N 70 40980
NASA CR-108485

INVESTIGATION OF CRACK GROWTH THRESHOLD OF INCONEL 718 EXPOSED TO HIGH PRESSURE OXYGEN

By

C. F. Tiffany, J. N. Masters and W. D. Bixler

CASE FILE COPY

Prepared For

NATIONAL AERONAUTICS AND SPACE ADMINISTRATION

Contract NAS9-10913

THE BOEING COMPANY

NOTICE

This report was prepared as an account of Government sponsored work. Neither the United States, nor the National Aeronautics and Space Administration (NASA), nor any person acting on behalf of NASA:

A.) Makes any warranty or representation, expressed or implied, with respect to the accuracy, completeness, or usefulness of the information contained in this report, or that the use of any information, apparatus, method, or process disclosed in this report may not infringe privately owned rights; or

B.) Assumes any liabilities with respect to the use of, or for damages resulting from the use of any information, apparatus, method or process disclosed in this report.

As used above, "person acting on behalf of NASA" includes any employee or contractor of NASA, or employee of such contractor, to the extent that such employee or contractor of NASA, or employee of such contractor prepares, disseminates, or provides access to, any information pursuant to his employment or contract with NASA, or his employment with such contractor.

Requests for copies of this report should be referred to

National Aeronautics and Space Administration
Office of Scientific and Technical Information
Attention: AFSS-A
Washington, D.C. 20546

NASA CR-108485

FINAL REPORT

INVESTIGATION OF CRACK GROWTH THRESHOLD OF INCONEL 718 EXPOSED TO HIGH PRESSURE OXYGEN

By

C. F. Tiffany, J. N. Masters and W. D. Bixler

Prepared for

NATIONAL AERONAUTICS AND SPACE ADMINISTRATION

August 1970

Contract NAS 9-10913

Technical Management

NASA Manned Spacecraft Center

Houston, Texas

Royce G. Forman

Aerospace Group

THE BOEING COMPANY

Seattle, Washington

INVESTIGATION OF CRACK GROWTH THRESHOLD OF INCONEL 718 EXPOSED TO HIGH PRESSURE OXYGEN

By

C. F. Tiffany, J. N. Masters and W. D. Bixler

ABSTRACT

Fracture and subcritical flaw growth characteristics were experimentally determined for forging and electron beam (EB) welded Inconel 718 tankage material in environments of high pressure gaseous and liquid oxygen. Static fracture, sustained load, cyclic load and combined sustained/cyclic load tests were conducted using precracked surface flawed specimens. Specimen thicknesses, welding and heat treating procedures, and environments were selected to simulate those of either the Apollo Service Module/Electrical Power System (SM/EPS) LOX tank or the Lunar Module/Environmental Control System (LM/ECS) GOX tank. For both tanks, the failure mode was found to be leakage at proof and operating stress levels, and no environmentally induced subcritical flaw growth was observed. In addition, cyclic flaw growth rates at stress levels and stress ratios applicable to the SM/EPS LOX tank are essentially zero.

KEY WORDS

Apollo 13

Inconel 718

High pressure oxygen

Fracture Characteristics

FOREWORD

As part of the Apollo 13 investigation, NASA requested the Aerospace Group of the Boeing Company to perform an experimental study of the flaw growth and fracture characteristics of EB welded Inconel 718 tankage material in an environment of high pressure oxygen. This program was performed under NASA Contract NAS 9-10913 during the period from April 24, 1970 to May 25, 1970, and the results are reported herein. The work was administered under the direction of Mr. R. G. Forman at NASA/MSC.

This program was performed by the Structures Research and Development organization, C. F. Tiffany, Section Chief. J. N. Masters was Program Supervisor, and W. D. Bixler, Technical Leader. Structural testing of specimens was conducted by A. A. Ottlyk and C. C. Mahnken. Metallurgical and welding support was provided by R. E. Regan and W. C. Butterfield. Don Good prepared the art work.

The information contained in this report is also released as Boeing Document D180-10073-1.

SUMMARY

The experimental work described herein was undertaken to investigate the fracture and flaw growth characteristics of forging and EB welded Inconel 718 in an environment of high pressure oxygen. The primary objective was to determine whether or not there was a structural deficiency in the SM/EPS LOX tank which could have contributed to the Apollo 13 incident. Since the GOX tank is also made of EB welded Inconel 718, a secondary study was included on that tank.

The program was thus conducted in two major parts. Part I simulated the SM/EPS LOX tank processing, thicknesses, and service conditions; Part II simulated the LM/ECS GOX tank processing, thicknesses, and service conditions. All fracture tests were conducted using uniaxially loaded precracked surface flawed specimens. Static, sustained, cyclic, and combined sustained/cyclic (suslic) loads were applied to specimens with flaws in base metal, in weld nugget centerline (℄) and in weld heat affected zone (HAZ).

Part I consisted primarily of testing in LOX at 1000 psi pressure and -190°F. Additional reference tests were run in an air/gaseous nitrogen mixture at -190°F. Fracture tests were conducted at room temperature, -190°F, and -320°F. Welded specimens, (which were tested in the as-welded condition) were nominally 0.111 inches thick; base metal specimens were nominally 0.059 inches thick.

Part II consisted of flaw growth tests in room temperature gaseous oxygen at 1000 psi pressure, and static tests in air at room temperature. Specimen dimensions and processing procedures were tailored to simulate the LM/ECS GOX tank (i.e., aged welded specimens were nominally 0.062 inches thick; base metal specimens were nominally 0.031 inches thick).

The following major observations were made from the study conducted:

1. The probable failure mode in both the SM/EPS LOX tank and the LM/ECS GOX tank is leakage at both proof and operating stress levels.

2. No environmentally induced subcritical flaw growth was observed in testing Inconel 718 in a high pressure oxygen environment for either the SM/EPS LOX tank or the LM/ECS GOX tank.

3. Cyclic flaw growth rates at stress levels and stress ratios applicable to the SM/EPS LOX tank (R = 0.95) are essentially zero.

From these observations, the following conclusions were arrived at relative to the Apollo 13 SM/EPS LOX tank:

1. No catastrophic brittle failure occurred.

2. Flaw growth through-the-thickness during flight to produce leakage or a subsequent ductile failure is only a very remote possibility.

Therefore, the SM/EPS LOX tank material did not contribute directly to the Apollo 13 incident.

TABLE OF CONTENTS

		PAGE
	SUMMARY	iv
1.0	INTRODUCTION	1
2.0	BACKGROUND	3
	2.1 Critical Flaw Sizes - Failure Mode	3
	2.2 Subcritical Flaw Growth	6
	2.3 Initial Flaw Sizes - The Proof Test	7
3.0	MATERIALS	9
4.0	PROCEDURES	11
	4.1 Specimen Fabrication	11
	4.2 Static and Flaw Growth Test Setups	13
	4.3 Experimental Approach for Static,Sustained, Cyclic and Sustained/Cyclic (Suslic) Load Tests	13
	4.4 Stress Intensity Solution	15
5.0	TEST RESULTS AND ANALYSIS	17
	5.1 Mechanical Properties	17
	5.2 Fracture Tests	17
	5.3 Sustained Load and Growth on Loading Tests	19
	5.4 Sustained/Cyclic (Suslic) Tests	21
	5.5 Special Flaw Growth Tests	22
	5.6 Comparison of Flaw Extension Methods and Specimen Width Requirements	22
	5.7 Cycle to Leakage Tests	24
6.0	OBSERVATIONS AND CONCLUSIONS	27
	REFERENCES	29

LIST OF ILLUSTRATIONS

		PAGE
1	Shape Parameter Curves for Surface and Internal Flaws	31
2	Applied Stress vs. Flaw Size	32
3	Stress Intensity Magnification Factors for Deep Surface Flaws	33
4	Growth-On-Loading in 2219 - T87 Aluminum Weldment in Air at Room Temperature	34
5	Comparison of Surface Flaw and Center Crack Data	35
6	Effect of R Value on Cyclic Life	36
7	The Effect of Wall Thickness on the Value of the Proof Test	37
8	Hemispherical SM/EPS LOX Tank Forging	38
9a	Weld Blank (Part I)	39
9b	Weld Blank (Part II)	39
10	60 KV Sciaky Electron Beam Welding Facility	40
11	SM/EPS LOX Tank Weld Simulation (Part I)	41
12a	Forging Tensile Specimen (Part I)	42
12b	Weldment Tensile Specimen (Part I)	42
13a	Forging Fracture Specimen (Part I)	43
13b	Weldment Fracture Specimen (Part I)	43
14	LM/ECS GOX Tank Weld Simulation (Part II)	44
15a	Forging Tensile Specimen (Part II)	45
15b	Weldment Tensile Specimen (Part II)	45
16a	Forging Fracture Specimen (Part II)	46
16b	Weldment Fracture Specimen (Part II)	46
17	Environmental Temperature Control System for Non-hazardous Tests	47
18	Cyclic Load Profile for Sustained/Cyclic Tests Performed in LOX at -190°F and 1000 psi	48

List of Illustrations (Continued)

		PAGE
19	Overall View of Dead Load Test Setup for Hazardous Testing	49
20	Schematic of Oxygen System for Parts I and II Testing	50
21	Specimen Mounting Pressure Caps	51
22	Temperature Conditioning System for Hazardous Testing (Part I)	52
23	Three Way Control Valves for Temperature Conditioning System-Hazardous Testing (Part I)	53
24	Mechanical Properties of Inconel 718 Used in Assessment of SM/EPS LOX Tank (Part I)	54
25	Static Fracture Tests of Inconel 718 Forging at Various Temperatures (Part I)	55
26	Static Fracture Tests of Inconel 718 Weldments at Various Temperatures (Part I)	56
27	Test Results of Inconel 718 Forging at -190°F for SM/EPS LOX Tank Assessment (Part I)	57
28	Test Results of Inconel 718 Weldment at -190°F for SM/EPS LOX Tank Assessment - Flaws in ℄ (Part I)	58
29	Test Results of Inconel 718 Weldment at -190°F for SM/EPS LOX Tank Assessment - Flaws in HAZ (Part I)	59
30	Test Results of Inconel 718 Forging at 70°F for LM/ECS GOX Tank Assessment (Part II)	60
31	Test Results of Inconel 718 Weldment at 70°F for LM/ECS GOX Tank Assessment (Part II)	61
32	Fractographs of Inconel 718 Forging Specimens Stressed to 140 ksi - 8X Polarized Light (Part I)	62
33	Fractographs of Inconel 718 Weldment Specimens Stressed to Approximately 100 ksi - 8X Polarized Light (Part I)	63
34	Fractographs of Inconel 718 Forging Specimens Stressed to 140 ksi-8X Polarized Light (Part II)	64
35	Fractographs of Inconel 718 Weldment Specimens Stressed to 100 ksi - 8X Polarized Light (Part II)	65

List of Illustrations (Continued)

		PAGE
36	Fractographs of Inconel 718 Weldment Specimens Stressed to 120 ksi - 8X Polarized Light (Part II)	66
37	Special Tests of Inconel 718 Weldments (Part I)	67
38	Fractographs of Inconel 718 Weldment Specimens Stressed to 80 ksi - Flaws in ℄ - 8X White Light (Part I)	68
39	Cyclic Tests to Leakage at R = 0 of Inconel 718 Forging in Air at 70°F (Part I)	69
40	Flaw Growth Rates to Leakage for Inconel 718 (Parts I and II)	70

LIST OF TABLES

		PAGE
I	Mechanical Properties of Inconel 718 from SM/EPS LOX Tank Forging (Part I)	71
II	Mechanical Properties of Inconel 718 from SM/EPS LOX Tank Weldments (Part I)	71
III	Mechanical Properties of Inconel 718 Used in Assessment of the LM/ECS GOX Tank (Part II)	72
IV	Static Fracture Tests of Inconel 718 in Air At 70°F (Part I)	73
V	Static Fracture Tests of Inconel 718 in Air/GN_2 at - 190°F (Part I)	74
VI	Static Fracture Tests of Inconel 718 in LN_2 at -320°F (Part I)	74
VII	Static Fracture Tests of Inconel 718 in Air at 70°F (Part II)	75
VIII	Sustained Tests of Inconel 718 Forging in LOX at -190°F and 1000 psi (Part I)	76
IX	Sustained Tests of Inconel 718 Weldment in LOX at -190°F and 1000 psi - Flaws in ℄ (Part I)	77
X	Sustained Tests of Inconel 718 Weldment in LOX at - 190°F and 1000 psi - Flaws in HAZ (Part I)	78
XI	Load/Unload Tests of Inconel 718 in Air/GN_2 at -190°F (Part I)	79
XII	Sustained Tests of Inconel 718 Forging in GOX at 70°F and 1000 psi (Part II)	80
XIII	Sustained Tests of Inconel 718 Weldment in GOX at 70°F and 1000 psi - Flaws in ℄ (Part II)	81
XIV	Sustained Tests of Inconel 718 Weldment in GOX at 70°F and 1000 psi - Flaws in HAZ (Part II)	82
XV	Load/Unload Tests of Inconel in Air at 70°F (Part II)	83
XVI	Sustained/Cyclic (Suslic) Tests of Inconel 718 Forging in LOX at -190°F and 1000 psi (part I)	84
XVII	Sustained/Cyclic (Suslic) Tests of Inconel 718 Weldment in LOX at -190°F and 1000 psi - Flaws in HAZ (Part I)	85

List of Tables (Continued)

		PAGE
XVIIIa	Cyclic Test of Inconel 718 Forging in Air/GN_2 at -190°F (Part I)	86
XVIIIb	Cyclic Test of Inconel 718 Weldment in Air/GN_2 at 190°F Flaws in HAZ (Part I)	86
XVIIIc	Cyclic/Load to Leakage Test of Inconel 718 Weldment in Air/ GN_2 at -190°F - Flaws in HAZ (Part I)	86
XVIIId	Proof/Cyclic/Load Test of Inconel 718 Weldment in Air-Flaws in HAZ (Part I)	86
XIXa	Comparison of Flaw Extension Methods and Specimen Width on 3 Hour Sustained Load Tests in Air/GN_2 at -190°F - Flaws in ℄ (Part I)	87
XIXb	Battelle Inconel 718 Weldment (T.I.G.) Sustained Loaded for 3 Hours in LOX at -297°F (Part I)	87
XXa	Cyclic Tests to Leakage at R=0 of Inconel 718 Forging in Air at 70°F (Part I)	88
XXb	Cyclic Test to Leakage at R = 0.095 of Inconel 718 Weldment in Air/GN_2 at -190°F - Flaw in HAZ (Part I)	88
XXc	Cyclic Test to Leakage at R=0 of Inconel 718 Weldment in Air at 70°F - Flaw in HAZ (Part II)	88

1.0 INTRODUCTION

The objective of this investigation was to determine the fracture and flaw growth characteristics of Inconel 718 tank materials in high pressure oxygen environments as applicable to the Apollo Service Module/Electrical Power System (SM/EPS) LOX tank and the Lunar Module/Environmental Control System (LM/ECS) GOX tank. The program was conducted in two major parts as indicated below:

Program	Environ-ment	SPECIMENS TESTED [1]					
		Tensiles	Static Fracture	Sustained	Load/ Unload	Cyclic	Suslic [2]
Part I SM/EPS LOX Tank	Air at 70° F	B W	B W			B	
	LOX at -190°F & 1000 psi			B W			B W
	Air/GN_2 at -190°F	B W	B W	W	B W	B W	
	LN_2 at -320°F	B W	B W				
Part II LM/ECS GOX Tank	Air at 70°F	B W	B W		B W		
	GOX at 70°F and 1000 psi			B W		W	

[1] B = Base Metal Specimens
W = Weldment Specimens

[2] Combined Sustained/Cyclic Loading

2.0 BACKGROUND

The prediction of failure mode, and the estimation of minimum structural life of metallic pressure vessels requires understanding of three major factors. These are the initial flaw sizes, the critical flaw sizes (i.e., the sizes required to cause fracture at a given stress level), and the subcritical flaw growth characteristics.

2.1 Critical Flaw Sizes-Failure Mode

The failure mode of a pressure vessel is dependent upon the fracture toughness of the material, thickness, and the applied stress level. For combinations of these variables in which the critical flaw size is small with respect to thickness, the failure mode is complete fracture, and the vessel is termed "thick walled".

For surface flaws in uniformly stressed "thick walled" vessels, the critical flaw sizes can be calculated using the expression:

$$(a/Q)_{cr} = \frac{1}{1.21\pi}\left(\frac{K_{Ic}}{\sigma}\right)^2 \qquad (1)$$

where:

a	=	depth (semi-minor axis) of a semi-elliptical surface flaw
Q	=	flaw shape parameter (see Figure 1)
σ	=	uniform stress applied perpendicular to the plane of crack
K_{Ic}	=	plane strain stress intensity factor or fracture toughness of the material.

Figure 2 is a graphical representation of Equation (1).

If the critical flaw sizes approach or exceed the wall thickness, the vessel is termed "thin walled". In order to predict critical flaw sizes as well as failure modes and operational life of "thin walled" vessels, it is necessary to know the stress intensity for flaws which become very deep with respect to the wall thickness. The stress intensity solution for semi-elliptical surface flaws shown in Equation (1) was derived

by Irwin (Reference 1) and has been found to be reasonably accurate for flaw depths up to about 50 percent of the material thickness. At greater depths, the applied stress intensity is magnified due to the effect of the free surface near the flaw tip. This means that in "thin walled" vessels the flaw tip stress intensity can attain the critical value (i.e., the K_{Ic} value) at a flaw size which is significantly smaller than that which would be predicted using Equation (1).

Kobayashi (Reference 2) has developed an approximate solution for deep surface flaws which are long with respect to their depth (i.e., small a/2c values). The results are shown in terms of a stress intensity magnification factor (M_K), versus a/t in Figure 3. This factor is applied to the original Irwin equation to obtain the stress intensity for deep surface flaws. As Figure 3 illustrates, the magnification reaches a maximum value of about 60 percent. Experimental data obtained on several materials appears to provide a fair degree of substantiation to the available solution (References 3 and 4) for flaws of moderate aspect ratios (i.e., a/2c values from 0.10 to 0.20). Kobayashi's solution tends to slightly underestimate the magnification for longer flaws.

Kobayashi's original solution was limited to depth-to-thickness ratios (a/t) of 0.70. The curve was later extended to greater depths for engineering use (i.e., the dotted part of Figure 3) as substantiating data became available. In Reference 4 it was found that use of this type of a solution was practical up to the point where the plastic zone ahead of the flaw tip [1] was very large with respect to the remaining unbroken ligament (t_n). For shallow flaws in brittle materials, the fracturing process is very abrupt. The amount of flaw growth prior to failure, under a rising load, can usually be considered to be negligible. In this case, all important dimensions (i.e., a and ρ) are small with respect to thickness. However, as the plastic zone becomes large (e.g., $\rho/t_n \rightarrow 1.0$), important deviations occur. Foremost of these is that large amounts of stable crack extension can occur, under rising load, well before complete fracture. An example of this behavior is illustrated in Figure 4.

[1] The plastic zone size herein is estimated as $\rho = \frac{\pi}{16}\left(\frac{K_{Ic}}{\sigma_{ys}}\right)^2$

This figure, from Reference 5, shows the amount of flaw extension which takes place in 2219-T87 aluminum weldments. These specimens were loaded to a predetermined stress level and then the load was rapidly dropped to zero. After fatigue marking the flaw front and failing the specimens, the growth-on-loading was measured directly from the fracture face. Significantly, in fatigue tests at constant maximum stress this growth-on-loading appears to occur only on the first cycle. Growth on subsequent cycles proceeds at a much lower rate. Similar observations have been made for 2219-T87 aluminum weldments at -320 and -423°F (Reference 4) and for titanium alloys (References 4 and 6). In the extreme case, this slow flaw growth can result in the flaw growing completely through-the-thickness. The specimen finally fails, upon a further increase in load as a through-the-thickness crack. In this instance, of course, the surface flaw solutions are not meaningful in describing the fracture process. As would be expected, predicted failure stresses based upon plane stress data and the original surface flaw length (not depth) correspond quite well (Reference 4). This is shown in Figure 5. The solid curve represents the conventional stress-flaw size relation for through cracks in a titanium alloy for an experimentally determined K_{CN} value of 104.7 ksi $\sqrt{in.}$ The curve is based upon a finite width specimen of 4.0 inches, equal to the width of surface specimens tested. Data points for the surface flaw specimens are plotted in terms of gross failure stress versus initial flaw length (2c). The correspondence is seen to be good until, of course, net section stress begins to approach the yield strength.

The above noted examples fall into the category of "thin walled" tankage and are normally considered to be the type in which the predicted failure mode is leakage. There are, however, combinations of flaw lengths and depths with which a ductile fracture before leakage could possibly occur. This would require a very deep flaw (i.e., $\rho/t_n \rightarrow 1.0$) whose length was effectively that of a critical through crack length at the applicable operating or proof stress level. No known systematic study of this type of flaw has been attempted.

2.2 Subcritical Flaw Growth

An initial subcritical flaw $(a/Q)_i$, as shown in Figure 2, can grow to critical size $(a/Q)_{cr}$ due to fatigue (cyclic stress) and environmentally induced sustained stress growth. Also, if the initial flaw is large with respect to the critical size, sustained growth may occur in a relatively inert environment.

The growth of an initial flaw to critical size is normally predicted in terms of cycles or time at load from the results of fracture specimen tests and fracture mechanics analysis. It has been shown (References 7, 8 and 9) that for a given environment and cyclic loading profile that the time or cycles to failure depends primarily upon the magnitude of the initial stress intensity (K_{Ii}) as compared to the critical stress intensity, K_{Ic} (i.e., cycles or time to failure $= f(K_{Ii}/K_{Ic})$).

The most important characteristic observed in all sustained stress flaw growth experiments performed to date is the existence of a threshold stress intensity level for a given material in a given environment. This stress intensity is designated as K_{TH}. The observation has been that, below a given stress intensity, flaw growth has not been detected and above this value, growth does occur and can result in fracture or leakage. Threshold values vary widely and have been found to be affected by alloy, heat treat level, grain direction, material form (e.g., base metal and weldment), temperature, and environment.

Considerable experimental and analytical work has been performed on the problem of fatigue crack growth (References 7, 8, 9, 10, 11, 12, 13 and 14). Much of this work has involved study of the effect of varying stress intensity ratios, R (i.e., $R = K_{min}/K_{max}$). It has been observed that cyclic crack growth rates very rapidly decrease as R starts to exceed about 0.80 to 0.90. Figure 6 taken from Reference 14 illustrates this point. The experimental points shown are from thin surface flaw tests of 6Al-4V titanium.

2.3 Initial Flaw Sizes - The Proof Test

As noted in Paragraph 2.2, the growth of subcritical flaws has been found to be primarily dependent upon the magnitude of the initial stress intensity as compared to the critical value. A successful proof test to a load level above the operating level provides an indication of the maximum possible initial to critical stress intensity ratio. This maximum stress intensity ratio is related to the proof test factor, α , as follows (Reference 9).

$$\text{max.} \quad (K_{Ii}/K_{Ic}) = 1/\alpha \tag{2}$$

The effect of material thickness on the information gained in a proof test is illustrated schematically in Figure 7. As noted there are three general cases of interest:

I. The critical flaw depths for relatively long (i.e., $Q \rightarrow 1.0$) surface flaws at the proof and operating stress levels are less than the wall thickness;

II. The critical flaw depth of a relatively long surface flaw is less than the thickness at the proof stress level, but at operating stress level it exceeds the wall thickness.

III. The critical depth of relatively long surface flaws at the proof and operating stress levels exceed the wall thickness.

In the first case, the predicted fracture mode would be catastrophic at both the proof and operating stress levels if failure should occur. In case II, the predicted failure mode at proof stress level is catastrophic and at operating stress level it is leakage. In either case the allowable K_{Ii}/K_{Ic} ratio is less than the K_{TH}/K_{Ic} ratio to allow for cyclic growth to the extent necessary to prevent service operation at or above the K_{TH}. In the third case either the material has such a high toughness or

the vessel wall is so thin that flaws cannot attain critical size at either the proof or operating stress level. Consequently, the predicted failure mode at both the proof and operating pressure is leakage. With regard to the maximum possible initial flaw size that could exist in the vessel after a successful proof test, all that can be said is that it is less than the wall thickness, otherwise the vessel would have leaked during the test. [1]

Obviously, in this case the proof test does not provide assurance against leakage due to multiple pressure cycles, since the initial flaw that was nearly through the thickness could grow through in a very few number of operational cycles. However, if the sustained stress threshold stress intensity, K_{TH} to critical stress intensity ratio is used as the maximum allowable K_{Ii}/K_{Ic}, the proof test should provide some assurance against leakage during a single prolonged operational cycle.

[1] With regard to the case of a very long and deep flaw which might be approaching criticallity as an effective through crack (see Paragraph 2.1), it does appear that the proof test can provide some assurance that service failure will not occur by this mode, (i.e., K_i/K_C in operation $\approx 1/\alpha$)

3.0 MATERIALS

One hemispherical SM/EPS LOX tank forging made of Inconel 718 was supplied by NASA/MSC Houston, Texas to conduct this investigation. The forging was about 0.40 inches thick with a diameter of 25 inches as illustrated in Figure 8. Prior to receival of the forging at Boeing, it had been heat treated at 1800°F for 1 hour, air cooled and then aged at 1325°F for 8 hours, furnace cooled to 1150°F, held for 10 hours and air cooled.

4.0 PROCEDURES

4.1 Specimen Fabrication

Precracked surface flawed specimens were used for all fracture tests including static fracture, sustained load, cyclic, and combined sustained/cyclic load tests. Overall dimensions of the specimens were tailored to the size and shape of the available forging. As illustrated in Figure 8 specimens for Part I (SM/EPS LOX tank) and Part II (LM/ECS GOX tank) investigations were obtained from the same hemispherical forging as described below:

Part I

Weld blanks were machined to the configuration shown in Figure 9a; having a basic weld preparation thickness of 0.139 inches to simulate actual tank material thickness prior to welding. The weld blank halves were electron beam (EB) welded together in a vacuum using a 60KV Sciaky EB welding machine as shown in Figure 10. The weld schedule used on the specimens varied somewhat from that used on the actual SM/EPS LOX tank, since available Boeing equipment has lower voltage, higher amperage capability than that used on the tank. A typical micrograph of the actual tank weld was obtained and weld settings were arrived at that would closely simulate the actual tank weld. The welding schedule used is presented in Figure 11 along with a photomicrograph of the weld. Final machining of the weldments along with the forging blanks into tensile and fracture specimen configurations shown in Figures 12a, 12b, 13a and 13b was then accomplished. The final machined thickness of the forging and weldment specimens was 0.059 and 0.111 inches respectively, which was representative of actual tank wall thicknesses. After final machining, the welded specimens were radiographic inspected. These specimens did not receive any thermal treatment after receipt of the tank forging at Boeing.

Part II

Weld blanks were machined to the configuration shown in Figure 9b; having a basic weld preparation thickness of 0.075 inches to simulate actual tank material thickness prior to welding. The weld blank halves were EB welded together using the same machine used in Part I welding. Again, as in Part I specimen fabrication, weld settings had to be established to simulate actual tank welds. After viewing a typical weld micrograph, the weld settings presented in Figure 14 were established. The resulting weld is also shown in Figure 14 which closely simulates the actual tank weld. These weldments plus rough machined forging specimen blanks were then thermally aged to duplicate the LM/EPS GOX tank fabrication history. Aging was done at 1325°F for 8 hours, furnace cooled at 100°F per hour to 1150°F, held for 10 hours and then air cooled. Final machining of the weldments along with the forging blanks into tensile and fracture specimen configurations shown in Figures 15a, 15b, 16a and 16b was then accomplished. After final machining the welded specimens were radiographic inspected. The final machined thickness of the forging and weldment specimens was 0.031 and 0.062 inches, respectively, which was representative of the actual tank wall thicknesses.

Parts I and II investigations utilized surface flaws that were introduced into the fracture specimens by using an electric discharge machine to form a starter notch and then extending the notch by low stress/high cycle tension-tension fatigue. The fatigue extension was accomplished at a maximum gross stress of 40 ksi at 1800 cpm. From 2000 to 36,000 cycles were required, depending upon the initial notch dimensions and whether or not the material was forging or weldment. All precracking was done in air at room temperature. The flaws put in Parts I and II welded specimens were located in the centerline (℄) and in the heat affected zone (HAZ). The flaws on the weld centerline were introduced from the bottom side of the weld (opposite the side the specimen was welded from) to simulate flaws exposed to the environments the tanks contained. The flaws in the HAZ were located 0.007 inches outside of the fusion line referenced at the bottom side of the weld. These flaws in the HAZ were introduced from the top side of the weld so that various depth flaws (greater than 50 percent of the thickness) would have the flaw tips terminating in the HAZ.

4.2 Static and Flaw Growth Test Setups

The same testing machines and setups were used for both Part I and Part II testing. All non-hazardous tests were conducted in an environmentally controlled laboratory at the Boeing Space Center. This includes all tensile, static fracture, sustained in air and cycled in air specimens. Where temperatures other than 70°F were required, the environmental control system shown schematically in Figure 17 was employed. By manual control of gaseous and liquid nitrogen supplies, any temperature between -320°F and 70°F can be maintained. All non-hazardous tests were conducted in a 120,000 lb. Baldwin universal testing machine with an MTS programmer.

Hazardous tests involving high pressure oxygen at -190°F and 70°F were conducted at Boeing's remote Tulalip Test Site. Dead load machines of 10,000 and 30,000 lb. capacity were used for the sustained and sustained/cyclic testing. The sustained/cyclic (suslic) load profile shown in Figure 18 was accomplished by automatically removing a certain portion of the dead weights for one-half hour and then replacing them for one-half hour. An overall view of two of the three dead load machines used is shown in Figure 19 without specimens. A schematic of the system is also shown in Figure 20. High pressure gaseous oxygen, regulated down to 1000 psi was supplied to a small cup mounted on the specimen. A cup with a pressure transducer pickup was also mounted on the back side of the specimen to sense the pressure rise occurring when the flaw grew through-the-thickness. These cups are shown in Figure 21. Temperature conditioning of the gaseous oxygen to -190°F was accomplished automatically using a gaseous/liquid nitrogen system as schematically shown in Figure 22 and pictorially presented in Figure 23. Three way valves were used to mix the proper amount of gaseous and liquid nitrogen to maintain the test temperature. The test temperature was generally maintained with ± 10°F and the pressure within ± 50 psi.

4.3 Experimental Approach for Static, Sustained, Cyclic and Sustained/Cyclic (Suslic) Load Tests

The experimental approach used during this study was the same for both Parts I and II testing with the exception of the flaw sizes used. The targeted flaw shape $(a/2c)_i$

for Part I was 0.25 which was limited in part by the thickness of specimen required and also by the size and shape of the available forging. Because of the thinner test specimens required for Part II testing, smaller $(a/2c)_i$ ratios targeted at 0.15 were possible.

The mechanical property specimens were tested at a strain rate of 0.004 inch/inch/min. while the static fracture specimens were tested to failure in approximately one minute. Flaw sizes for the static fracture specimens were targeted so that failure would occur below the yield strength in an attempt to obtain valid plane strain fracture toughness values. In general, this necessitated going to deep flaws relative to the thickness and in turn resulted in the flaws growing through-the-thickness. To detect if and when the flaws grew through-the-thickness prior to failure for specimens tested at room temperature, the back side of the specimen was observed visually.

The first sustained tests were conducted with specimens of flaw depths ranging from 50 to 85 percent of the thickness and loaded to either the operating or proof stress. These stresses were based on a spherically shaped vessel having a 25 inch diameter for the SM/EPS LOX tank and a 11.9 inch diameter for the LM/ECS GOX tank. Some of the higher stressed/deeper flawed specimens grew through-the-thickness upon loading and were then unloaded but generally, the specimens were held at constant load for about 20 hours. After unloading, the specimens were low stress cycled in air to mark the flaw front and then pulled to failure. Evidence of growth was then observed by a separation between the initial fatigue crack extension and that of final marking. Depending on whether or not flaw growth was observed, the next group of specimens were loaded to lower or higher stress levels, respectively. In addition to determining the combinations of stress and flaw depth which caused growth and those which did not, it became necessary to separate growth-on-loading from environmental/time dependent growth. This was accomplished by loading specimens to predetermined stress levels and then immediately dropping the load to zero and observing the fracture face for growth after marking and failing the specimen.

Cyclic flaw growth tests were conducted with a sinusoidal shaped loading profile whereas the suslic tests were performed using the square wave loading profile as shown in Figure 18. Suslic tests were conducted to determine what effect, if any, a high stress ratio had on flaw growth as compared directly to sustain loaded specimens.

4.4 Stress Intensity Solution

Where stress intensity values are reported, they were based on the following expression:

$$K_I = 1.95 \ \sigma \ (a/Q)^{1/2} \ M_K$$

where

K_I	=	stress intensity
σ	=	gross stress
a	=	flaw depth
Q	=	shape parameter
M_K	=	Kobayashi's deep flaw magnification factor

Values of Q and M_K are shown in Figures 1 and 3.

5.0 TEST RESULTS AND ANALYSIS

5.1 Mechanical Properties

Mechanical property tests were conducted for the forging and weldment materials used in the SM/EPS LOX tank (Part I) and LM/ECS GOX tank (Part II) evaluations.

Part I

The forging and weldment material were tested at temperatures of 70°F in air, -190°F in air/gaseous nitrogen and at -320°F in liquid nitrogen. In addition to the extensometer used to measure strain on the forging and weldment tensile specimens, a mini-strain gage (0.06 inch long) was positioned on the weld nugget of the weldments. The results of these tensile tests are shown in Figure 24. The strength of Inconel 718 increases as the temperature decreases for both forging and weldment. Of interest is the large increase in the as-welded weld nugget yield strength at -320°F as compared to temperatures between -200°F and 70°F where the yield strength remained relatively constant. The detailed results are presented in Tables I and II, respectively, for the forging and weldment.

Part II

Tensile tests were conducted at 70°F in air for the forging and weldment material and the detailed results are presented in Table III. The forging material (re-aged Part I forging material) demonstrated a modest increase of 6 percent in yield strength compared to the forging used in Part I, whereas the aged weldments showed a significant increase in weld nugget yield strength of 63 percent relative to the Part I as-welded weldments.

5.2 Fracture Tests

Part I

Static fracture tests of the Inconel 718 forging and weldment material were conducted in air at 70°F, in air/gaseous nitrogen at -190°F and in liquid nitrogen at -320°F. The weldment specimens either had flaws located in the centerline (℄) or in the heat

affected zone (HAZ). The results of these tests are presented in Figures 25 and 26 while the detailed data are presented in Tables IV, V and VI. As both figures indicate, the failure stress increases as the temperature decreases. The specimens tested at 70°F were visually observed to have the flaws extend through-the-thickness prior to failure in plane stress as a through-the-thickness crack. This condition also existed for the weldments tested at -190°F based on the results of several intended sustain loaded specimens which had flaws that grew through-the-thickness upon reaching maximum load as shown in Figure 28. Based on these data it is assumed that all of the static fracture specimens having very deep flaws (> 70 percent of the thickness) did not fail in plane strain but had significant flaw extension prior to failure, to the point of growing through-the-thickness. No plane strain fracture toughness values were obtained from the fracture specimens that were representative of tank wall and weld thicknesses. The failure stresses were above the local weld yield strength for the welded specimens tested at 70°F and -190°F.

An attempt was made to obtain plane strain fracture of the weldment material by increasing the specimen thickness. Two specimens with nominal thicknesses of 0.22 inches were prepared; one was then tested at 70°F and the other at -190°F. Neither of the flaws of these specimens were observed to have grown through-the-thickness prior to failure. Failure for both specimens occurred at an apparent stress intensity of 91.0 ksi $\sqrt{in}$ at stress levels which were above the weld nugget yield strengths. To obtain a truly valid plane strain fracture toughness, failure would have to occur below the yield strength which would require an even thicker specimen than tested.

These fracture tests do show that the failure mode of either the forging or weldment is leakage at stresses less than the yield strength and that any proof test conducted does not guarantee any maximum possible initial flaw size less than the wall thickness. This is a clasic example of a Case III pressure vessel as discussed in Paragraph 2.3.

Part II

Static fracture tests of the Inconel 718 forging and weldment material were conducted in air at 70°F. The weldment specimens either had flaws located in the ℄ or HAZ. All of the specimens tested were observed to have flaws that grew through-the-thickness prior to failure as shown in Figures 30 and 31, much the same as the specimens tested in Part I. The detail data for these tests is presented in Table VII. From the data obtained, a curve was generated for both forging and weldment material representing a lower bound above which flaw growth through-the-thickness could be expected. With both materials, flaw growth through-the-thickness could be expected when stressed to the proof stress if a flaw greater than 90 percent of the thickness was present. This is assuming the flaw was relatively long with respect to the depth ($a/2c = 0.15$).

The same result was obtained with these tests as in Part I, mainly that no plane strain fracture toughness values were generated from specimens that were representative of tank wall and weld thicknesses. These fracture tests do show that the failure mode of either the forging or weldment is leakage at stresses below the yield strength and that any proof test conducted does not guarantee any maximum possible initial flaw size less than the wall thickness.

5.3 Sustained Load and Growth on Loading Tests

Part I

Inconel 718 forging and weldment specimens were sustain loaded in LOX at -190°F and 1000 psi for a minimum of 20 hours. The weldment specimens either had flaws located in the ℄ or HAZ. The results of these tests are presented in Figures 27, 28 and 29, while the detailed data are presented in Tables VIII, IX and X. Flaw growth was observed in both the forging and weldment materials for particular combinations of stress and flaw depth, but because of the growth through-the-thickness observed with the static fracture specimens additional tests were conducted to separate time dependent, sustained load flaw growth from growth-on-loading. Key specimens that showed flaw growth after being sustain loaded for a minimum of 20 hours were

duplicated with specimens of similar depth flaws and loaded to the same stress level and then immediately unloaded. These load/unload specimen tests were conducted in an air/gaseous nitrogen environment at -190°F and the detailed data for these specimens are presented in Table XI. These specimens indicated as much growth as the specimens they duplicated, thereby proving that what was observed as growth in the sustained specimens was indeed growth occurring during loading the specimen and not environmentally induced. Fractographs of specimens showing growth are presented in Figures 32 and 33 for comparison. One notable exception to the growth-on-loading observed occurred when one welded specimen with a flaw in the ℄ grew through-the-thickness after being loaded for 37 minutes. This specimen had an 82 percent deep flaw and was loaded to 120 ksi as illustrated in Figure 28. The amount of growth occurring on loading for this specimen was probably appreciable as adjacent specimens did grow through-the-thickness upon loading. It is believed that the time dependent flaw growth indicated by this specimen was not environmentally induced but a function of the flaw condition and stress level, and would have occurred in any inert environment.

For both the forging and weldment materials, it was possible to generate a curve above which flaw growth-on-loading could be expected to occur as indicated in Figures 27, 28 and 29. As illustrated in Figure 27 for the forging material, a flaw depth of greater than about 50 percent of the thickness could grow upon applying the proof pressure. No flaw growth could be expected when stressed to the maximum design operating stress (σ_{MDOP}) for flaw depths up to about 90 percent of the thickness. A curve was also generated from the data obtained for the weldment material, above which flaw growth through-the-thickness could be expected. Specifically, flaw growth through-the-thickness could result if stressed to the proof level and a flaw was present which had a depth greater than 90 percent of the thickness. These observations are based on flaws that had an $a/2c = 0.25$.

In summary, within the range of stress levels and flaw sizes tested, the high pressure oxygen environment at -190°F and 1000 psi did not promote flaw growth of Inconel 718 forging or EB weldment material.

Part II

Inconel 718 forging and weldment specimens were sustain loaded in GOX at 70°F and 1000 psi for a minimum of 20 hours. The weldment specimens either had flaws located in the ℄ or HAZ. The results of these tests are presented in Figures 30 and 31, while the detailed data are presented in Tables XII, XIII and XIV. Just as observed during the Part I sustained testing, several specimens had an indication of flaw growth after being loaded for about 20 hours in the oxygen environment. Again, load/unload specimens were tested in air and found to have as much flaw growth as the sustained specimens they duplicated. The results of these load/unload specimens are also illustrated in Figures 30 and 31 along with the detail data presented in Table XV. Fractographs of specimens exhibiting flaw growth are presented in Figures 34, 35 and 36.

5.4 Sustained/Cyclic (Suslic) Tests

Suslic tests with the loading profile shown in Figure 18 were conducted to simulate actual in-flight pressure conditions within the SM/EPS LOX tank. The cyclic rate of 1 cph was slightly higher than the actual rate experienced with the Apollo 13 tank, but felt to be conservative. These tests were intended to determine if high flaw growth rates existed with Inconel 718 in an oxygen environment at high minimum to maximum stress ratios (R = 0.95).

Suslic tests were conducted with the forging and weldment material in LOX at -190°F and 1000 psi. The weldment specimens had flaws located in the HAZ. The selection of the HAZ was somewhat arbitrary since no discernible differences had been observed in the results obtained with flaws located in the ℄ or HAZ during static fracture and sustain tests. The results of the suslic tests are presented in Figures 27 and 29 for the forging and weldment materials, respectively. The detailed data are presented in Tables XVI and XVII. As indicated, some of the tests were conducted at a more conservative stress ratio (R = 0.895) value before the actual R value of 0.950 for the Apollo 13 tank was made known. For the suslic tests performed at maximum

stress levels and flaw sizes below the no flaw growth-on-loading curves, the results showed that flaw growth was less than 0.001 inches, even after 55.5 cycles (55.5 hours). Suslic specimens tested above the growth-on-loading curves, exhibited flaw growth on the same order of magnitude as that observed for the growth-on-loading specimens.

Based on these test results, it appears that suslic flaw growth rates at high R values (0.950) with Inconel 718 in oxygen are essentially zero.

5.5 Special Flaw Growth Tests

Several special tests were conducted to determine the amount of flaw growth produced by cycling Inconel 718 specimens at high R values (0.950) for 15,000 cycles. These tests were conducted in an air/gaseous nitrogen environment at -190°F and the results are presented in Figure 27 for the forging test and in Figure 37 for the weldment tests. The detail data for each specimen is contained in Tables XVIIIa, XVIIIb, XVIIIc and XVIIId. No specimens exhibited more than 0.001 inches of flaw growth after the 15,000 cycles. One welded specimen, tested to simulate various stress conditions experienced by the Apollo 13 SM/EPS LOX tank, did not show any flaw growth after 12 room temperature proof cycles to 75 ksi, 15,000 high R value (0.950) cycles to 52.1 ksi at -190°F and one final cycle to 67.7 ksi.

These results along with those of the suslic tests discussed in Paragraph 5.4 indicates that essentially zero flaw growth rates are obtained when Inconel 718 is subjected to high R value (0.950) cycles and stress levels below proof in either high pressure oxygen or air/gaseous nitrogen at -190°F.

5.6 Comparison of Flaw Extension Methods and Specimen Width Requirements

Because of the apparent differences in the sustained load behavior of Inconel 718 weldments in LOX at -297°F as reported in Reference 15 and the results obtained during Part I testing with weldments in LOX at -190°F and 1000 psi, an investigation was undertaken to determine if the different flaw extension methods or specimen width to flaw length ratios (W/2c) employed were responsible for the differences.

Reference 15 results had indicated significant sustained load growth at combinations of stress level and flaw size where no growth was observed in the Boeing generated data. It is realized that differences other than those noted above were present, such as TIG welds versus electron beam welds, but proving or disproving that these specimen preparation procedures mentioned above had any effect on the sustained load flaw growth characteristics would be helpful in understanding the behavior of Inconel 718.

Reference 15 generated data was obtained from surface flawed fracture specimens in which the initial crack extension was done with low stress cyclic bending rather than low stress cyclic tension as done with the Boeing prepared specimens. Bending stress levels of ± 45 ksi for weldment specimens were used by Reference 15 investigators. In addition, the specimen W/2c ratio was about 3.0 for the Reference 15 specimens as compared to a value of 4.0, established for the Boeing specimens. Previous tests (Reference 16) have indicated that at W/2c ratios less than 4.0, bending stresses become significant. These bending stresses are caused by the shift in neutral axis due to the presence of the flaw.

A specimen, 72W, was selected from Reference 15 as being typical of the specimens showing the sustain load flaw growth results obtained. This particular specimen had been stressed to a level of 80 ksi for a period of three hours in liquid oxygen and had indicated 0.011 inches of growth in the depth direction. Detailed data on this specimen are presented in Table XIXb. Three specimens were prepared at Boeing which had flaw sizes targeted at the 72W specimen flaw size. The first of these specimens had a W/2c ratio of about 4.0 with the crack extended in tension fatigue, the second had a W/2c ratio of about 3.0 with the crack extended in tension fatigue and the third had a W/2c ratio of 3.0 with the crack extended by complete reversal/bending fatigue. Maximum fatigue stress for all specimens was maintained at 45 ksi. The three specimens were sustain loaded at -190°F in an air/gaseous nitrogen environment at 80 ksi for three hours and then unloaded, marked and failed. Marking the flaw front was done in the same manner as the initial crack extension for each of the specimens. The results of these three specimens are shown in Figure 37 along

with the reference specimen, 72W. Neither of the two specimens, where the crack was extended by tension fatigue, showed any sustained load flaw growth, even though different W/2c ratios existed. The one specimen, where the crack was extended in bending fatigue, showed considerable growth. The growth observed was primarily in the flaw length direction. The detailed data for each specimen are presented in Table XIXa. Fractographs of all four specimens are presented in Figure 38 for comparison.

Although not as much growth was observed in the Boeing prepared, fatigued in bending specimen as the reference specimen 72W, the results indicate that probably part of the growth observed in the Reference 15 specimens was due to the manner in which the crack extension was accomplished. The smaller W/2c specimen did not show any growth under the stress condition tested. From this investigation, it appears that if a fracture specimen is to be tested in tension then the initial crack extension should also be performed in tension.

5.7 Cycle to Leakage Tests

Part I

Three forging specimens with varying depth flaws were cycled to leakage (the instant the flaw broke through the back surface) at 70°F in air at a stress level of 105 ksi. A cyclic rate of 40 cpm was used along with an R value of about zero. The number of cycles required to produce leakage as a function of initial flaw depth is presented in Figure 39. Cycle to leakage flaw growth rates were calculated and are presented in Figure 40 as a function of stress intensity. The detailed test data are presented in Tables XXa.

A single weldment specimen with a deep flaw located in the HAZ was cycled to leakage at -190°F in an environment of air/gaseous nitrogen and at a maximum stress of 87.2 ksi. A cyclic rate of 90 cpm was used along with R = 0.095. Four hundred and ninety-one (491) cycles were required to produce leakage which corresponds to an average flaw growth rate of 16.9 micro-inch/cycle. This growth rate result is also presented in Figure 40. The detailed test data for this specimen are presented in Table XXb.

Part II

A single weldment specimen with a flaw located in the HAZ was cycled to leakage at 70°F in air at a stress of 50 ksi. A cyclic rate of 40 cpm was used with R = 0. An average flaw size growth rate of 0.3 micro-inch/cycle was obtained and is also illustrated in Figure 40. The detailed test data for this specimen are presented in Table XXc.

In general, there appears to be good agreement in the flaw growth rates obtained between all the various forging and weldments cycled to leakage, regardless of the aging and test temperature. Reduced to the same stress level, all of the growth rates obtained would fall about on the same curve.

6.0 OBSERVATIONS AND CONCLUSIONS

The following major observations were made from the study conducted:

1. The probable failure mode in both the SM/EPS LOX tank and the LM/ECS GOX tank is leakage at both proof and operating stress levels.
2. No environmentally induced subcritical flaw growth was observed in testing Inconel 718 in an high pressure oxygen environment for either the SM/EPS LOX tank or the LM/ECS GOX tank.
3. Cyclic flaw growth rates at stress levels and stress ratios applicable to the SM/EPS LOX tank ($R = 0.95$) are essentially zero.

From these observations the following conclusions were arrived at relative to the Apollo 13 SM/EPS LOX tank:

1. No catastrophic brittle failure occurred.
2. Flaw growth through-the-thickness during flight to produce leakage or a subsequent ductile failure is only a very remote possibility.

Therefore, the SM/EPS LOX pressure vessel material was not directly responsible for the Apollo 13 incident.

REFERENCES

1. Irwin, G.R.; "Crack Extension Force for a Part-Through-Crack in a Plate", Journal of Applied Mechanics, Vol. 29, Trans. ASME, Vol. 84, Series E, December 1962.

2. Kobayashi, A.S.; "On the Magnification Factors of Deep Surface Flaws", Structural Development Research Memorandum No. 16, The Boeing Company, December 1965.

3. Tiffany, C.F., Masters, J.N., and Pall F.A.; "Some Fracture Considerations in the Design and Analysis of Spacecraft Pressure Vessels", presented at the ASM National Metals Congress, Chicago, October 1966.

4. Masters, J.N., Haese, W.P., and Finger, R.W.; "Investigation of Deep Flaws in Thin Walled Tanks", NASA CR-72606, December 1969.

5. Masters, J.N., Hall, L.R., Finger, R.W.; "Stress Corrosion of Metal Tank Materials", Rough Draft - Interim Final Report, NASA Contract NAS 3-12003, January 1970.

6. Bixler, W.D.; "Comparison of Flaw Growth Characteristics Under Cryogenic Proof and Ambient Test Conditions for Apollo Titanium Pressure Vessels".

7. Tiffany, C.F., and Lorenz, P.M.; "An Investigation of Low Cycle Fatigue Failures Using Applied Fracture Mechanics", ML-TDR-64-53, May 1964.

8. Tiffany, C.F., Lorenz, P.M., and Hall, L.R.; "Investigation of Plane Strain Flaw Growth in Thick-Walled Tanks", NASA CR-54837, February 1966.

9. ASTM Special Committee on Fracture Testing of High-Strength Metallic Materials, "Progress in the Measurement of Fracture Toughness and the Application of Fracture Mechanics to Engineering Problems", Materials Research and Standards, Vol. 4, No. 3, March 1964.

10. Hall, L.R.; "Plane-Strain Cyclic Flaw Growth in 2014-T62 Aluminum and 6Al-4V(ELI) Titanium", NASA CR-72396, November 1968.

11. Roberts, R. and Erdogan, R.; "The Effect of Mean Stress on Fatigue Crack Propagation in Plates Under Extension and Bending", ASME Paper No. 67, WA/MET-2, 1967.

12. Krafft, J.M.; "A Comparison of Cyclic Fatigue Crack Propagation With Single Cycle Crack Toughness and Plastic Flaw", Report to ASTM Fracture Toughness of High Strength Materials Special Committee, September 1965.

13. Forman, R.G., Kearney, V.E., and Engle, R.M.; "Numerical Analysis of Crack Propagation in Cyclic Loaded Structures", Journal of Basic Engineering, Trans. ASME, Series D, Vol. 89, pp. 459-464, September 1967.

14. Masters, J.N.; "Cyclic & Sustained Load Flaw Growth Characteristics of 6Al-4V Titanium", NASA CR-92231, July 1968.

15. Pettit, D.E., Feddersen, C.E., and Mindlin, H.; "Flaw Growth Behavior of Inconel 718 at Room and Cryogenic Temperature", NASA CR-101942, Battelle Memorial Institute, 1969.

16. Technical Proposal, "Experimental Study of the Growth of Surface Flaws", Document D2-121012-1, The Boeing Company, March 1969.

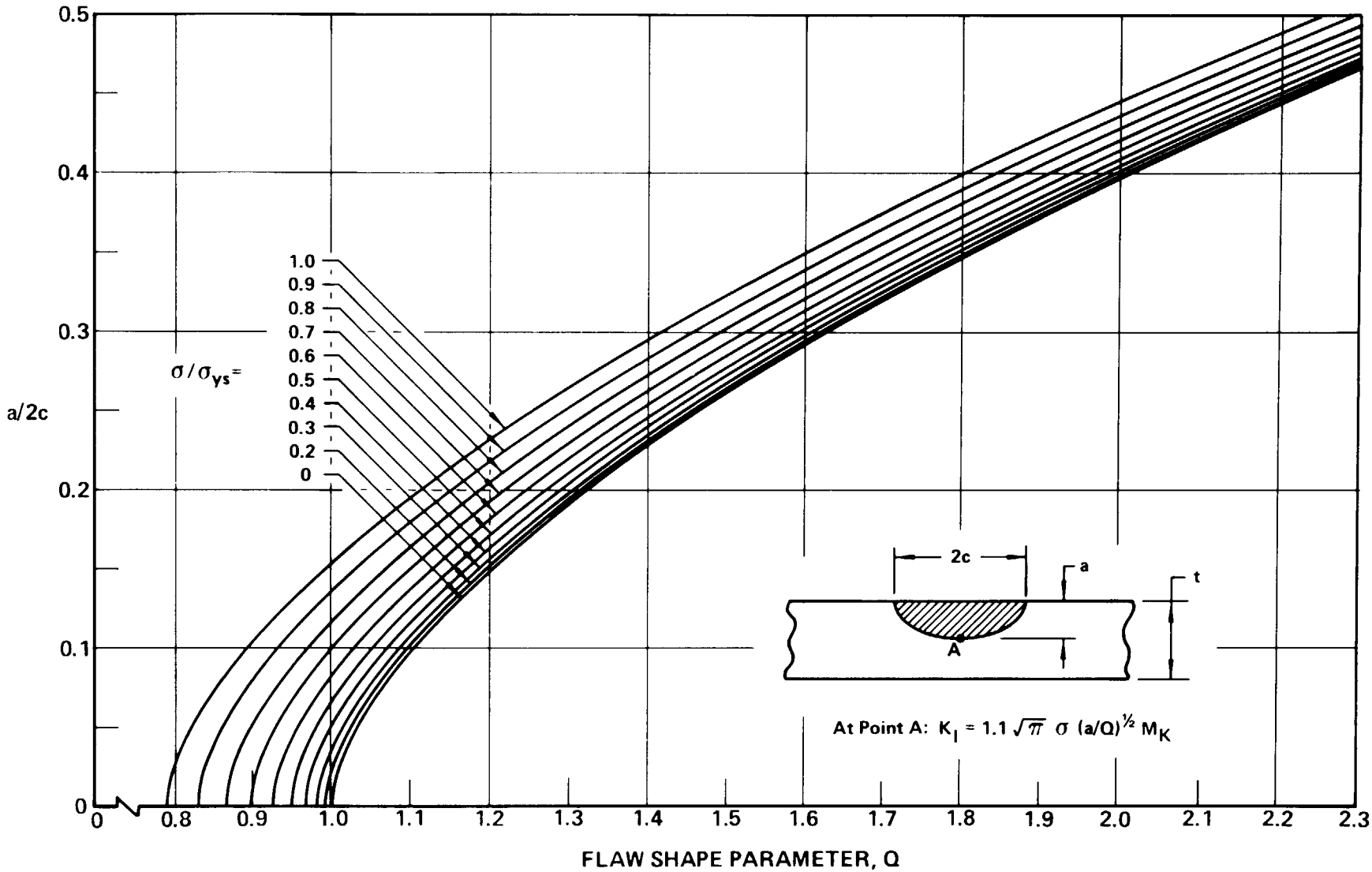

Figure 1 : SHAPE PARAMETER CURVES FOR SURFACE AND INTERNAL FLAWS

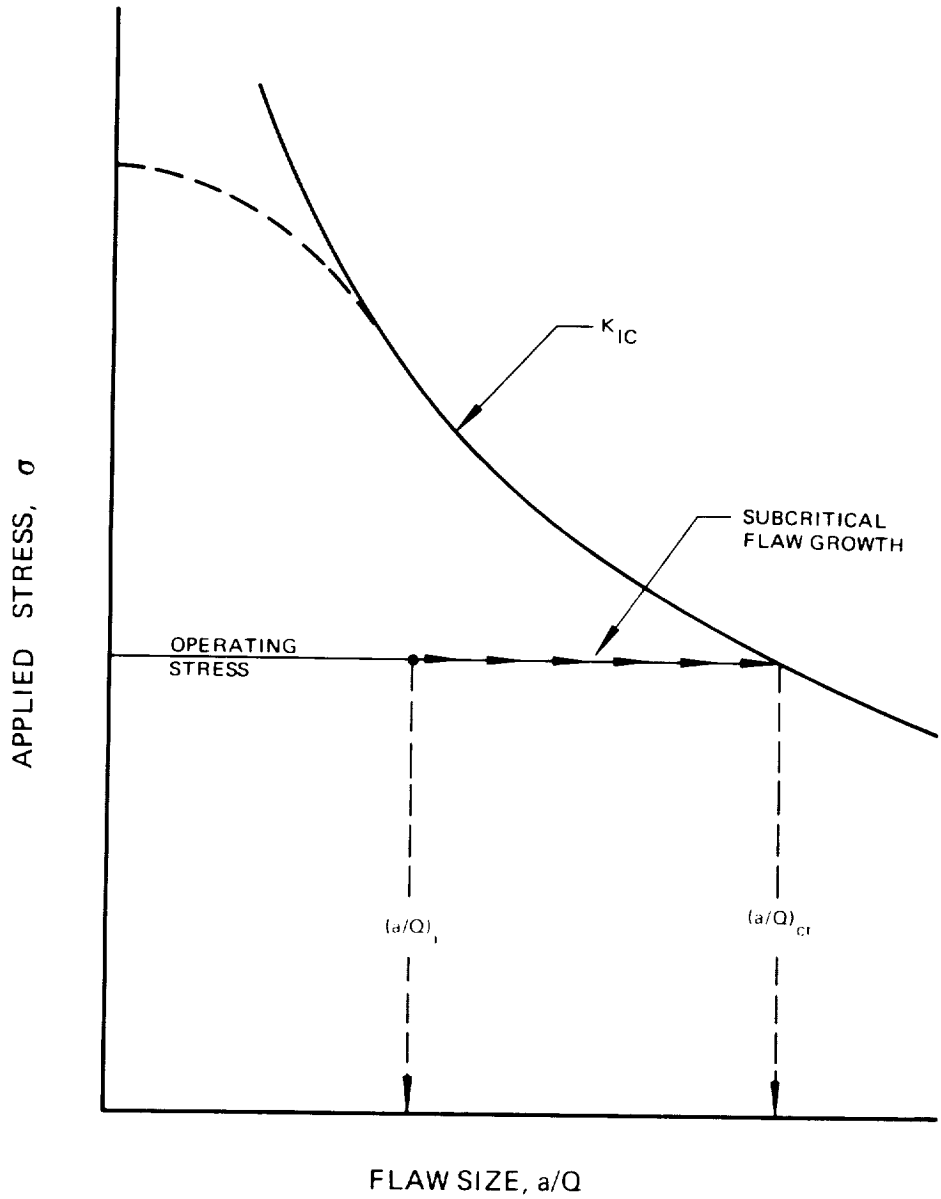

Figure 2: APPLIED STRESS VS. FLAW SIZE

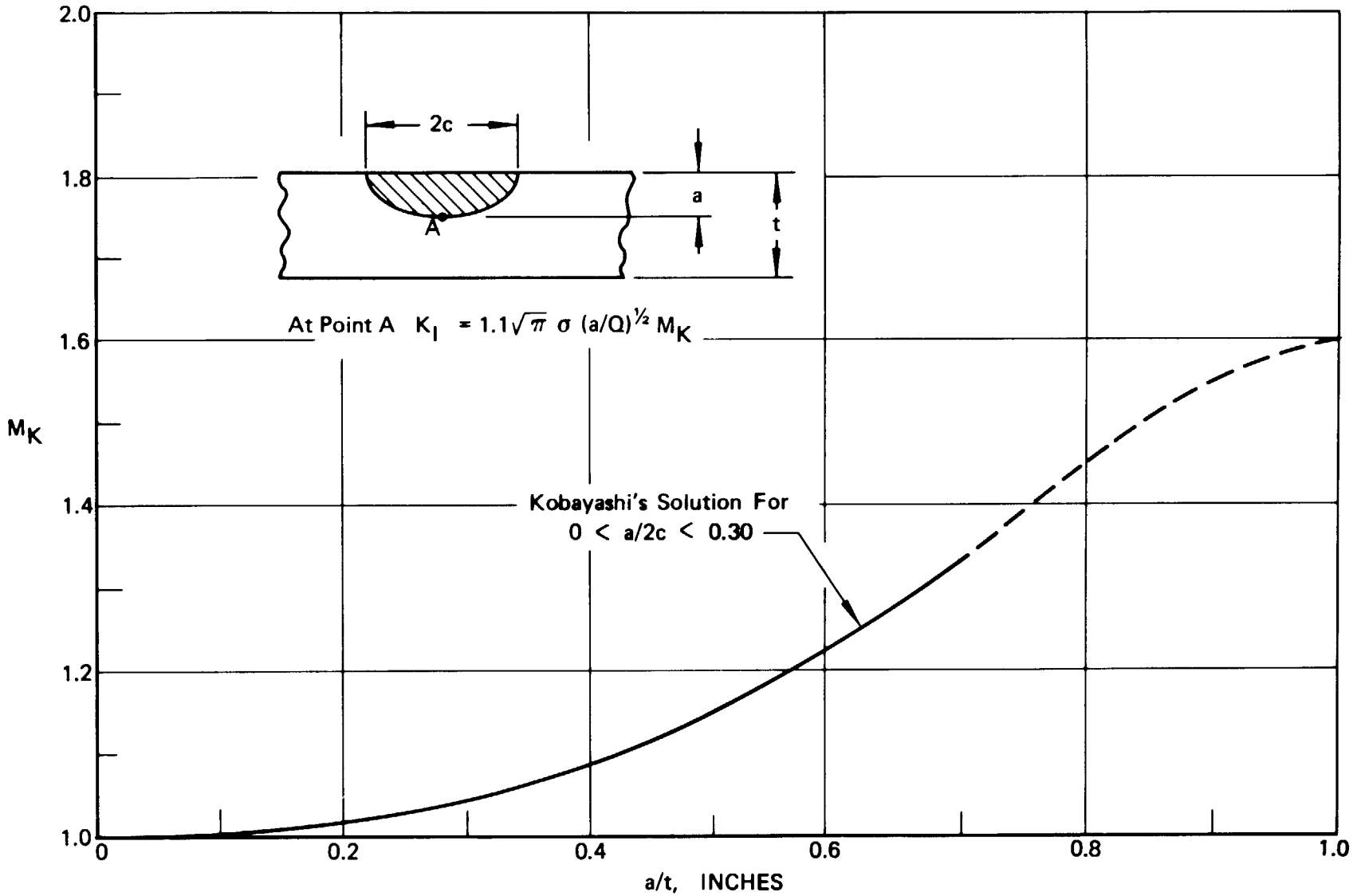

Figure 3: STRESS INTENSITY MAGNIFICATION FACTORS FOR DEEP SURFACE FLAWS

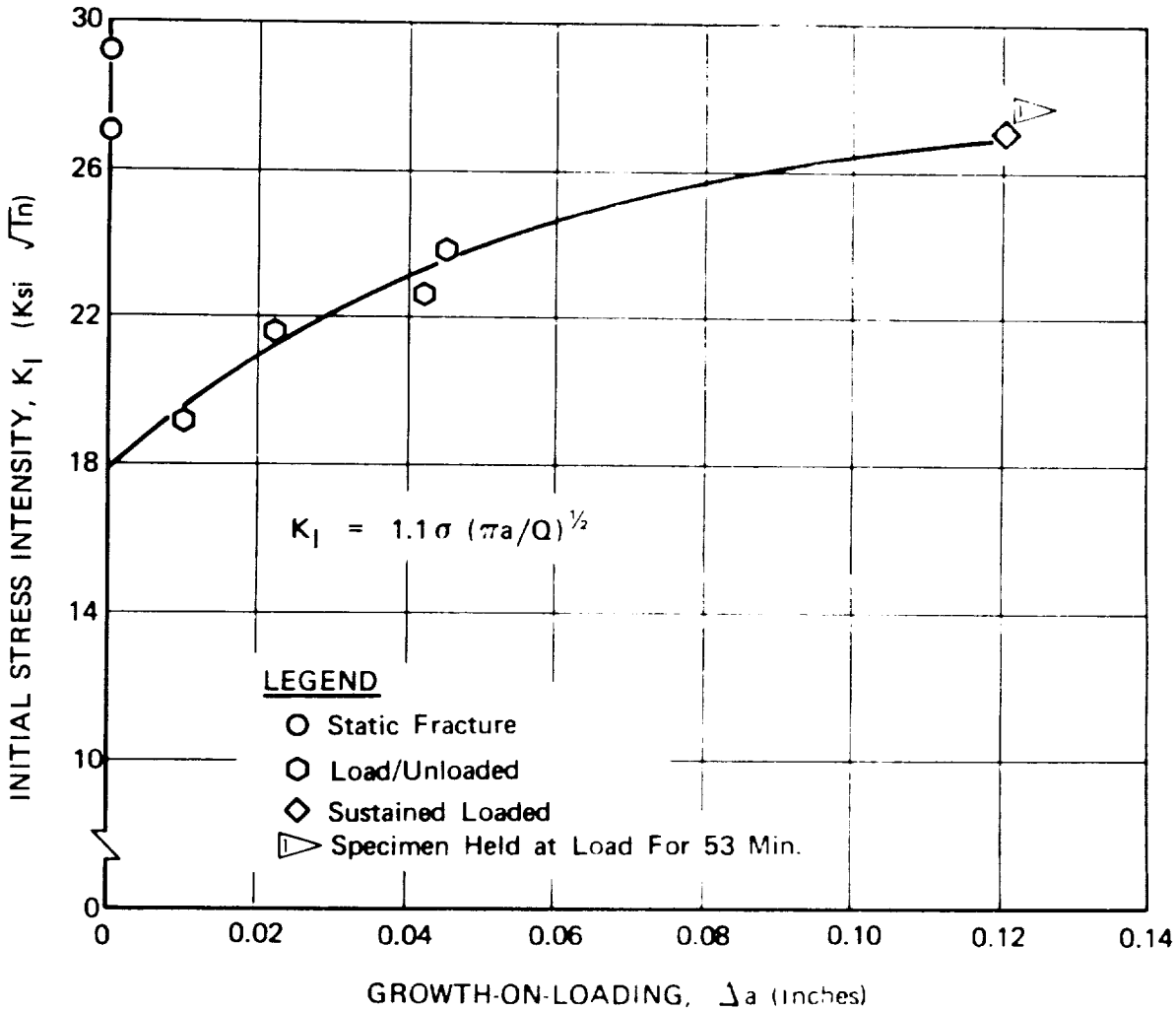

Figure 4: GROWTH-ON-LOADING IN 2219-T87 ALUMINUM WELDMENT IN AIR AT ROOM TEMPERATURE

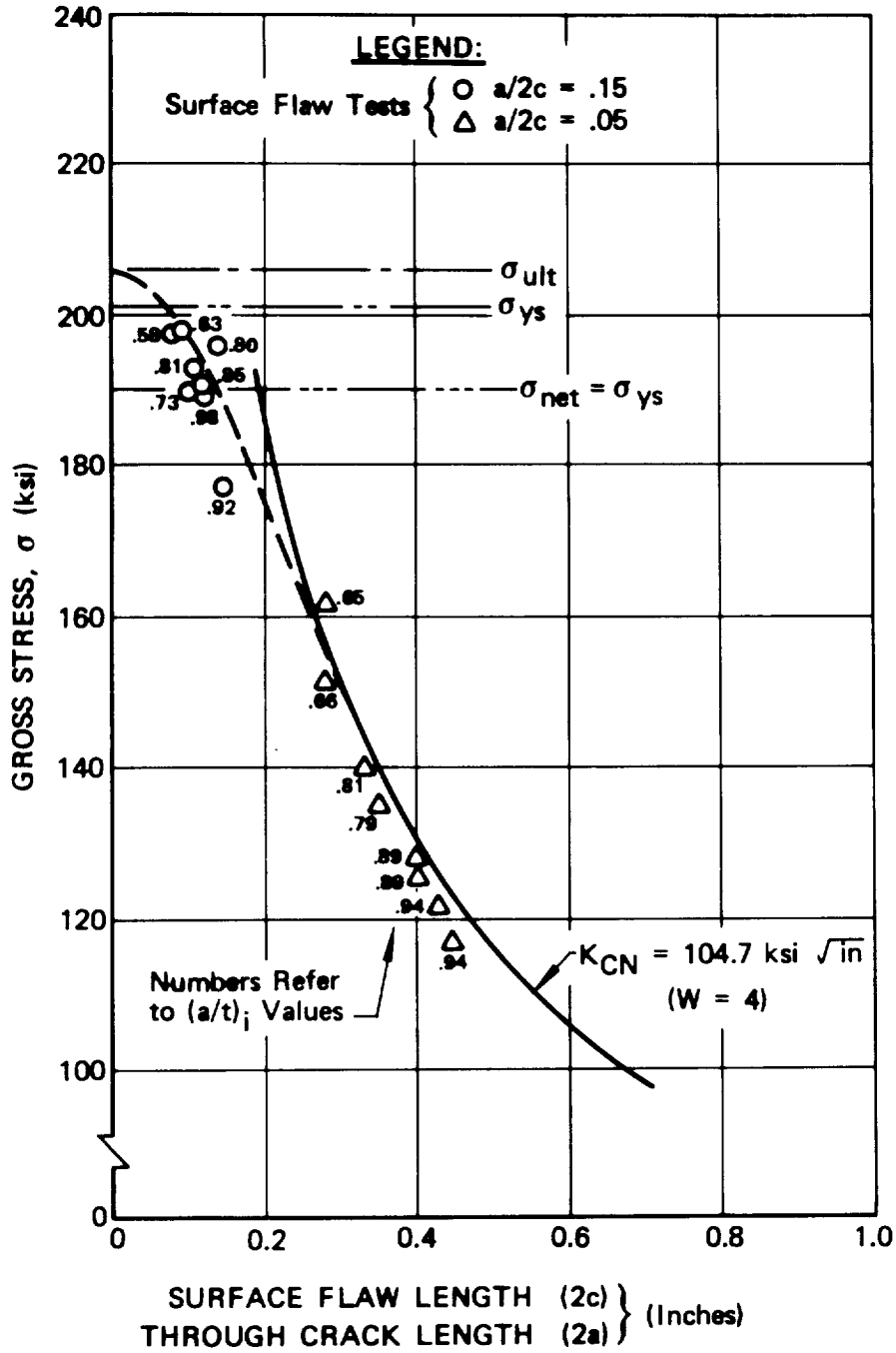

Figure 5: COMPARISON OF SURFACE FLAW & CENTER CRACK DATA
(t = 0.020", 5Al-2.5Sn Titanium Base Metal @ -423 °F)

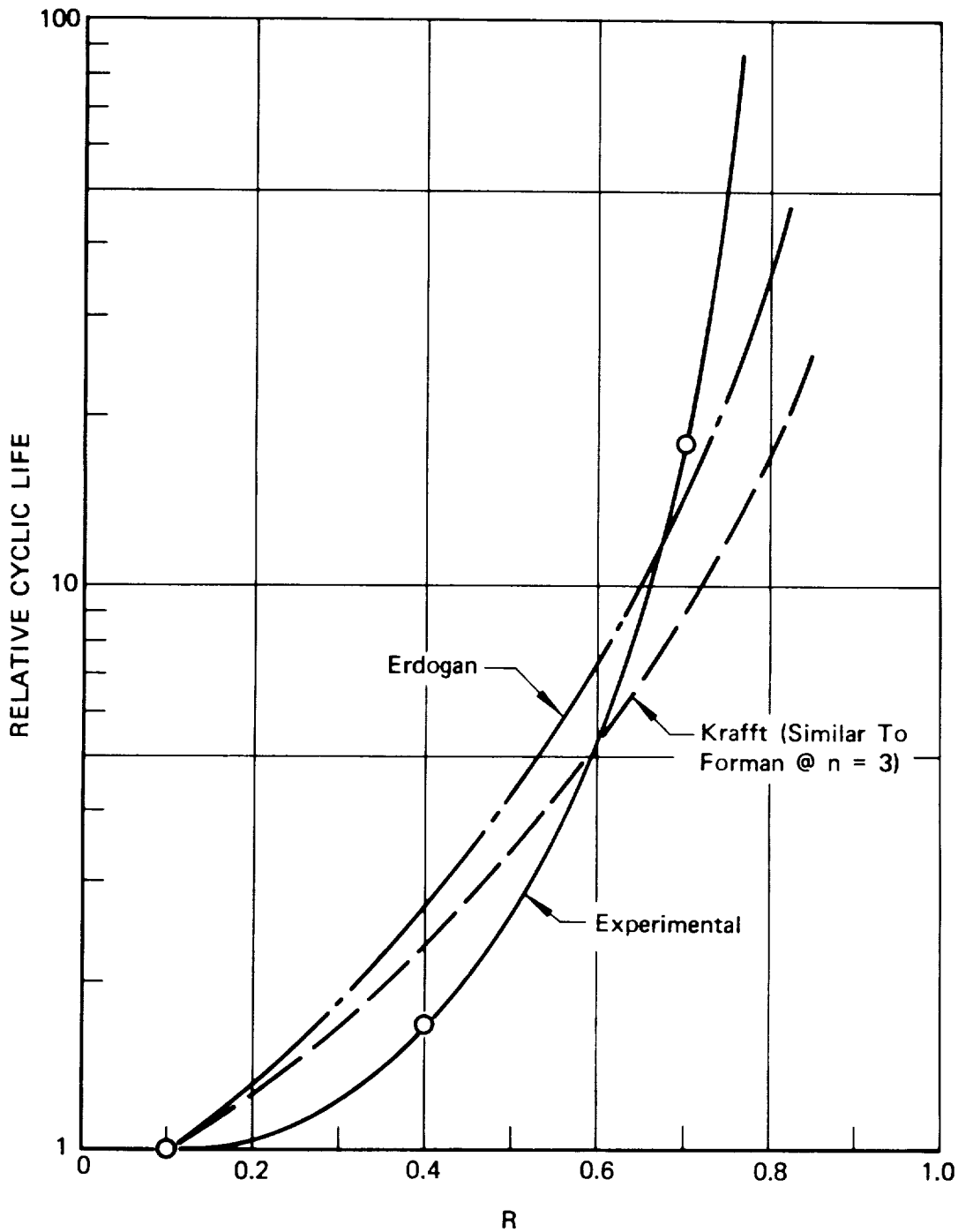

Figure 6: EFFECT OF R VALUE ON CYCLIC LIFE

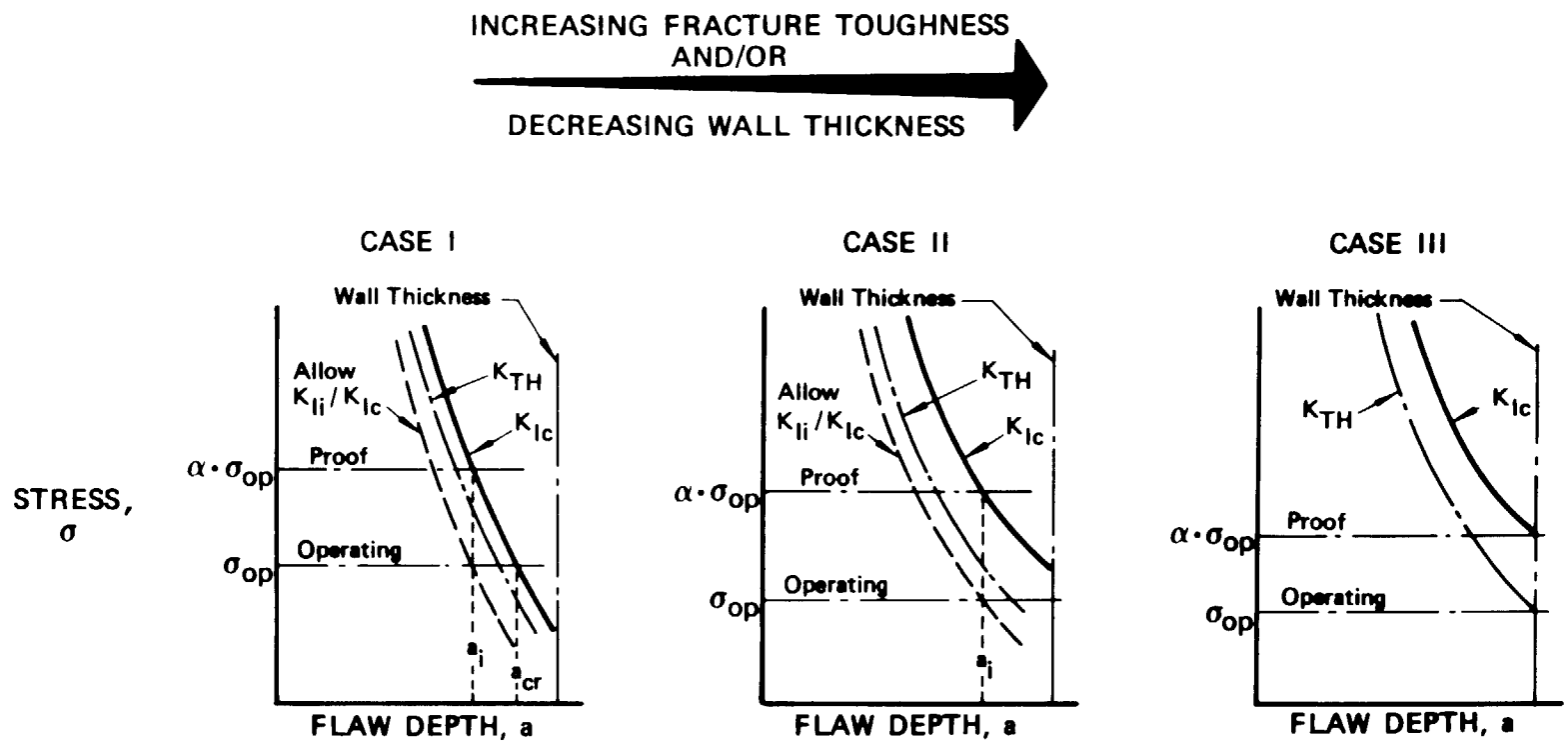

PROBABLE FRACTURE MODE	At Proof	Fracture	Fracture	Leakage
	At Operating	Fracture	Leakage	Leakage

REQUIRED MIN. PROOF TEST FACTOR

$$\alpha = \frac{1}{\text{Allow } K_{Ii}/K_{Ic}} \qquad \alpha = \frac{1}{\text{Allow } K_{Ii}/K_{Ic}} \qquad \alpha = \frac{1}{K_{TH}/K_{Ic}}$$

Figure 7: THE EFFECT OF WALL THICKNESS ON THE VALUE OF THE PROOF TEST

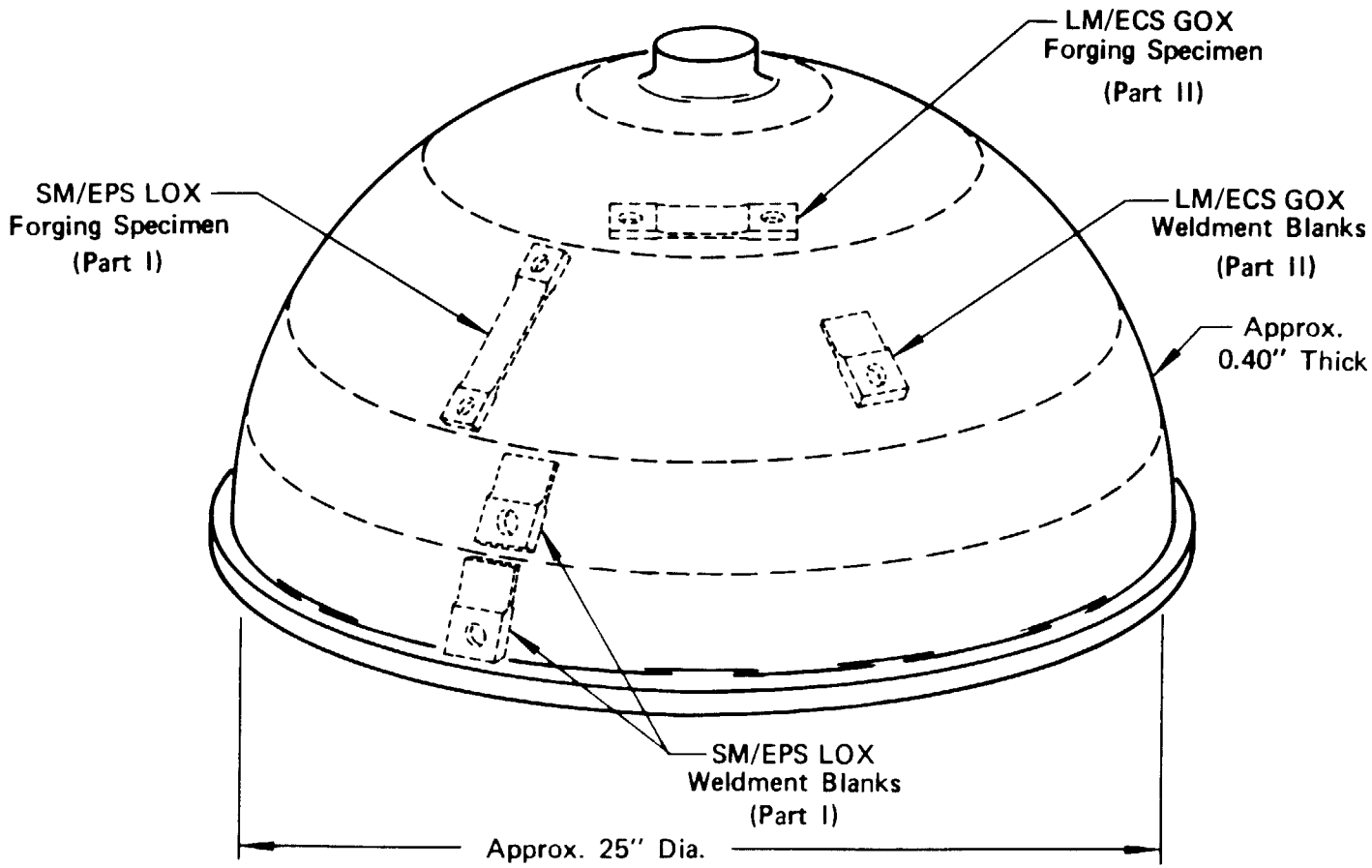

Figure 8: HEMISPHERICAL SM/EPS LOX TANK FORGING

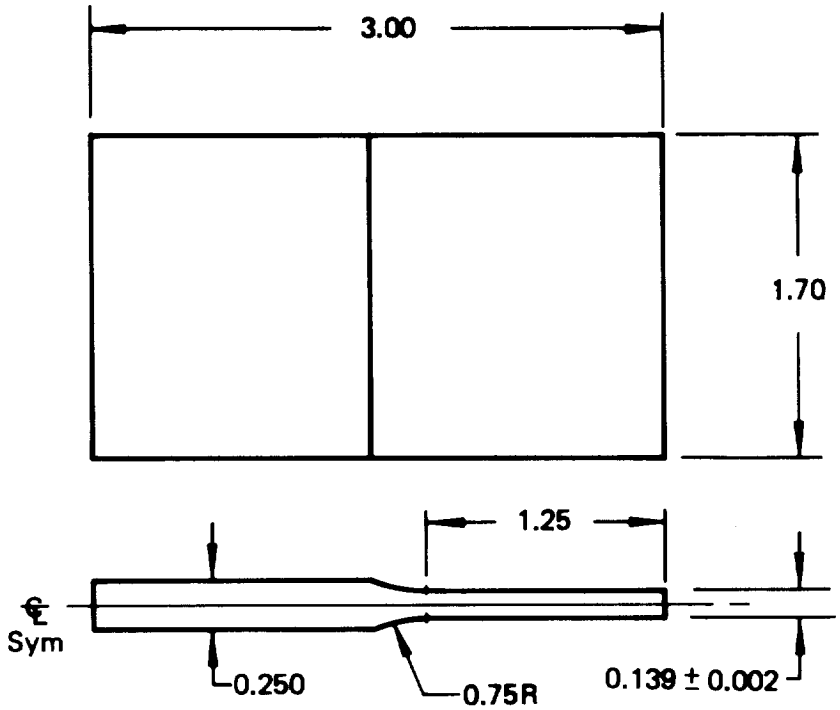

Figure 9a: WELD BLANK (PART I)

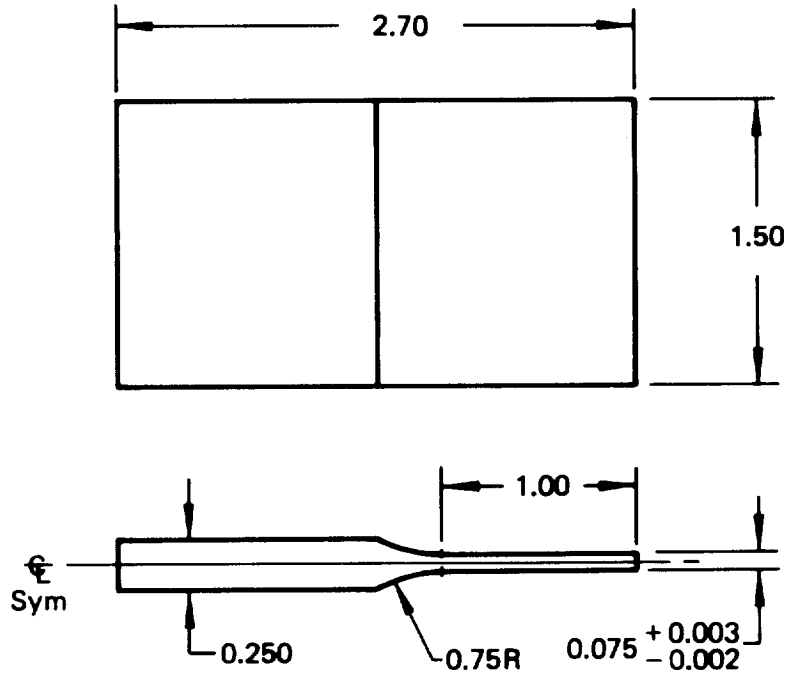

Figure 9b: WELD BLANK (PART II)

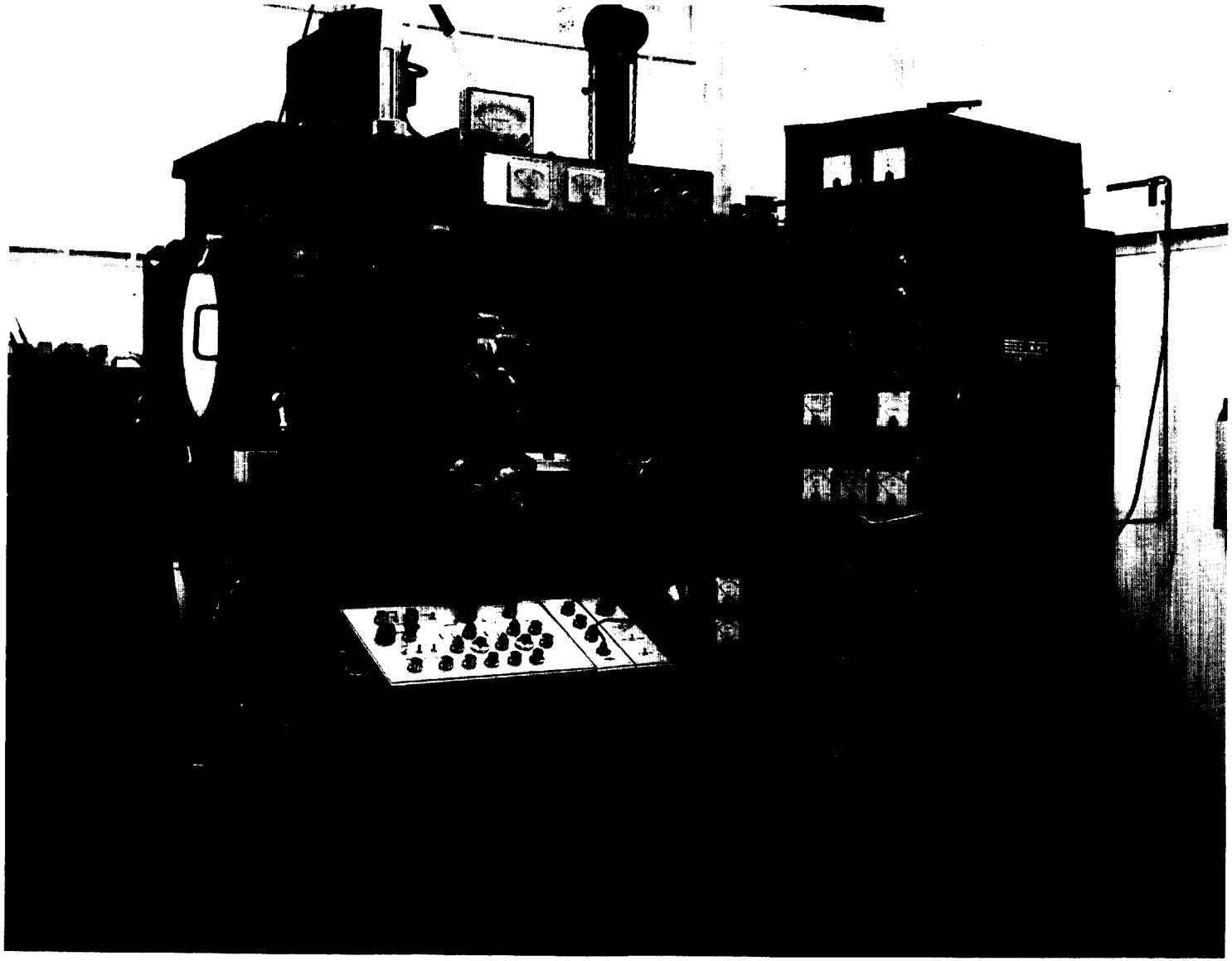

Figure 10: 60 KV SCIAKY ELECTRON BEAM WELDING FACILITY

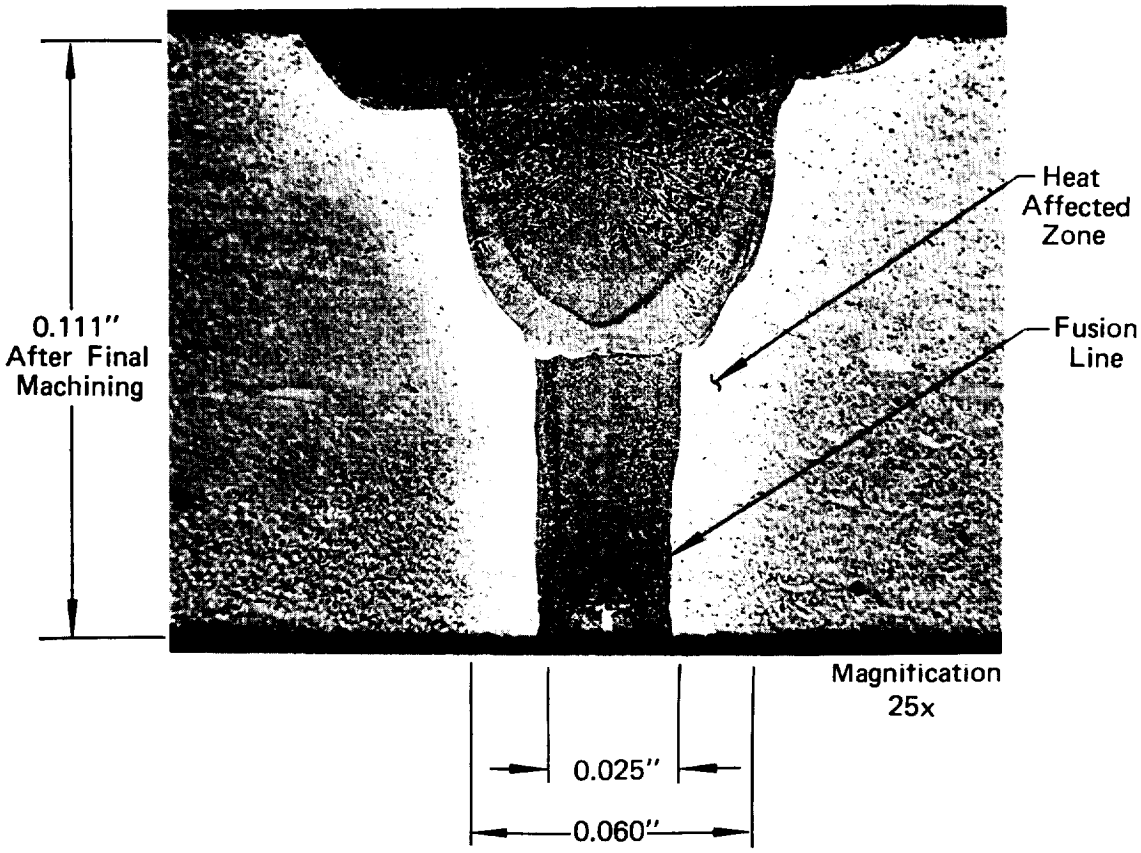

ELECTRON BEAM PASS	WELD DESCRIPTION	VOLTAGE (KV)	BEAM CURRENT (MA)	WELDING SPEED (IPM)	WELDING TECHNIQUE
1	Tack	50	10	45	---
2	Penetration	50	30	45	---
3	Partial Penetration	50	13	45	60 Cycle Circle Generator
4	Cover	50	12	45	3000 Cycle y Axis Oscillation

Figure 11: SM/EPS LOX TANK WELD SIMULATION (PART I)

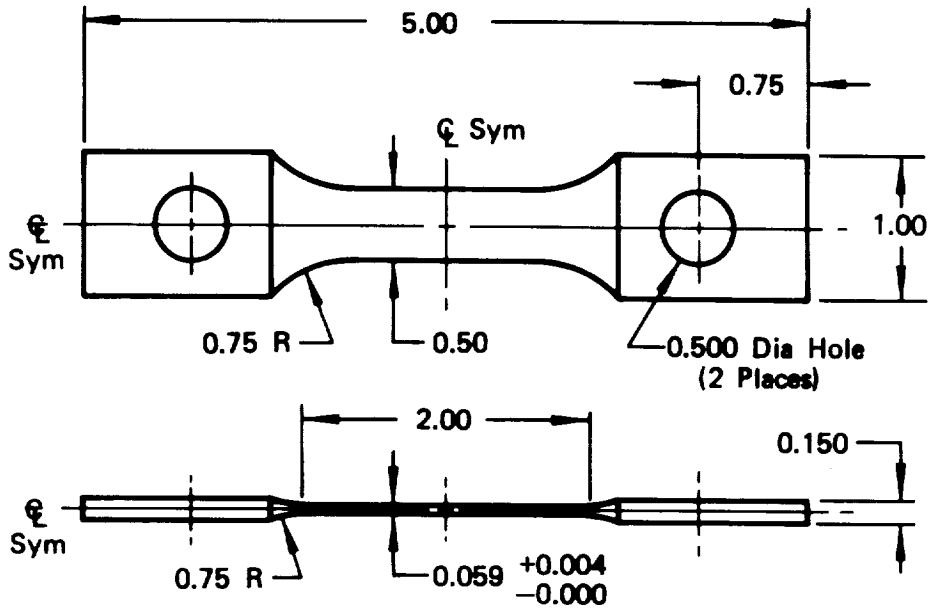

Figure 12a: FORGING TENSILE SPECIMEN (PART I)

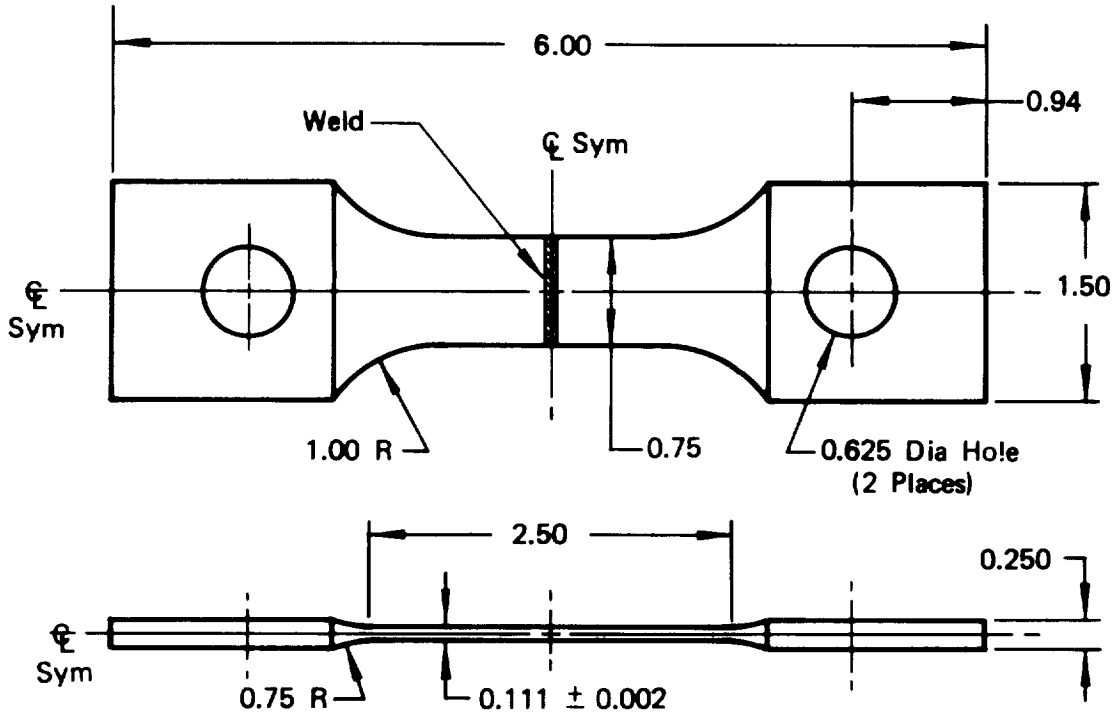

Figure 12b: WELDMENT TENSILE SPECIMEN (PART I)

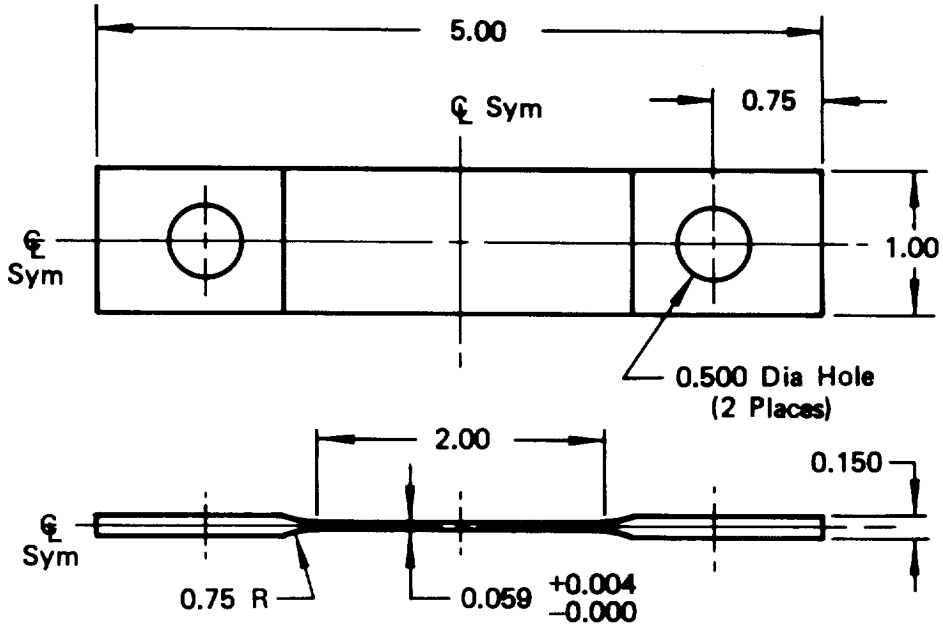

Figure 13a: FORGING FRACTURE SPECIMEN (PART I)

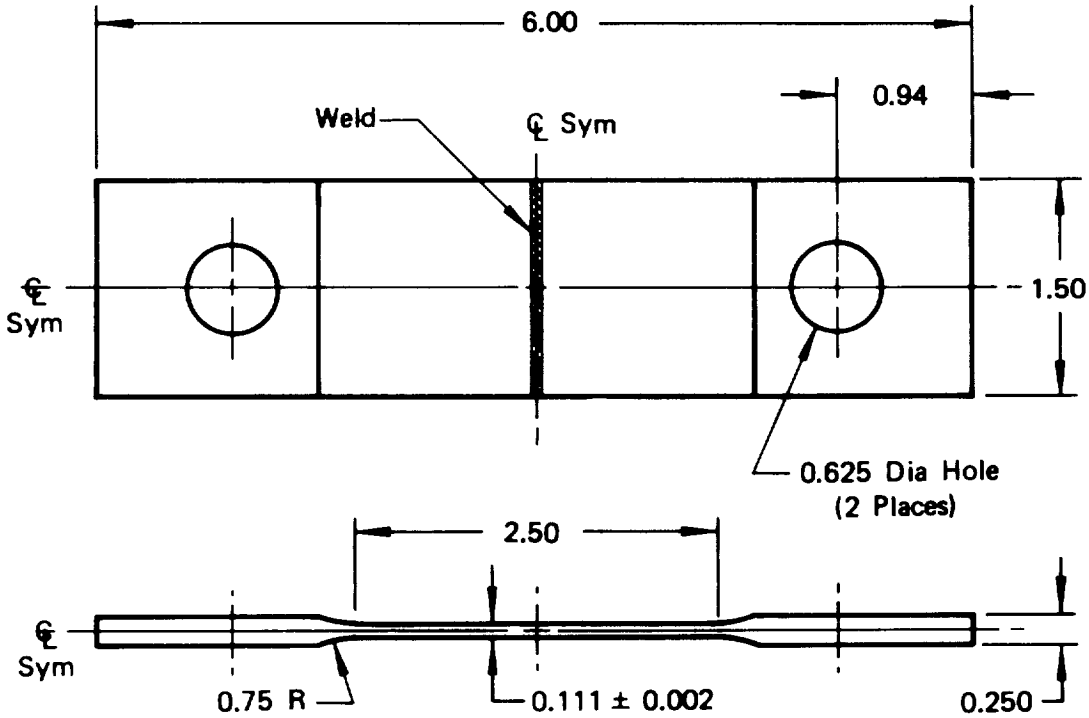

Figure 13b: WELDMENT FRACTURE SPECIMEN (PART I)

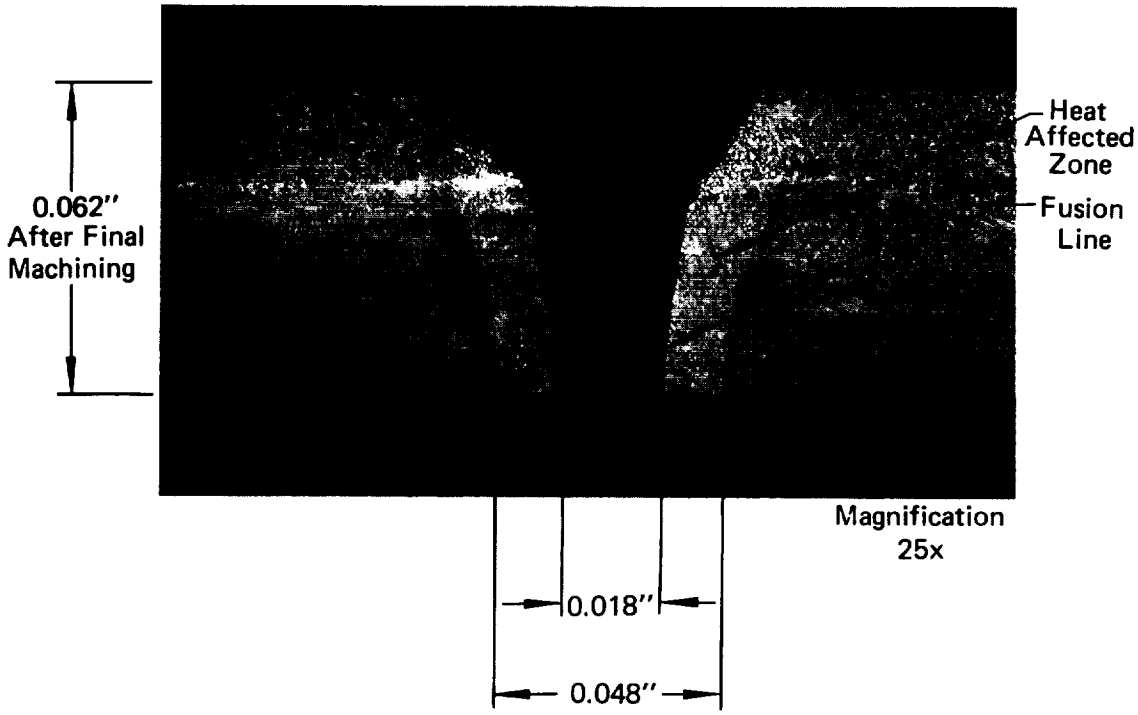

ELECTRON BEAM PASS	WELD DESCRIPTION	VOLTAGE (KV)	BEAM CURRENT (MA)	WELDING SPEED (IPM)	WELDING TECHNIQUE
1	Tack	50	5	45	---
2	Penetration	50	11	45	---
3	Cover	50	5	35	60 Cycle Circle Generator

Figure 14: LM/ECS GOX TANK WELD SIMULATION (PART II)

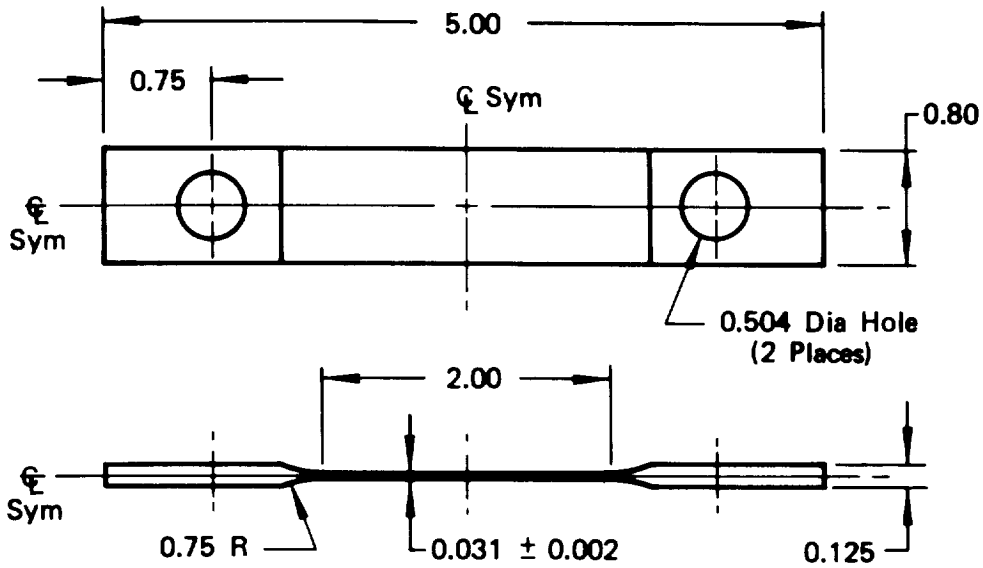

Figure 15a: FORGING TENSILE SPECIMEN (PART II)

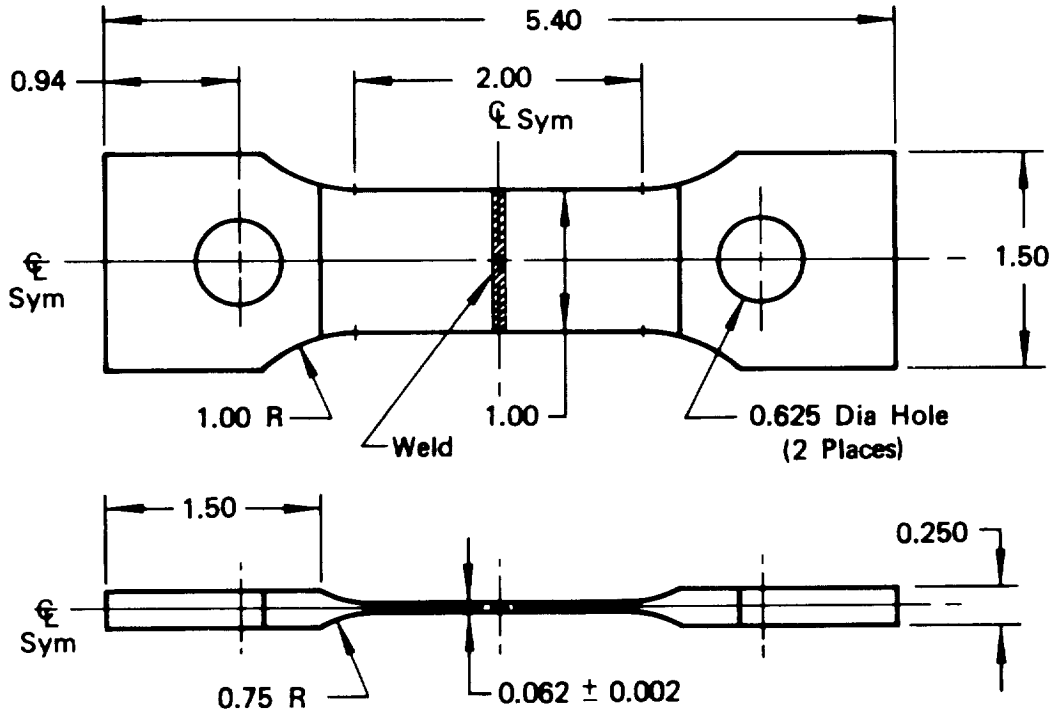

Figure 15b: WELDMENT TENSILE SPECIMEN (PART II)

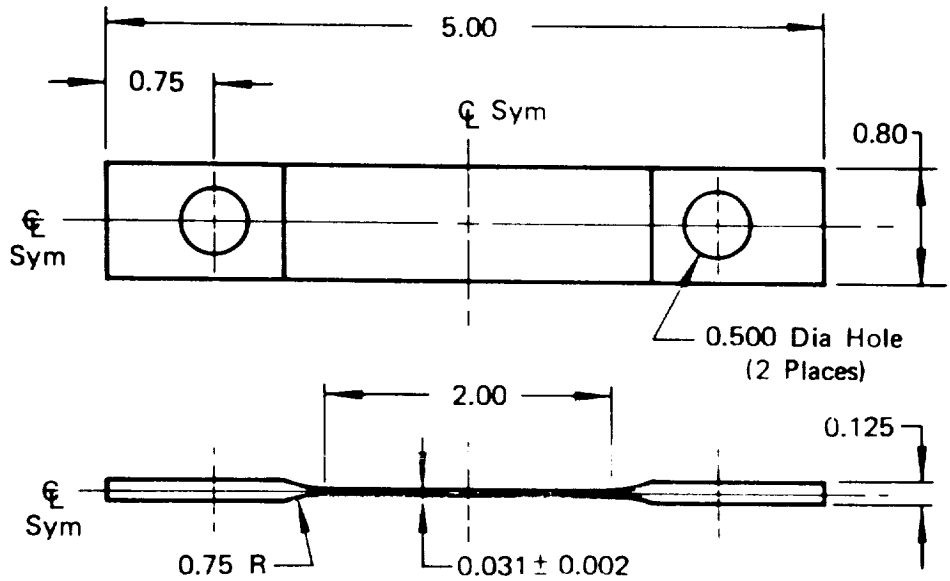

Figure 16a: FORGING FRACTURE SPECIMEN (PART II)

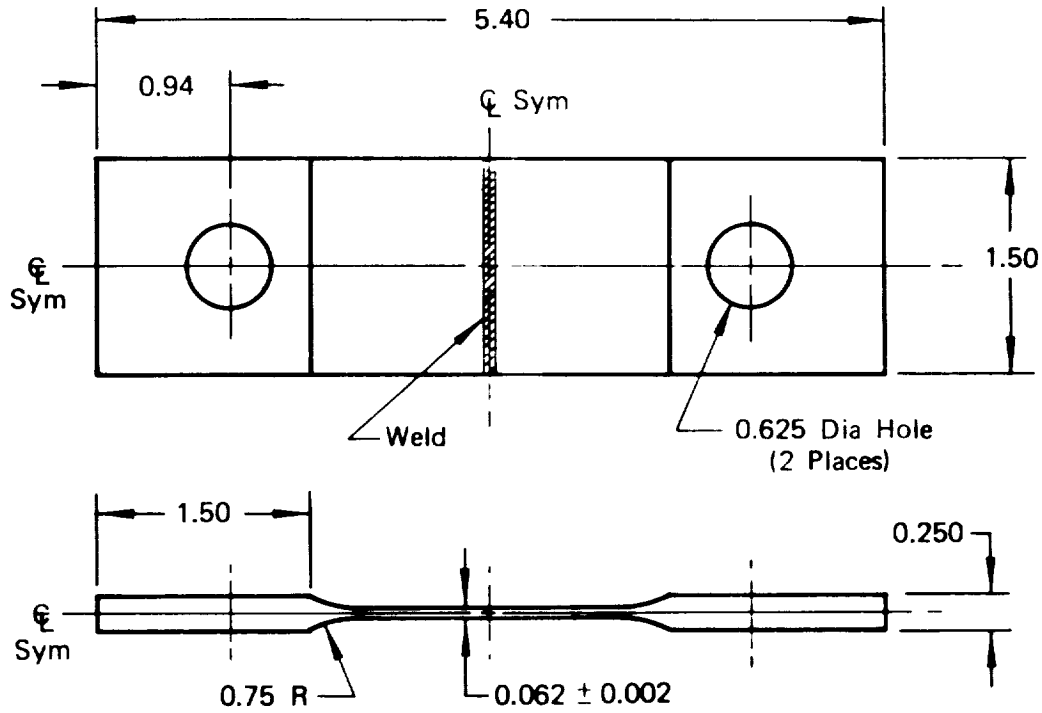

Figure 16b: WELDMENT FRACTURE SPECIMEN (PART II)

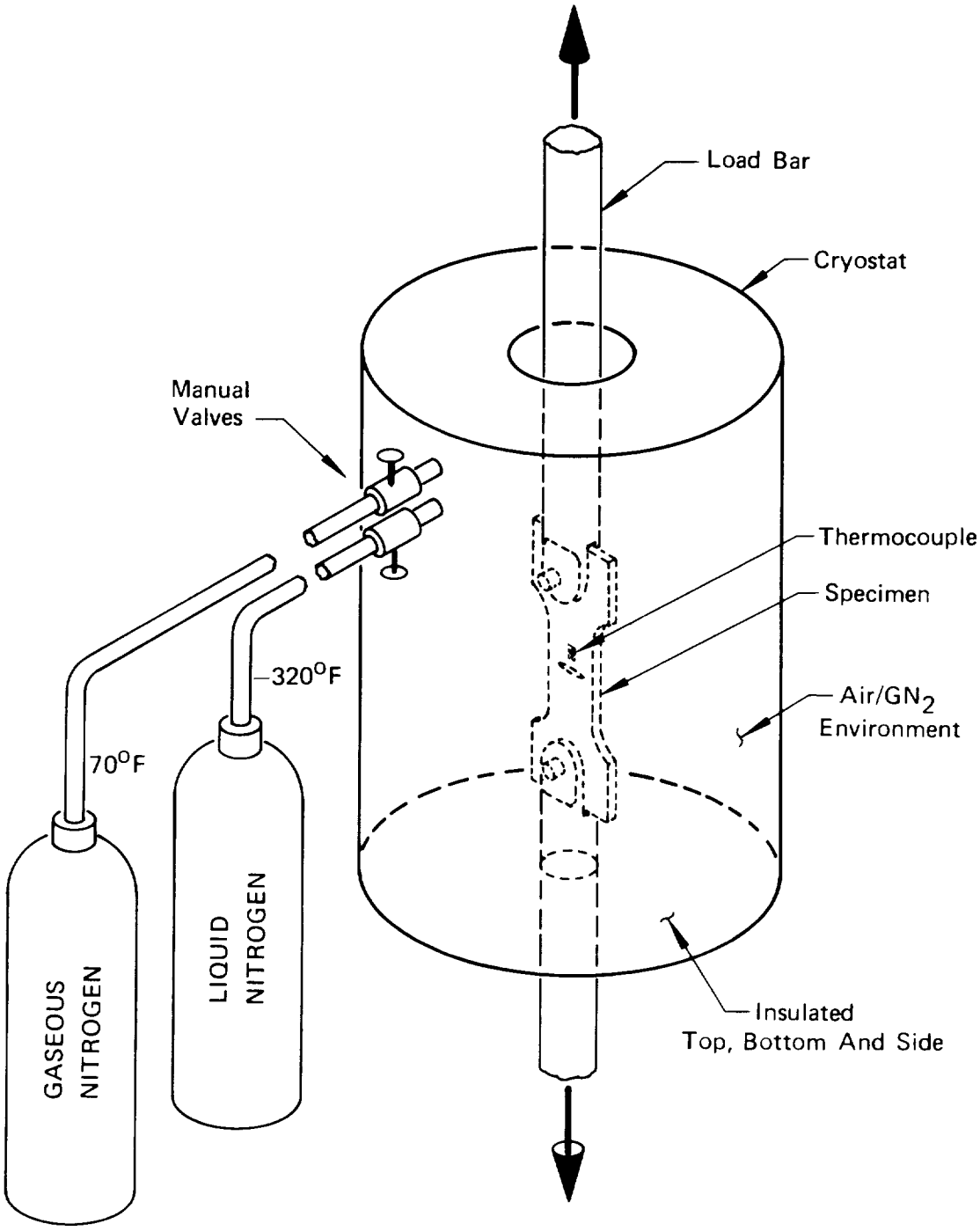

Figure 17: ENVIRONMENTAL TEMPERATURE CONTROL SYSTEM FOR NON–HAZARDOUS TESTS

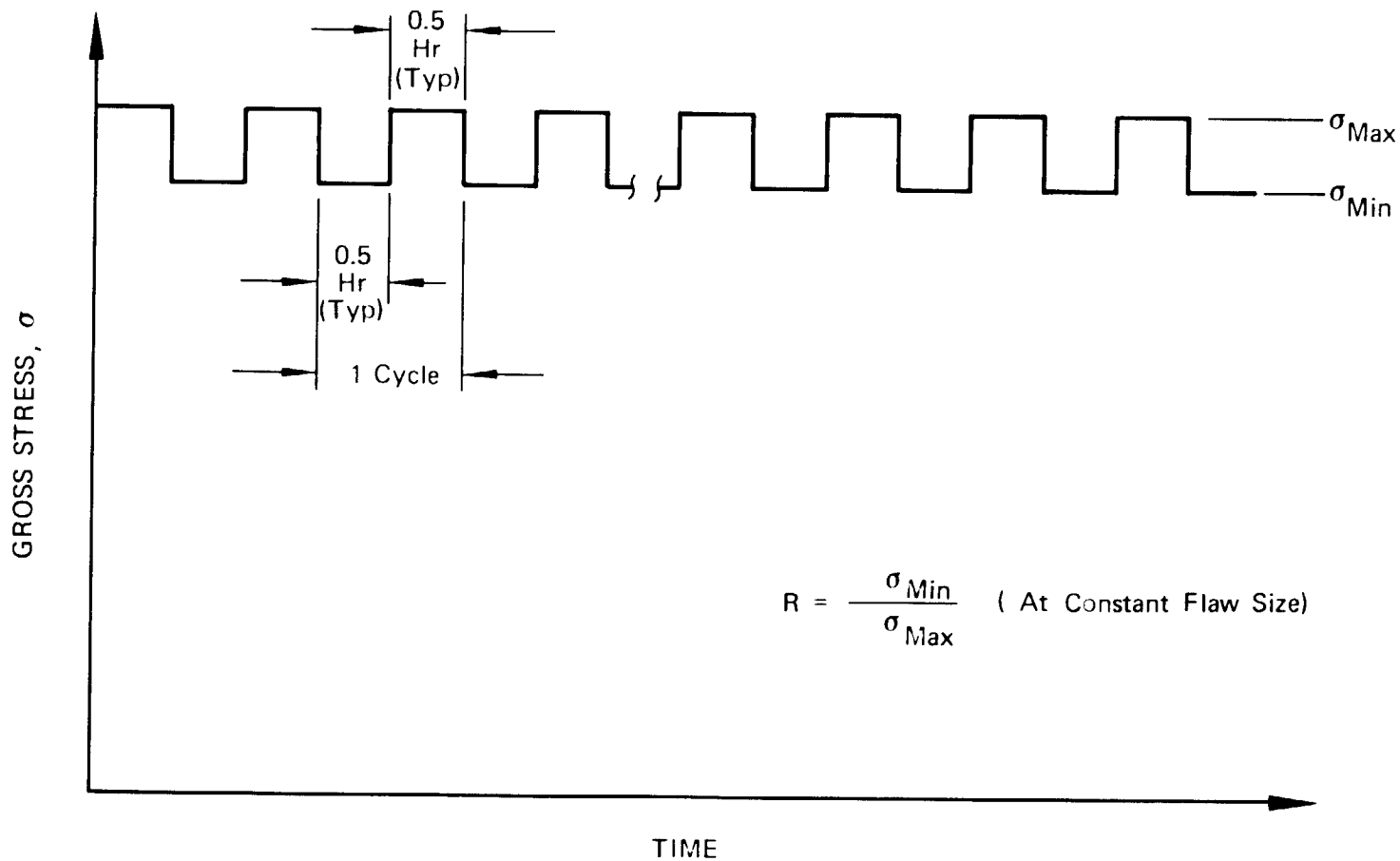

Figure 18: CYCLIC LOAD PROFILE FOR SUSTAINED/CYCLIC TESTS PERFORMED IN LOX AT −190°F AND 1000 PSI

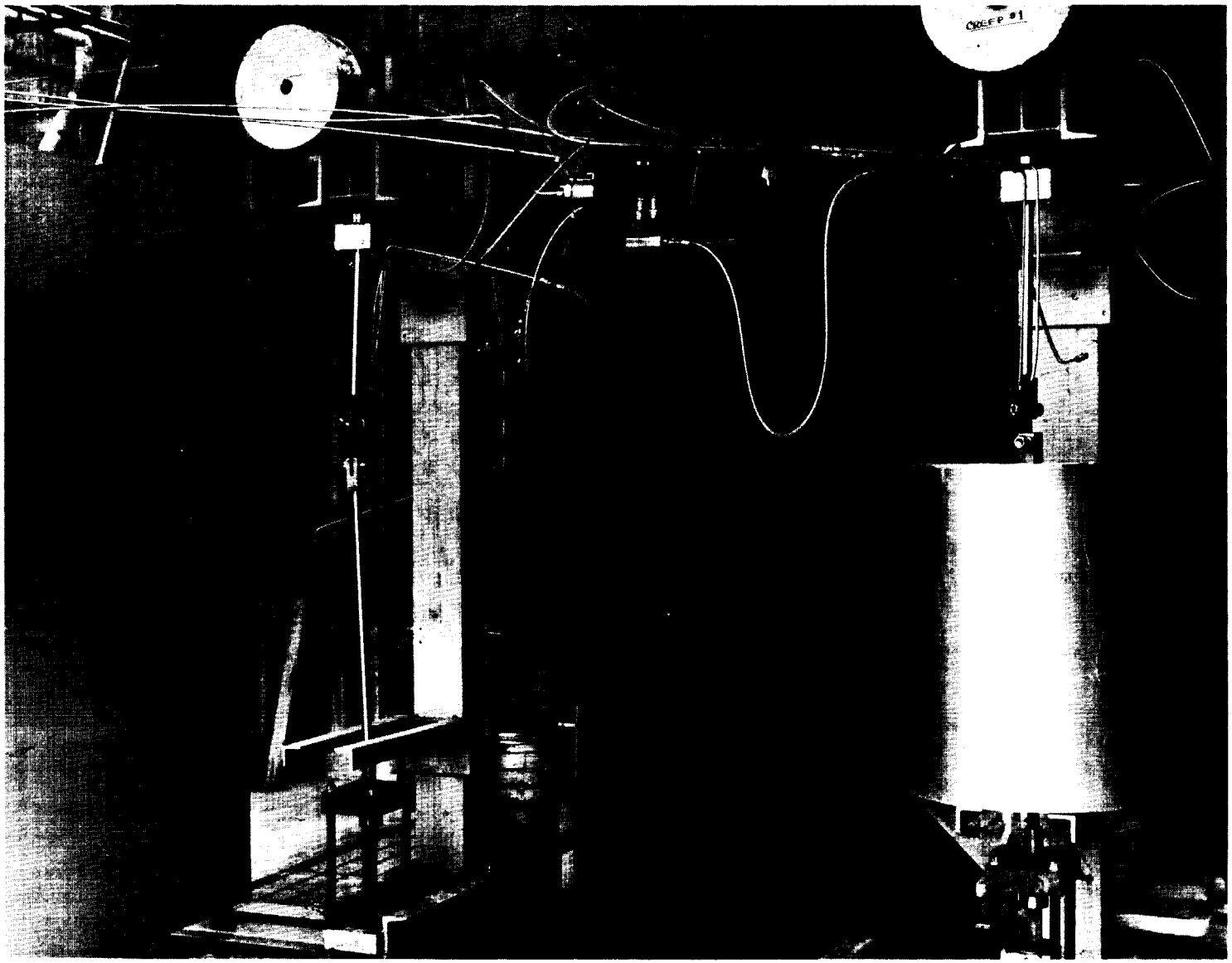

Figure 19: OVERALL VIEW OF DEAD LOAD TEST SETUP FOR HAZARDOUS TESTING

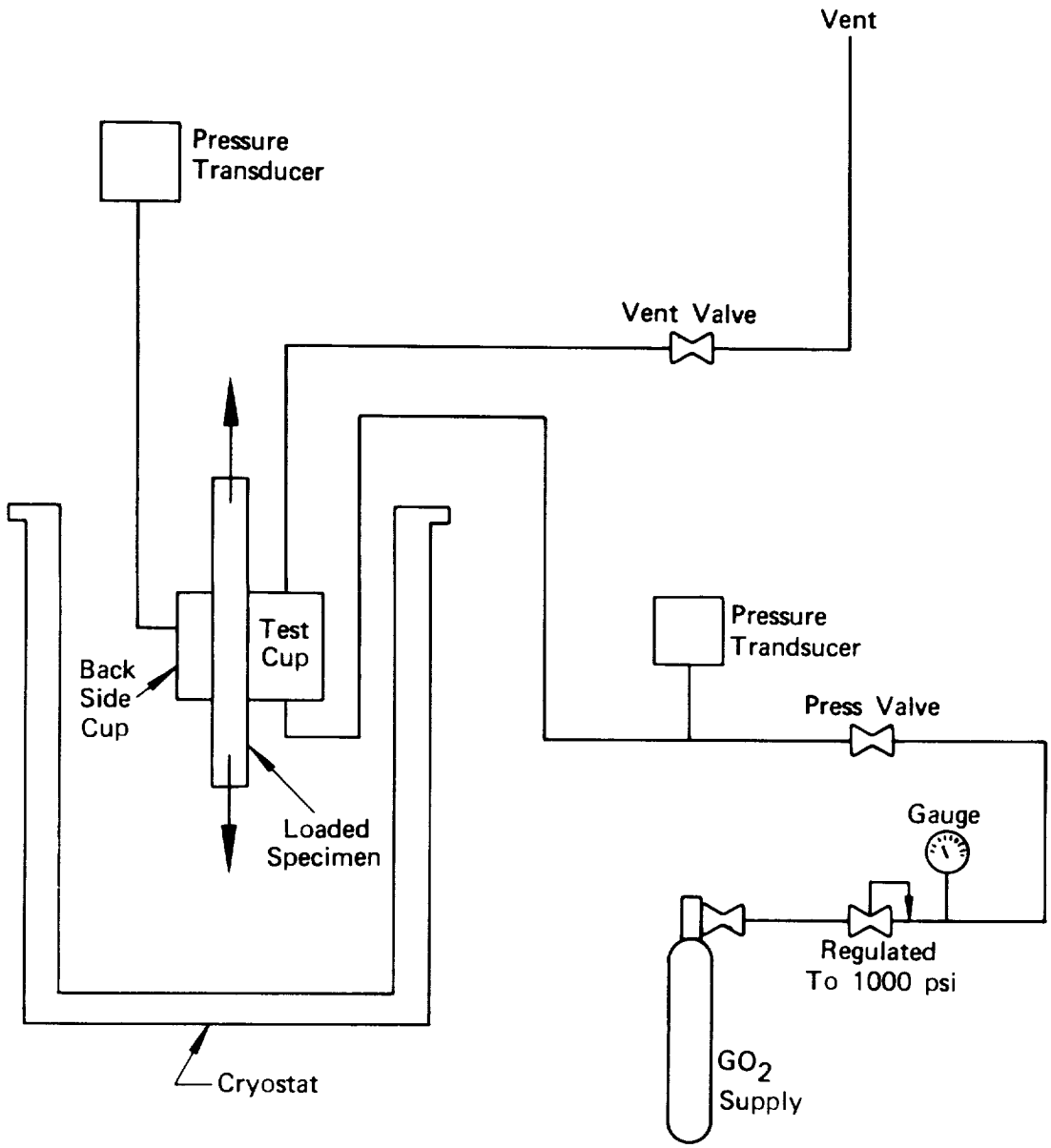

Figure 20: SCHEMATIC OF OXYGEN SYSTEM FOR PARTS I AND II TESTING

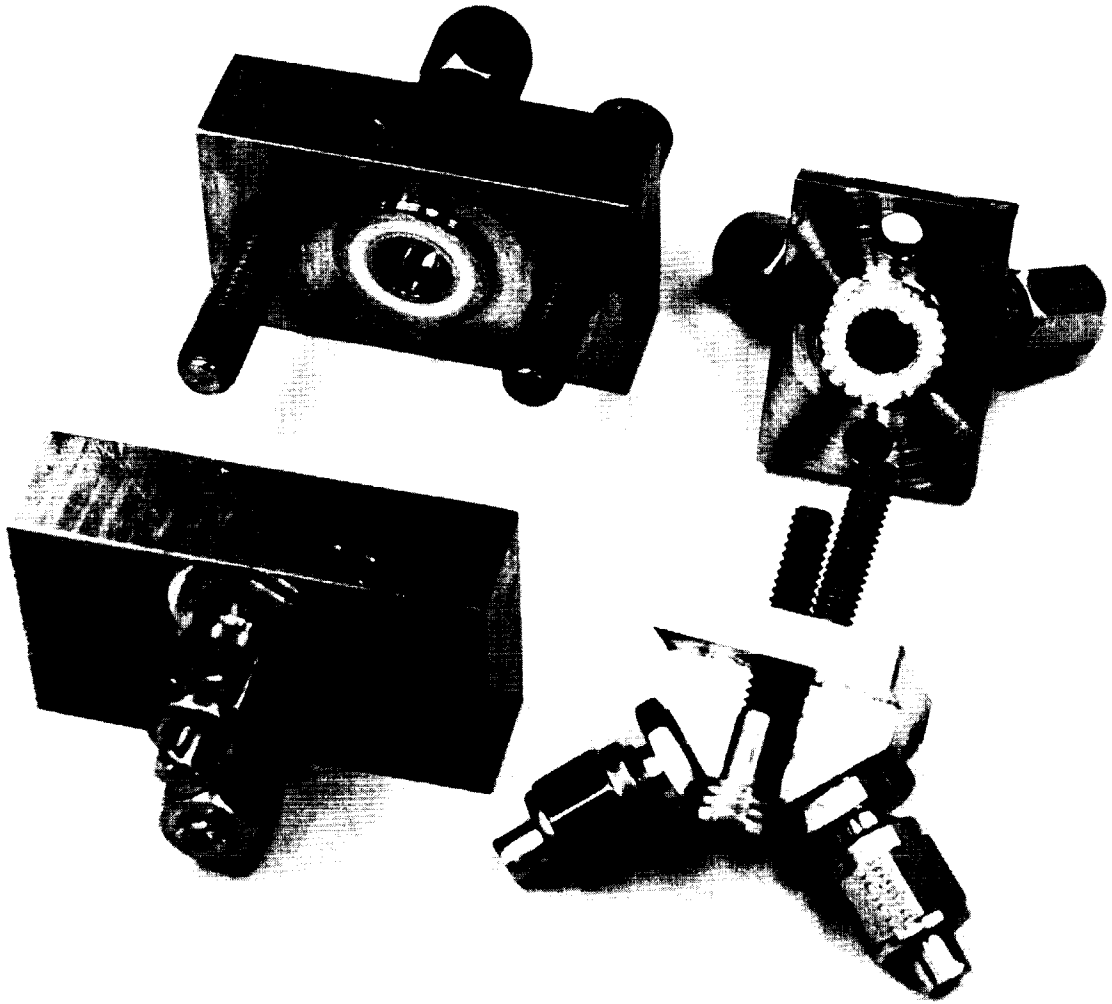

Figure 21: SPECIMEN MOUNTING PRESSURE CUPS

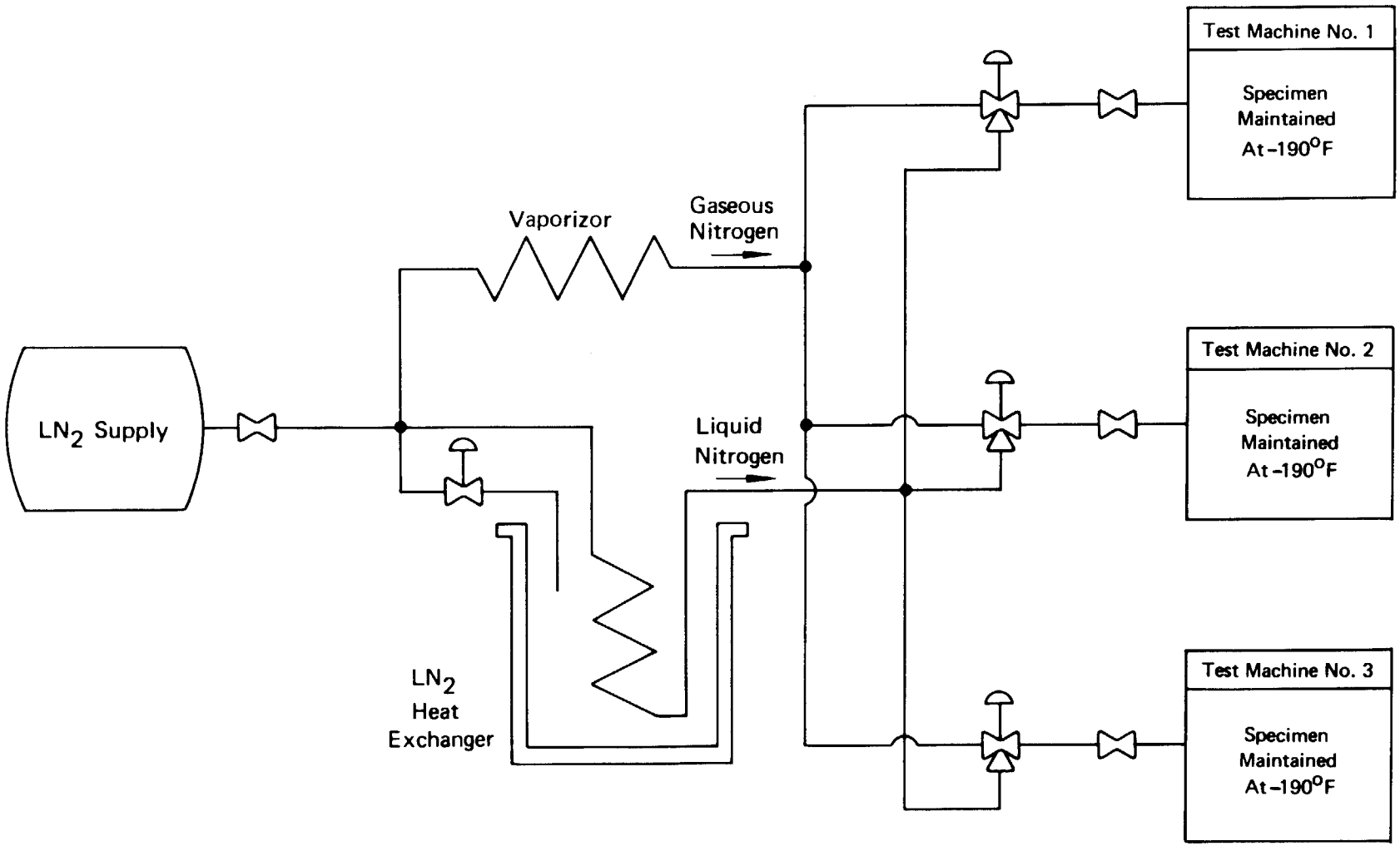

Figure 22: TEMPERATURE CONDITIONING SYSTEM FOR HAZARDOUS TESTING (PART I)

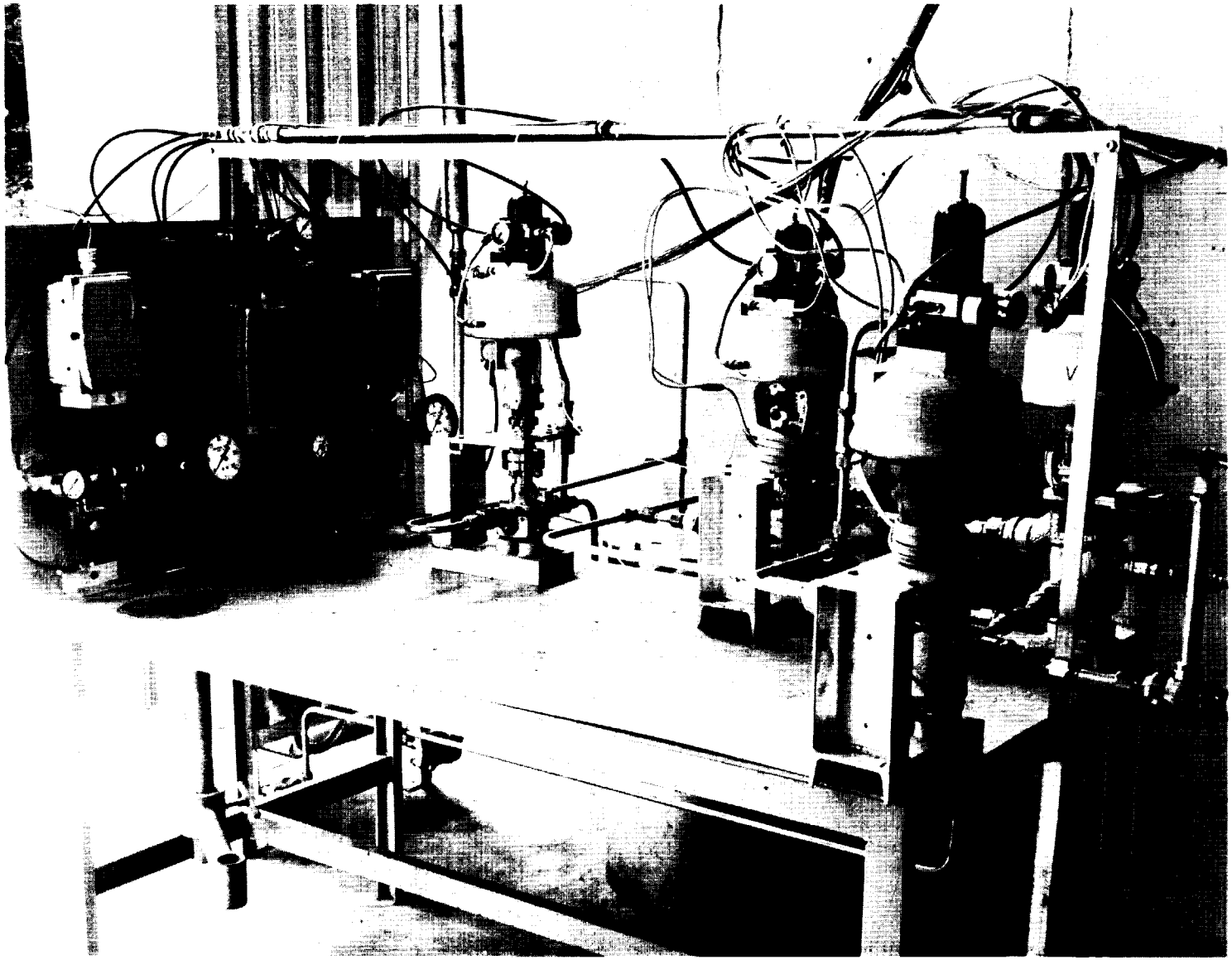

Figure 23: THREE WAY CONTROL VALVES FOR TEMPERATURE CONDITIONING SYSTEM – HAZARDOUS TESTING (PART I)

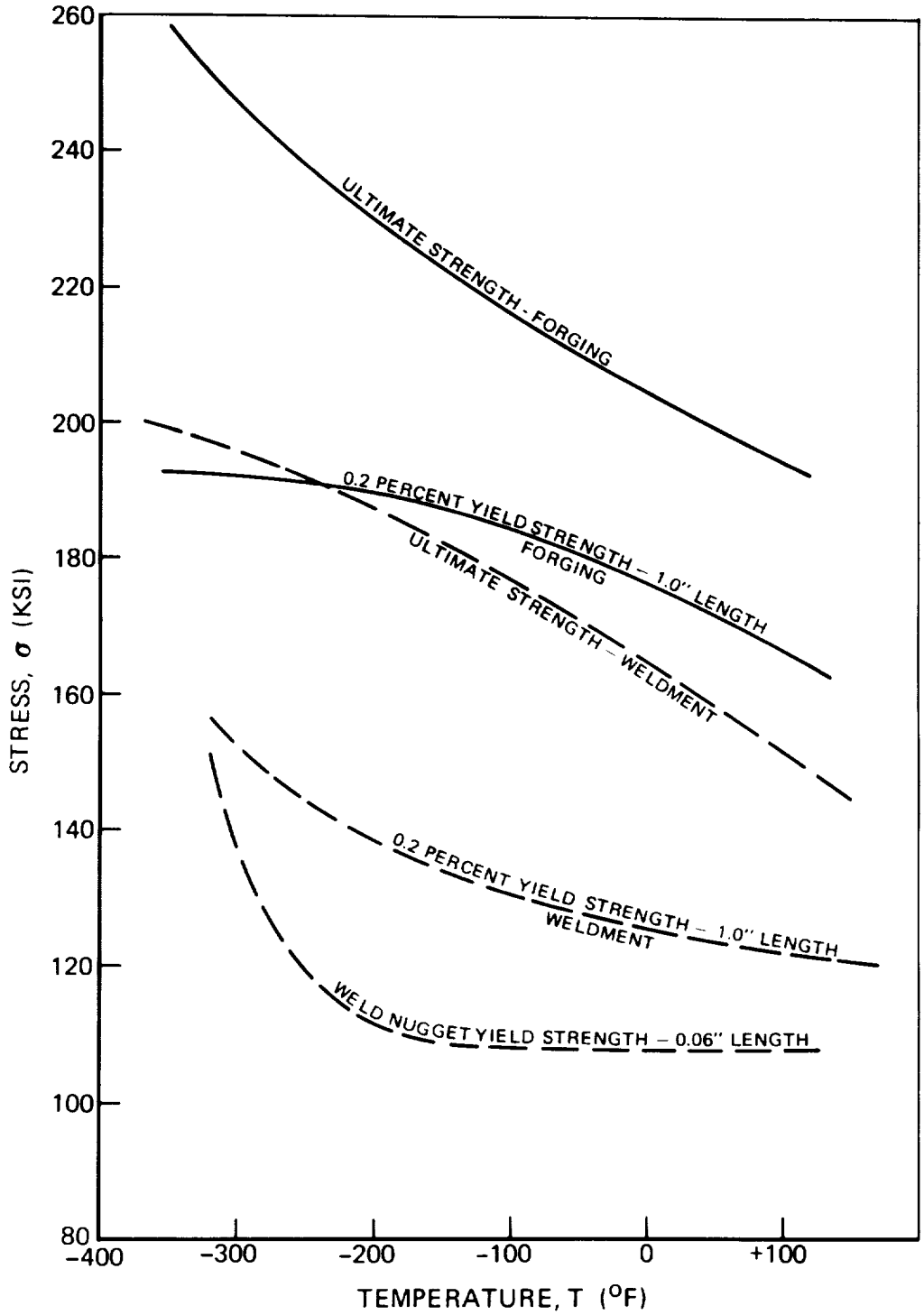

Figure 24: MECHANICAL PROPERTIES OF INCONEL 718 USED IN ASSESSMENT OF SM/EPS LOX TANK (PART I)

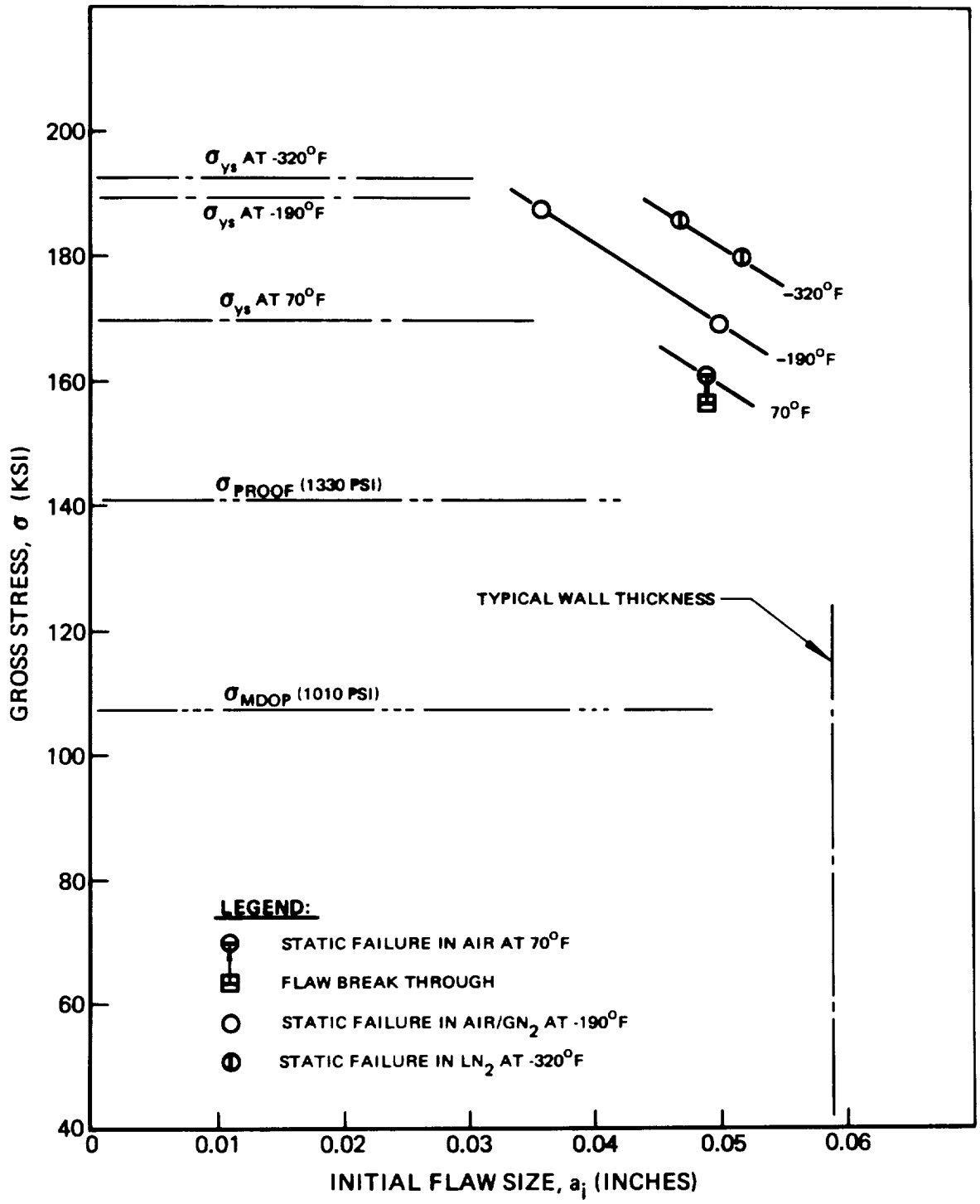

Figure 25: STATIC FRACTURE TESTS OF INCONEL 718 FORGING AT VARIOUS TEMPERATURES (PART I)

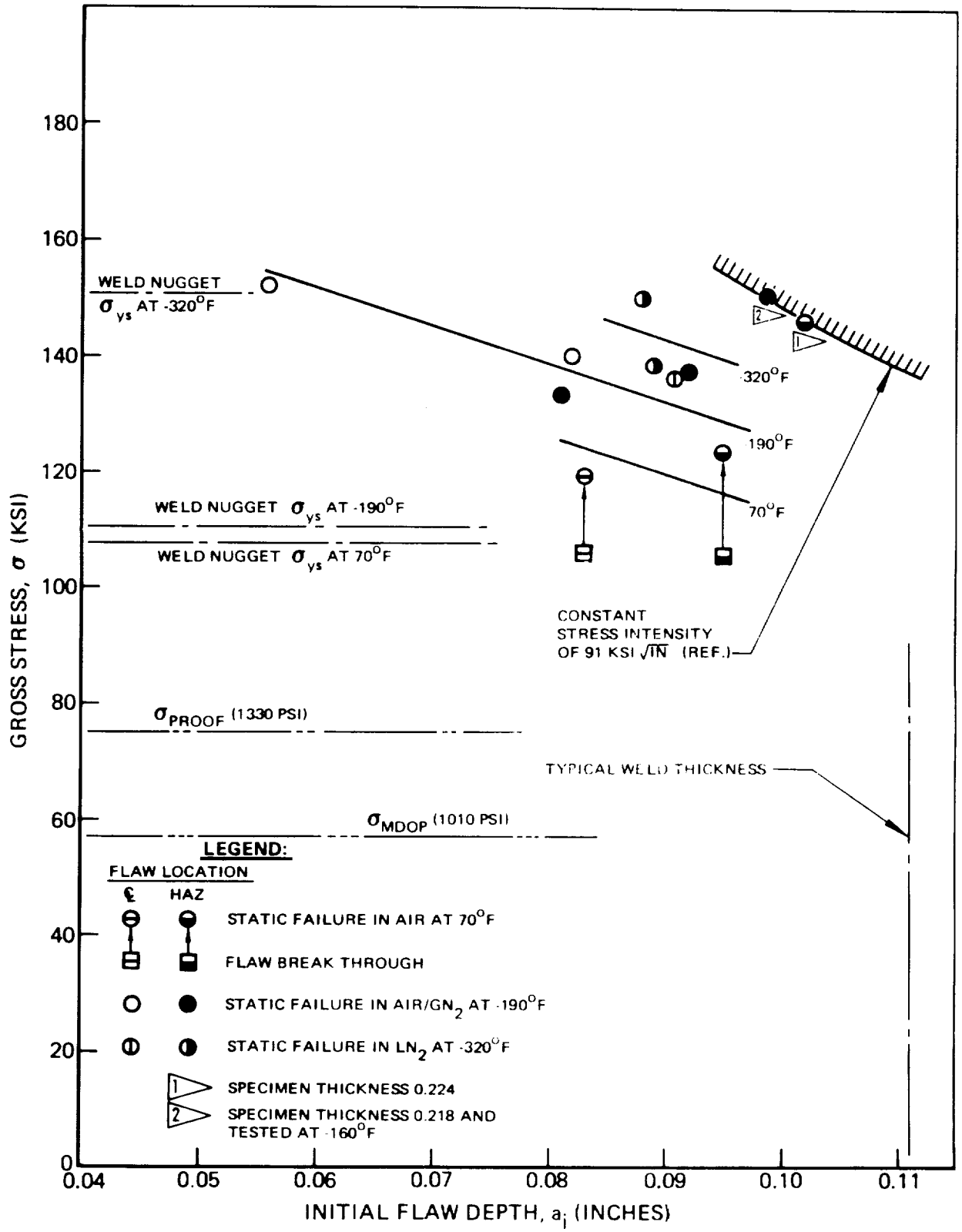

Figure 26: STATIC FRACTURE TESTS OF INCONEL 718 WELDMENT AT VARIOUS TEMPERATURES (PART I)

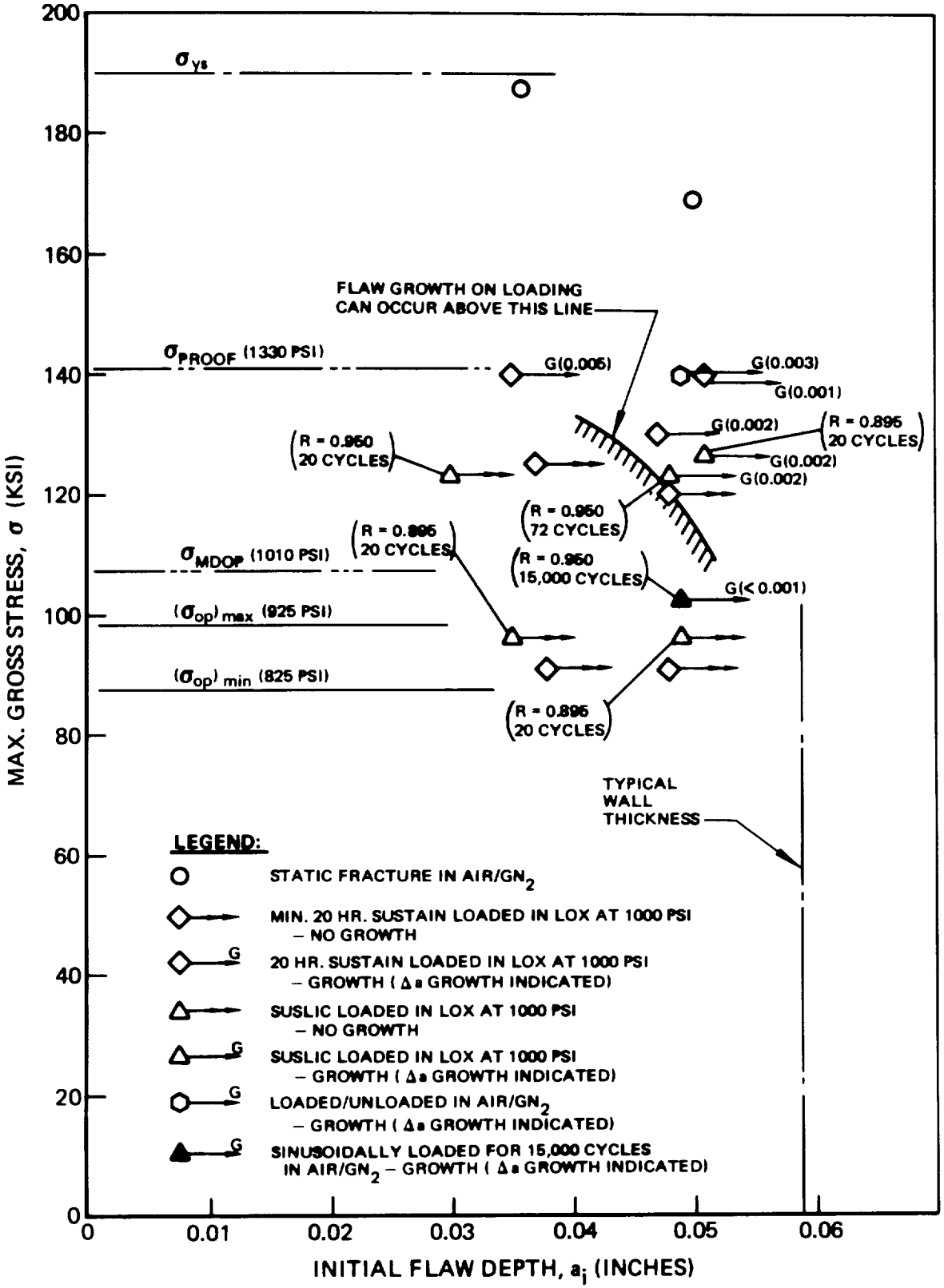

Figure 27: TEST RESULTS OF INCONEL 718 FORGING AT -190°F FOR SM/EPS LOX TANK ASSESSMENT (PART I)

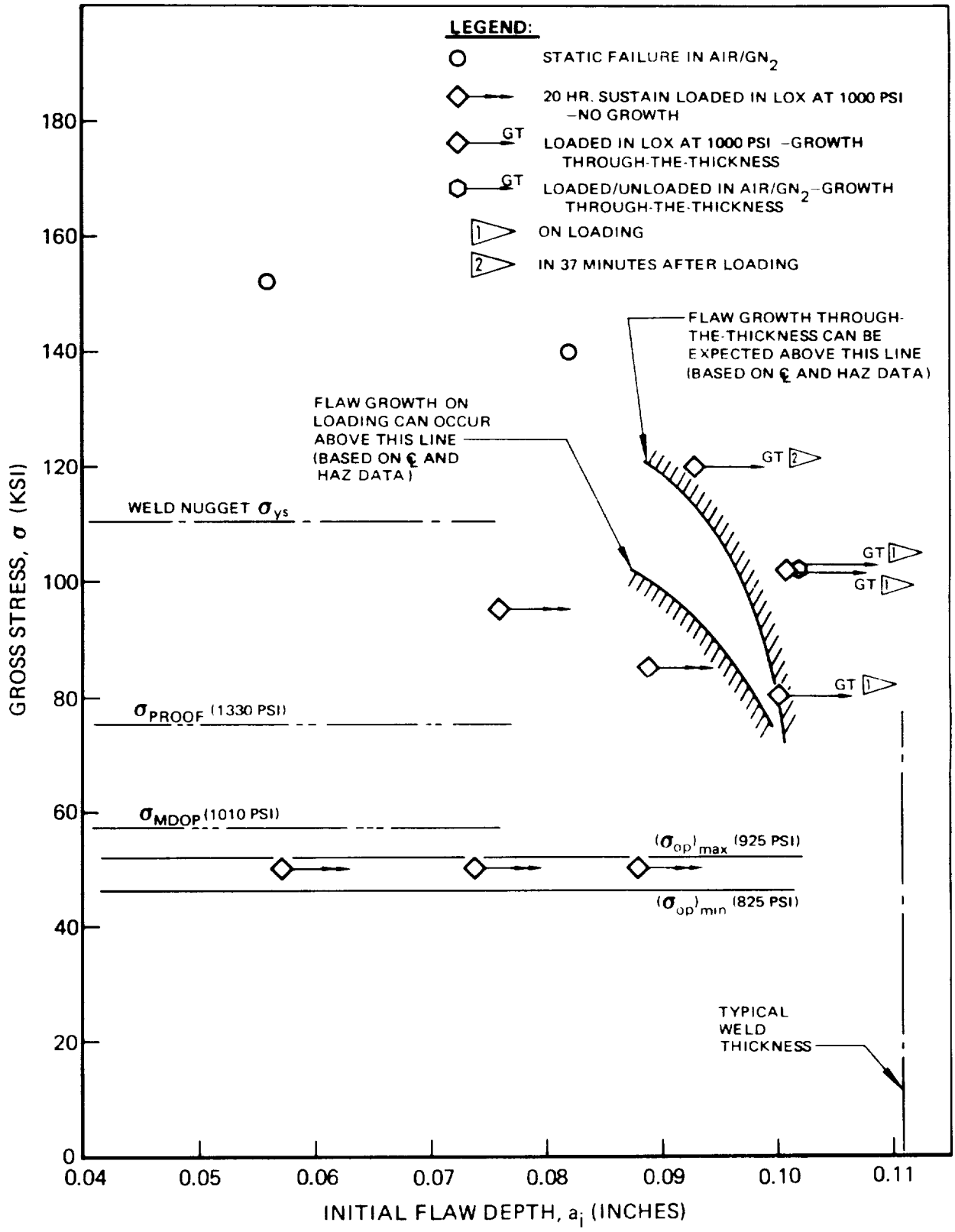

Figure 28: TEST RESULTS OF INCONEL 718 WELDMENT AT -190°F FOR SM/EPS LOX TANK ASSESSMENT– FLAWS IN ℄ (PART I)

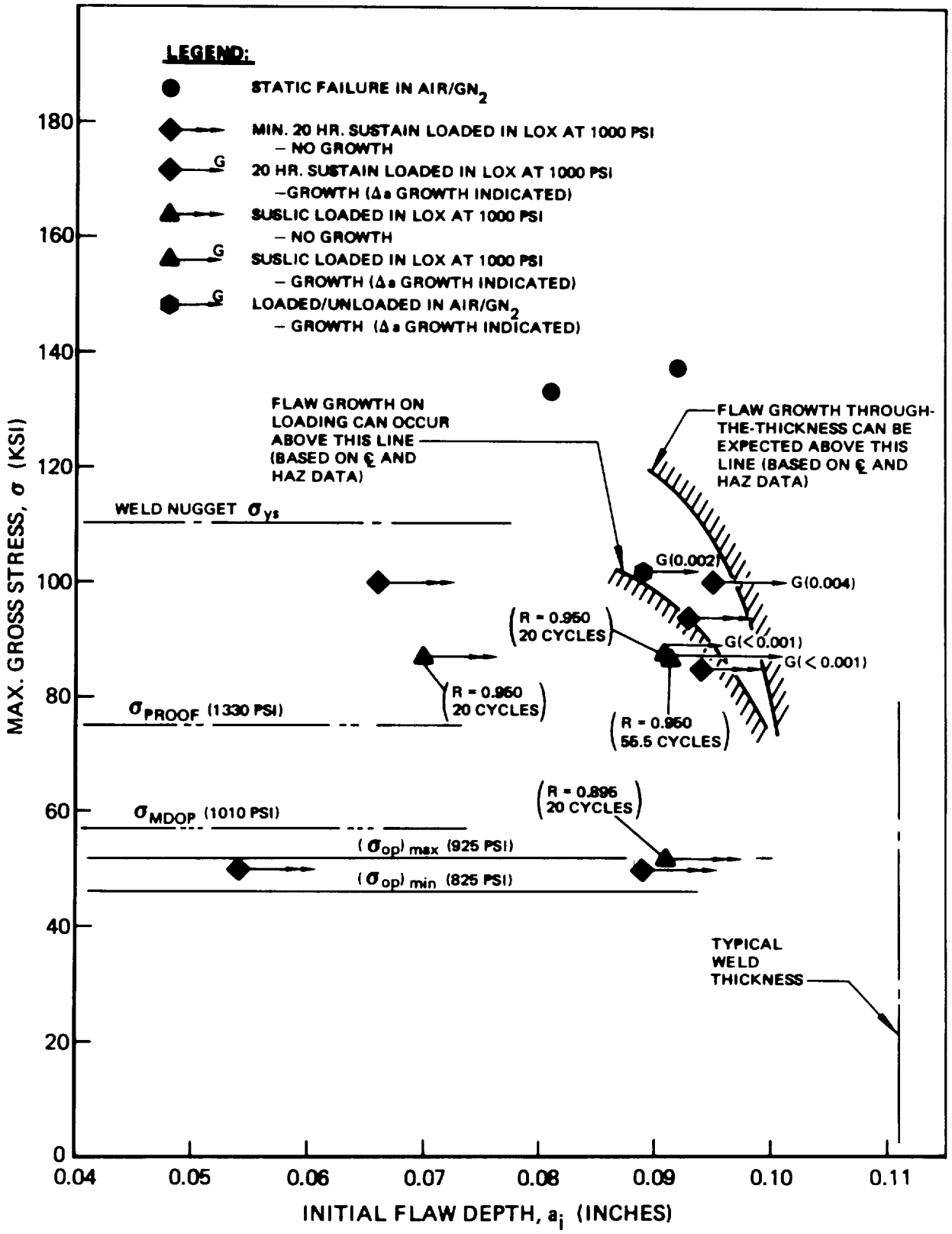

Figure 29: TEST RESULTS OF INCONEL 718 WELDMENT AT -190°F FOR SM/EPS LOX TANK ASSESSMENT – FLAWS IN HAZ (PART I)

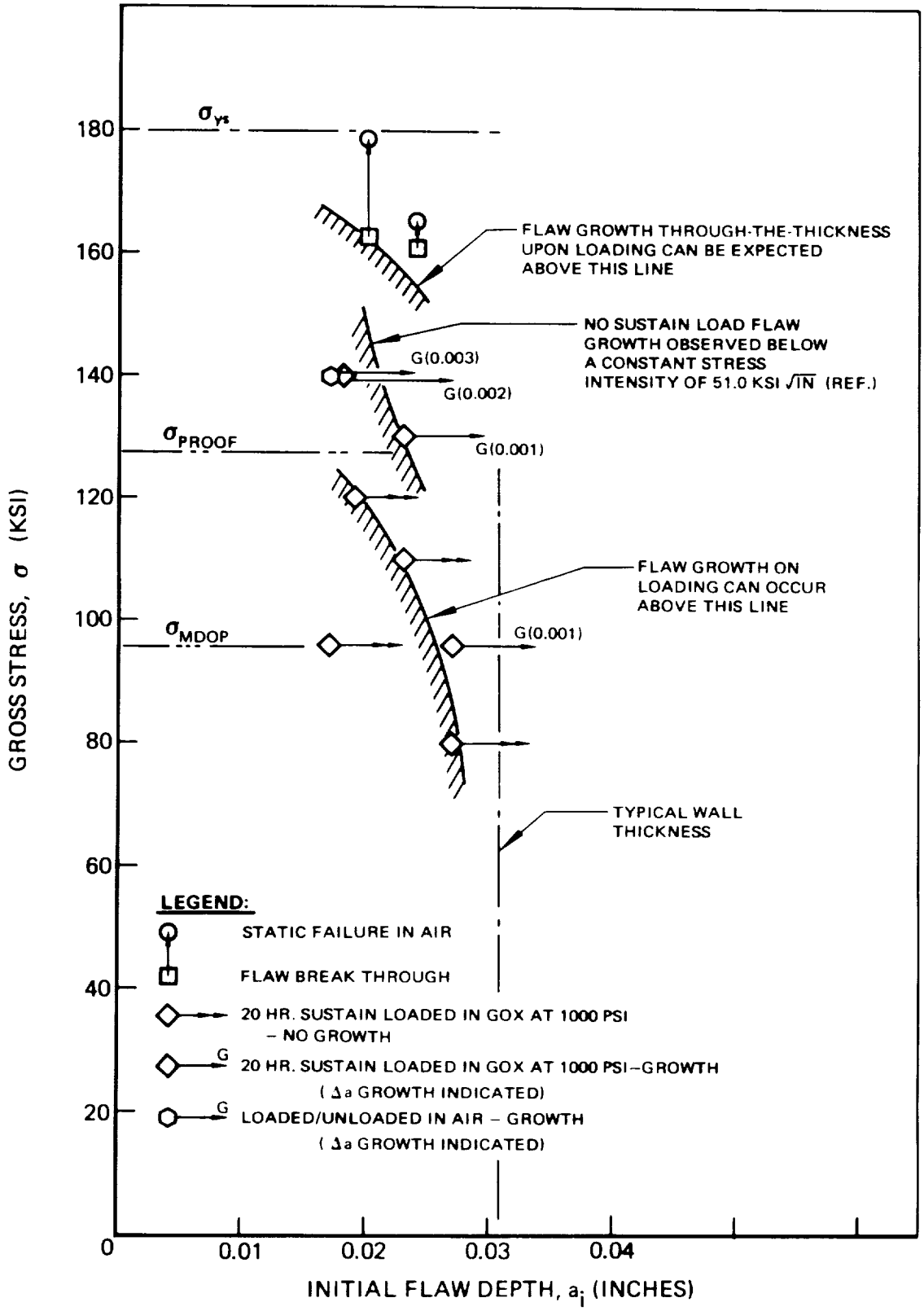

Figure 30: TEST RESULTS OF INCONEL 718 FORGING AT 70°F FOR LM/ECS GOX TANK ASSESSMENT (PART II)

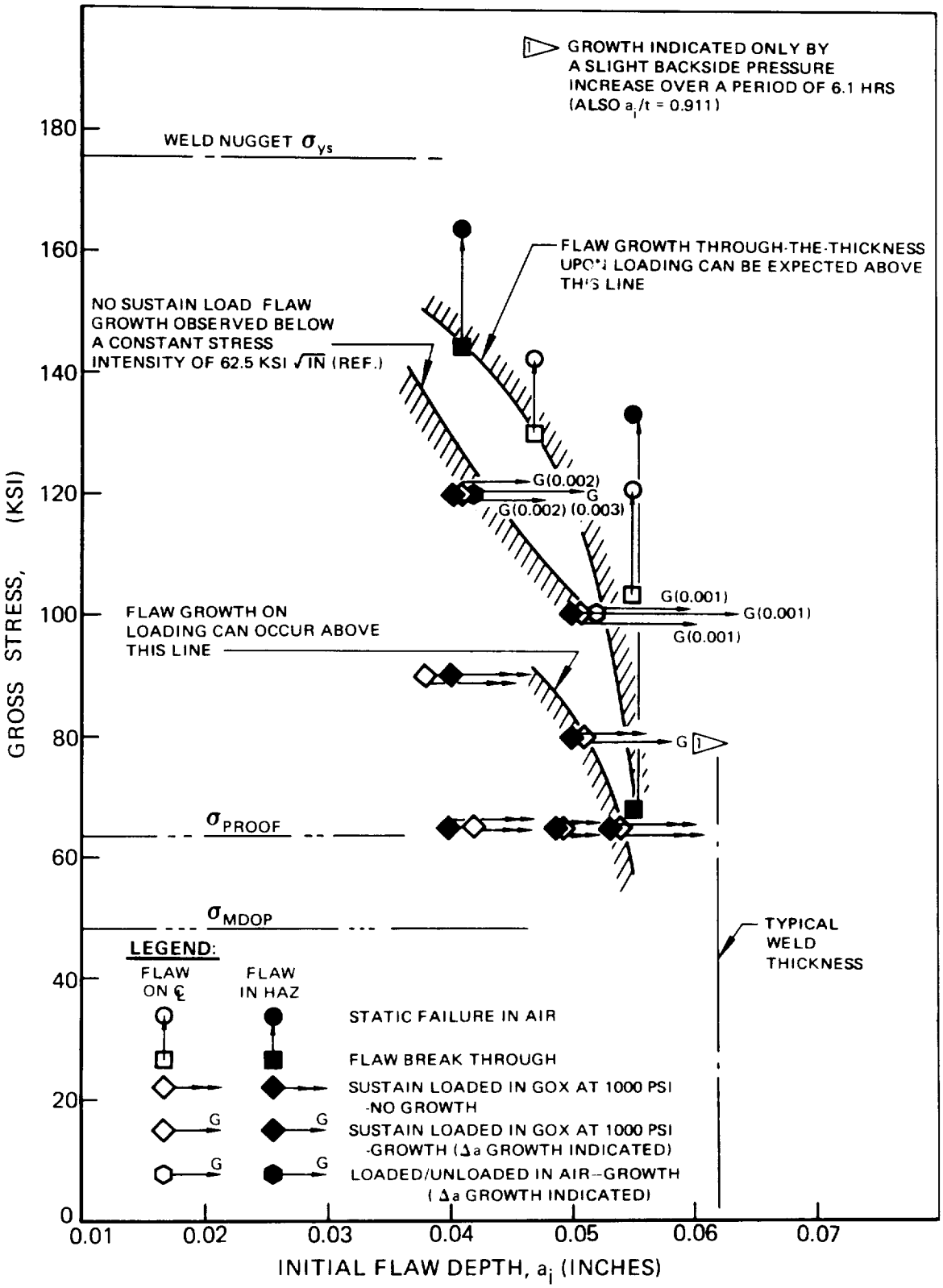

Figure 31: TEST RESULTS OF INCONEL 718 WELDMENT AT 70°F FOR LM/ECS GOX TANK ASSESSMENT (PART II)

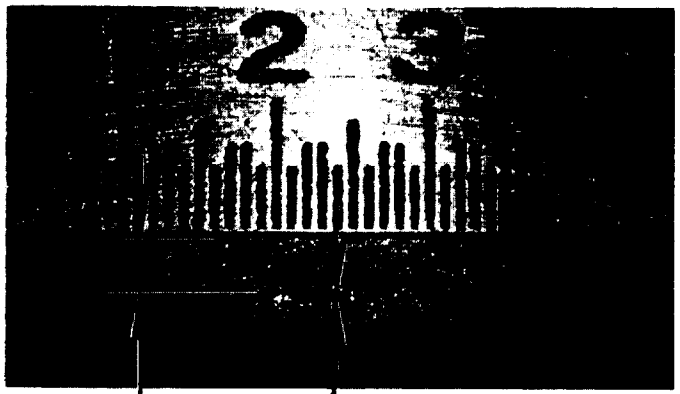

a_i = 0.035" Growth

Specimen B-13
Sustain Loaded For 20 Hrs. In
LOX at −190°F and 1000 psi

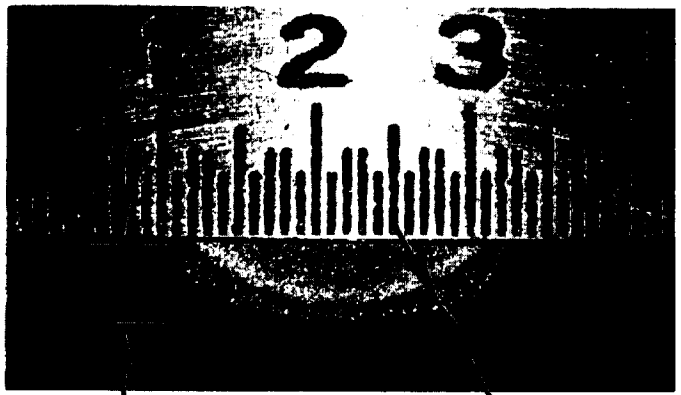

a_i = 0.051" Growth

Specimen B-6
Sustain Loaded For 20 Hrs. In
LOX at −190°F and 1000 psi

a_i = 0.049" Growth

Specimen B-15
Loaded/Unloaded In Air/GN_2 At −190°F

Figure 32: FRACTOGRAPHS OF INCONEL 718 FORGING SPECIMENS STRESSED TO 140 KSI – 8X POLARIZED LIGHT (PART I)

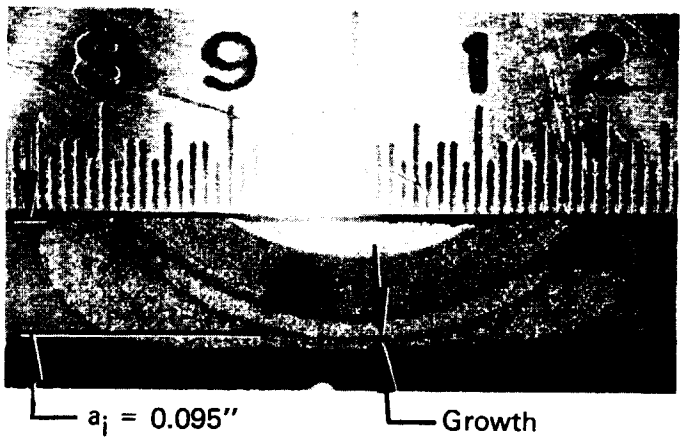

Specimen W-14 (Flaw In HAZ)
Sustain Loaded For 20.3 Hrs.
In LOX At −190°F And 1000 psi
σ = 100 ksi

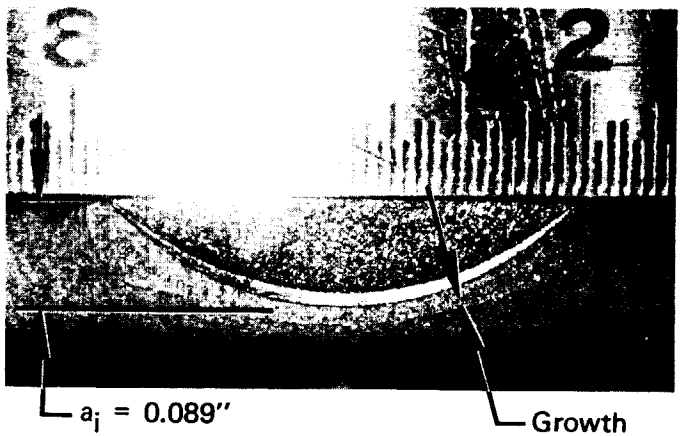

Specimen W-23 (Flaw In HAZ)
Loaded/Unloaded In Air/GN_2
At −190°F σ = 102 ksi

Figure 33: FRACTOGRAPHS OF INCONEL 718 WELDMENT SPECIMENS STRESSED TO APPROXIMATELY 100 KSI – 8X POLARIZED LIGHT (PART I)

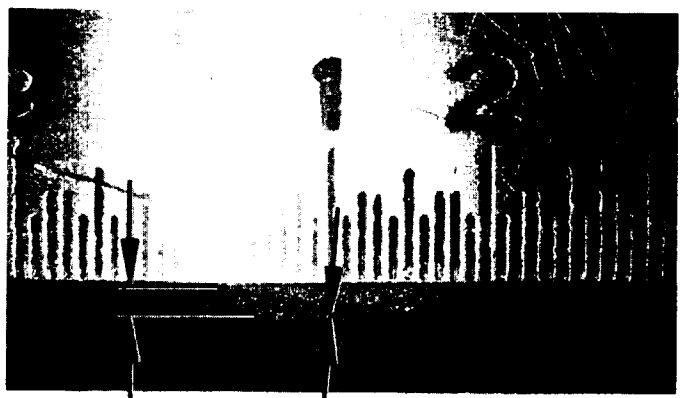

a_i = 0.018" Growth

Specimen LB-1
Sustain Loaded For 20 Hrs.
In GOX At 70°F And 1000 psi

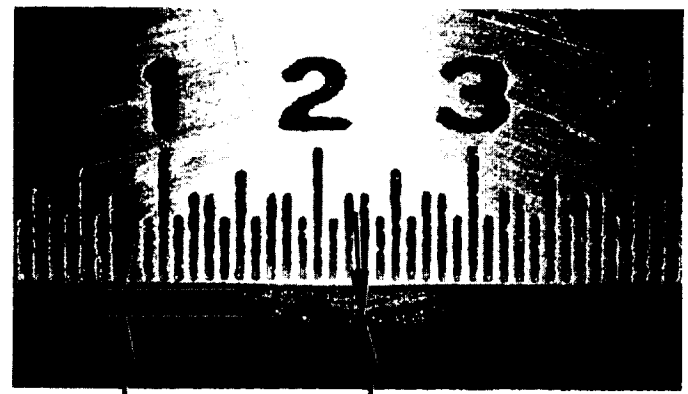

a_i = 0.017" Growth

Specimen LB-5
Loaded/Unloaded In Air At 70°F

Figure 34: FRACTOGRAPHS OF INCONEL 718 FORGING SPECIMENS STRESSED TO 140 KSI – 8X POLARIZED LIGHT (PART II)

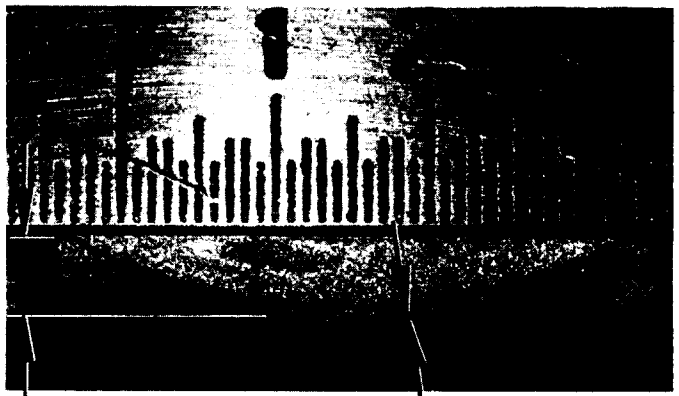

Specimen LW-1 (Flaw In ℄)
Sustain Loaded For 20 Hrs. In
GOX At 70°F And 1000 psi

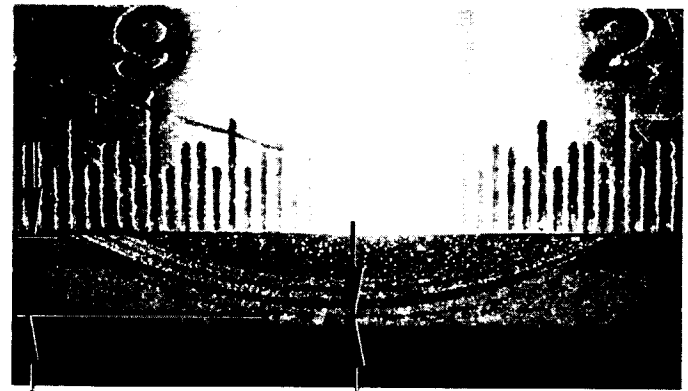

Specimen LW-14 (Flaw In HAZ)
Sustain Loaded For 20 Hrs. In
GOX At 70 °F And 1000 psi

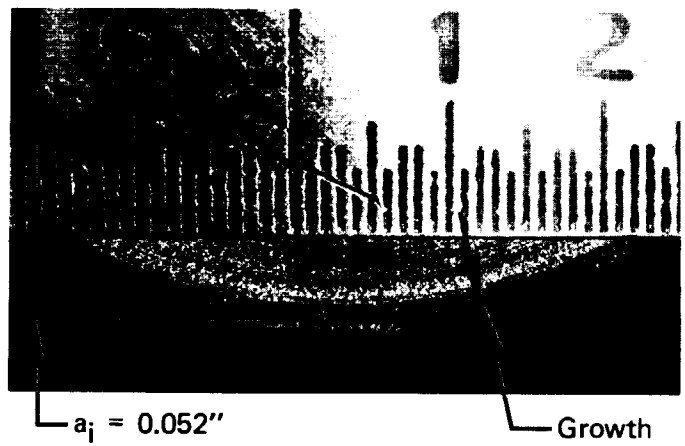

Specimen LW-8 (Flaw In ℄)
Loaded/Unloaded In Air At 70°F

Figure 35: FRACTOGRAPHS OF INCONEL 718 WELDMENT SPECIMENS STRESSED TO 100 KSI – 8X POLARIZED LIGHT (PART II)

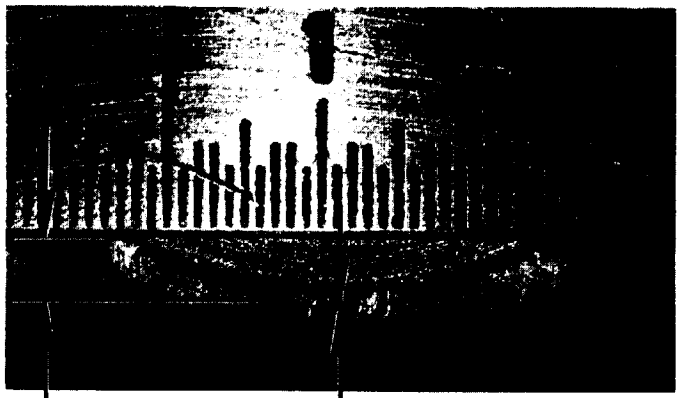

a_i = 0.041" Growth

Specimen LW-13 (Flaw In ℄)
Sustain Loaded For 20 Hrs.
In GOX At 70°F And 1000 psi

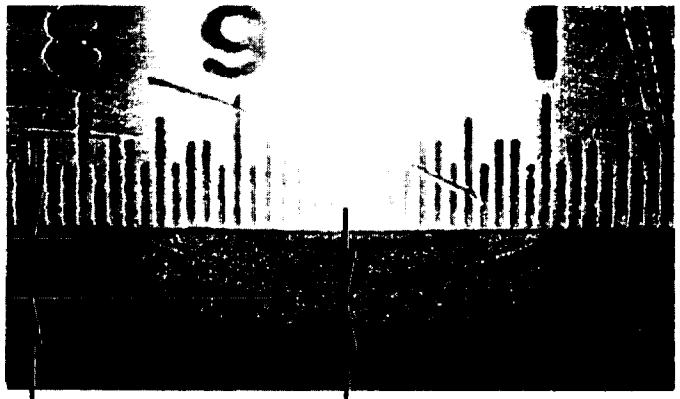

a_i = 0.041" Growth

Specimen LW-2 (Flaw In HAZ)
Sustain Loaded For 20 Hrs.
In GOX At 70°F And 1000 psi

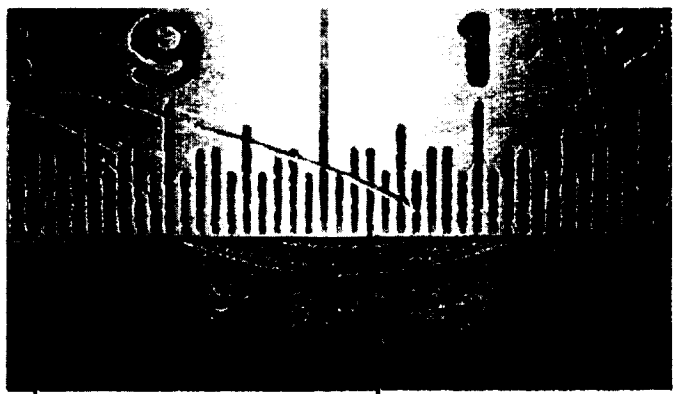

a_i = 0.042" Growth

Specimen LW-9 (Flaw In HAZ)
Loaded/Unloaded In Air At 70°F

Figure 36: FRACTOGRAPHS OF INCONEL 718 WELDMENT SPECIMENS STRESSED TO 120 KSI – 8X POLARIZED LIGHT (PART II)

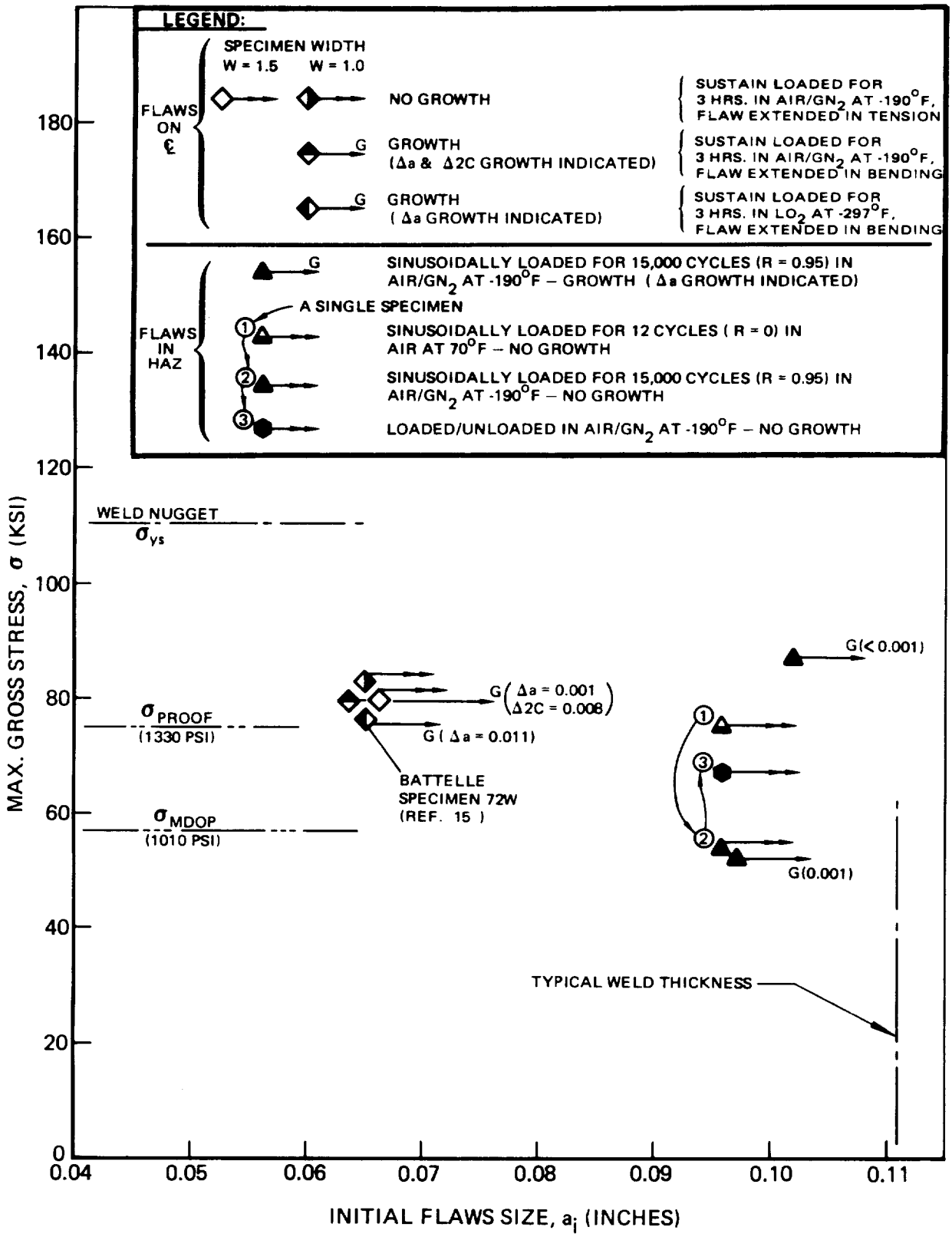

Figure 37: SPECIAL TESTS OF INCONEL 718 WELDMENTS (PART I)

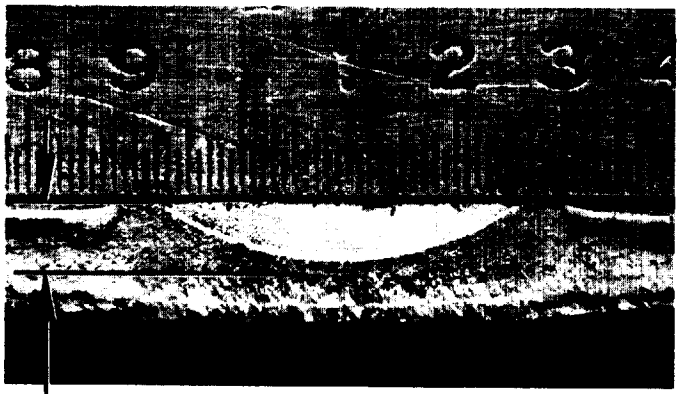

a_i = 0.066" No Growth

Specimen W-33 (Width = 1.5)
Sustain Loaded For 3 Hrs. In Air/GN_2
At −190°F (Flaw Extended In Tension)

a_i = 0.065" No Growth

Specimen W-34 (Width = 1.0)
Sustain Loaded For 3 Hrs. In Air/GN_2
At −190°F (Flaw Extended In Tension)

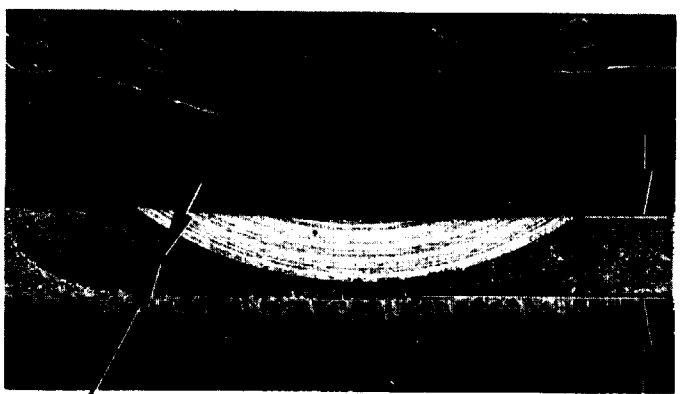

Growth a_i = 0.064"

Specimen W-35 (Width = 1.0)
Sustain Loaded For 3 Hrs. In Air/GN_2
At −190°F (Flaw Extended In Bending)

a_i = 0.065" Growth

Battelle Specimen 72W (Width = 1.0)
Sustain Loaded For 3 Hrs. In
LOX At −297°F (Flaw Extended In Bending)

Figure 38: FRACTOGRAPHS OF INCONEL 718 WELDMENT SPECIMENS STRESSED TO 80 KSI – FLAWS IN ℄ – 8X WHITE LIGHT (PART I)

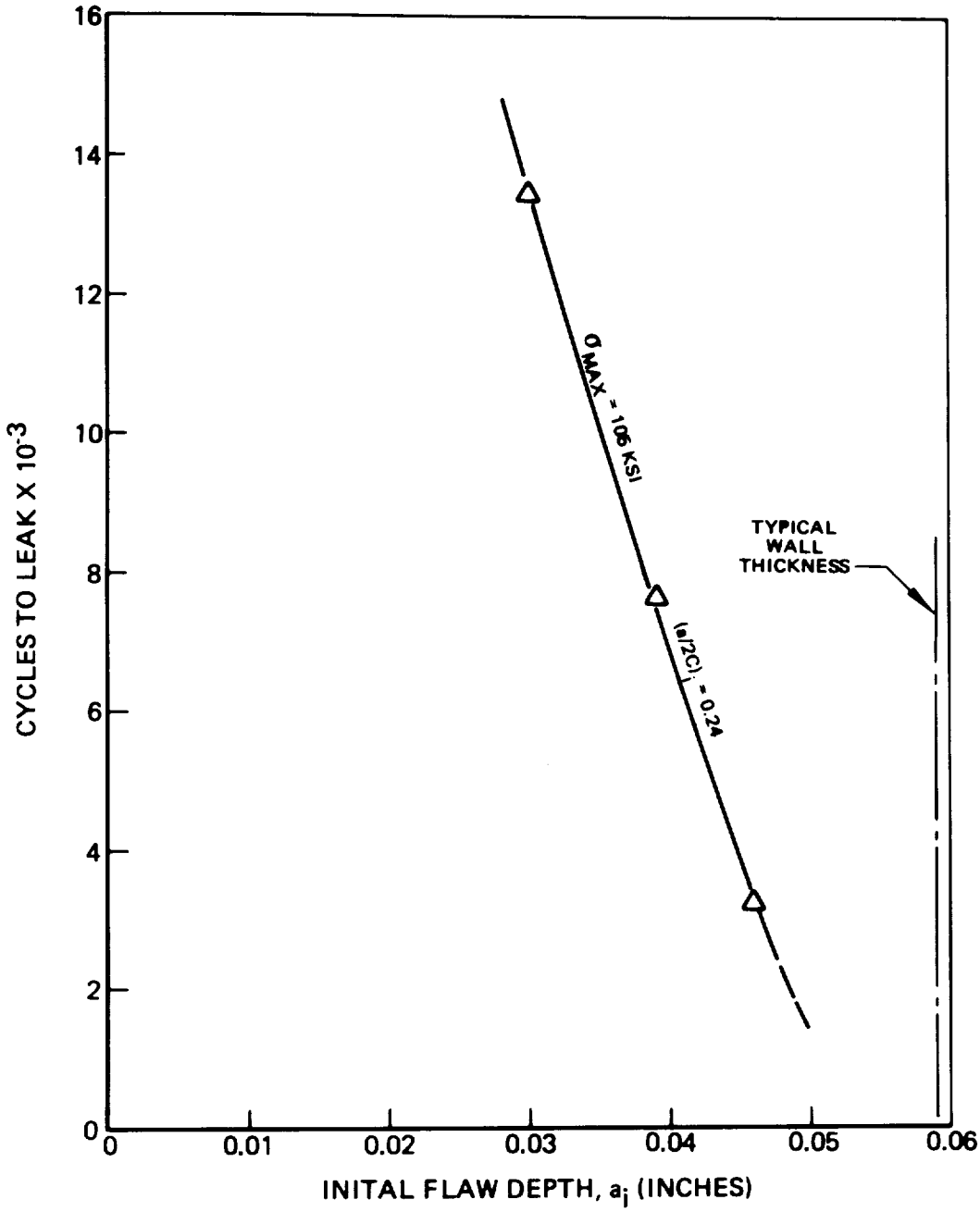

Figure 39: CYCLIC TESTS TO LEAKAGE AT R = 0 OF INCONEL 718 FORGING IN AIR AT 70°F (PART I)

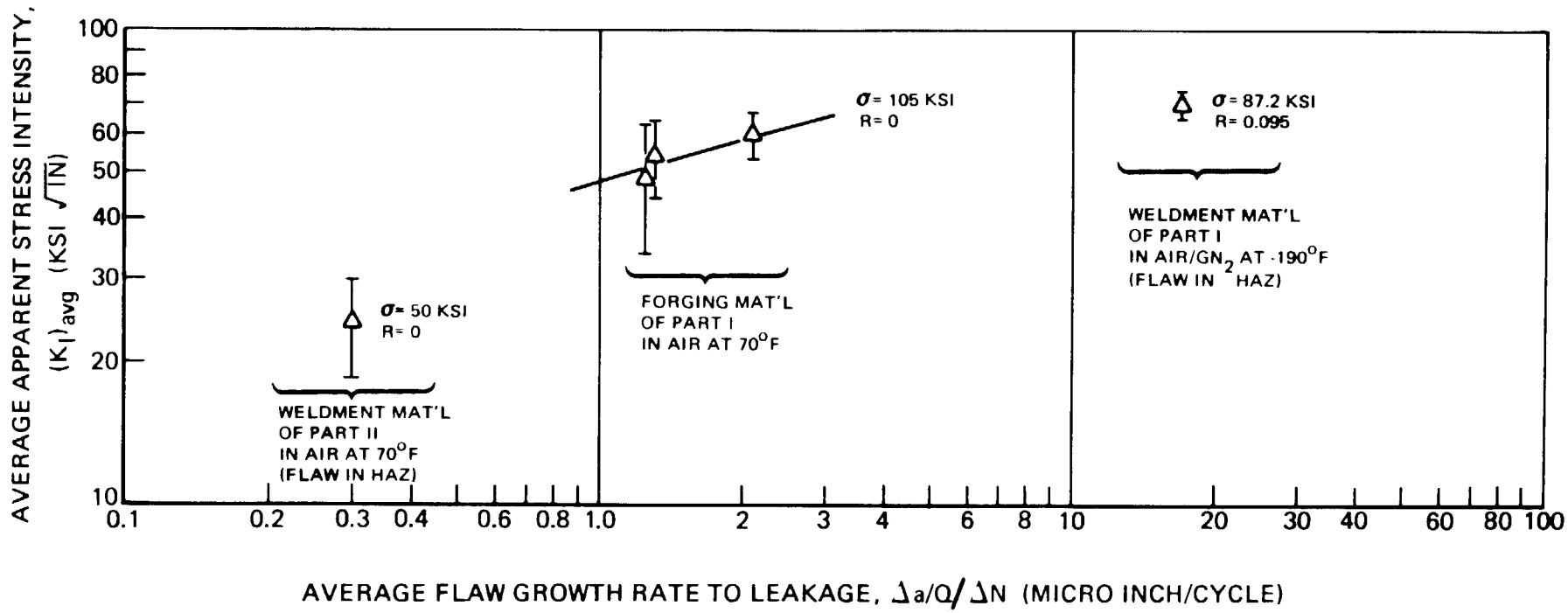

Figure 40: FLAW GROWTH RATES TO LEAKAGE FOR INCONEL 718 (PARTS I AND II)

Table I: MECHANICAL PROPERTIES OF INCONEL 718 FROM SM/EPS LOX TANK FORGING (PART I) [1]

SPECIMEN NUMBER	THICKNESS, t (Inch)	WIDTH, w (Inch)	ENVIRONMENT	TEMPERATURE (°F)	YIELD STRENGTH 0.2% OFFSET IN 1.0 INCH LENGTH (Ksi)	ULTIMATE STRENGTH (Ksi)	ELONGATION IN 1.0 INCH LENGTH (%)	REDUCTION IN AREA (%)
BT-1	0.060	0.508	Air	70	169.6	198.0	27	38
BT-2	0.061	0.509	Air	70	170.0	197.0	26	36
					Avg. 169.8	Avg. 197.5	Avg. 27	Avg. 37
BT-3	0.061	0.505	Air/GN_2	-190	190.2	229.3	19	35
BT-4	0.062	0.507	Air/GN_2	-190	188.2	227.7	21	45
					Avg. 189.2	Avg. 228.5	Avg. 20	Avg. 40
BT-5	0.060	0.498	LN_2	-320	192.5	251.3	34	41

[1] Heat Treated at 1800°F for 1 Hour and Air Cooled. Aged at 1325°F for 8 Hours, Furnace Cooled to 1150°F, Held for 10 Hours and Then Air Cooled.

Table II: MECHANICAL PROPERTIES OF INCONEL 718 FROM SM/EPS LOX TANK WELDMENTS (PART I) [2]

SPECIMEN NUMBER	THICKNESS, t (Inch)	WIDTH, w (Inch)	ENVIRONMENT	TEMPERTURE (°F)	WELD NUGGET YIELD STRENGTH 0.2% OFFSET IN 0.06 INCH LENGTH (Ksi)	YIELD STRENGTH 0.2% OFFSET IN 1.0 INCH LENGTH (Ksi)	ULTIMATE STRENGTH (Ksi)	ELONGATION IN 1.0 INCH LENGTH (%)	REDUCTION IN AREA (%)
WT-4	0.111	0.756	Air	70	112.5	125.7	158.0	3	31
WT-5	0.105	0.746	Air	70	103.1	120.2	153.7	2	35
					Avg. 107.8	Avg. 123.0	Avg. 155.9	Avg. 3	Avg. 33
WT-1	0.111	0.757	Air/GN_2	-190	111.1	136.8	186.5	4	30
WT-2	0.111	0.758	Air/GN_2	-190	109.4	138.4	186.7	4	29
					Avg. 110.3	Avg. 137.6	Avg. 186.6	Avg. 4	Avg. 30
WT-3	0.112	0.757	LN_2	-320	150.8	156.7	197.2	3	27

[2] As Welded Electron Beam.

Table III: MECHANICAL PROPERTIES OF INCONEL 718 USED IN ASSESSMENT OF THE LM/ECS GOX TANK [1] (PART II)

MATERIAL	SPECIMEN NUMBER	THICKNESS, t (Inch)	WIDTH, w (Inch)	ENVIRONMENT	TEMPERATURE (°F)	WELD NUGGET YIELD STRENGTH 0.2% OFFSET IN 0.06 INCH LENGTH (Ksi)	YIELD STRENGTH 0.2% OFFSET IN 1.0 INCH LENGTH (Ksi)	ULTIMATE STRENGTH (Ksi)	ELONGATION IN 1.0 INCH LENGTH (%)	REDUCTION IN AREA (%)
Forging	LBT-1	0.034	0.801	Air	70	N/A	180.9	206.6	22	32
	LBT-2	0.032	0.800	Air	70		178.3	203.4	16	39
							Avg. 179.6	Avg. 205.0	Avg. 19	Avg. 36
Weldment	LWT-1	0.062	0.992	Air	70	162.8	151.0	186.6	8	41
	LWT-2	0.056	1.001	Air	70	188.5	168.7	204.6	8	29
						Avg. 175.6	Avg. 159.9	Avg. 195.6	Avg. 8	Avg. 35

[1] Heat Treated at 1800°F for 1 Hour and Air Cooled. Aged at 1325°F for 8 Hours. Furnace Cooled to 1150°F, Held for 10 Hours and Then Air Cooled. Weldments Electron Beam Welded and Then Weldment and Forging Material Reaged at 1325°F for 8 Hours, Furnace Cooled to 1150°F, Held for 10 Hours and Air Cooled.

Table IV: STATIC FRACTURE TESTS OF INCONEL 718 IN AIR AT 70°F (PART I)

MATERIAL	SPECIMEN NUMBER	FLAW LOCATION	THICKNESS, t (Inch)	INITIAL FLAW DEPTH, a_i (Inch)	INITIAL FLAW LENGTH, $2c_i$ (Inch)	$(a/2c)_i$	GROSS STRESS AT FLAW BREAK THROUGH, σ_T (Ksi)	GROSS STRESS AT FAILURE, σ_F (Ksi)	YIELD STRENGTH, σ_{ys} (Ksi)	σ_T/σ_{ys}	σ_F/σ_{ys}	a_i/t
Forging	B12	–	0.059	0.049	0.197	0.248	156.5	161.0	169.8	0.921	0.947	0.831
Weldment	W13	℄	0.112	0.083	0.353	0.235	106.2	119.2	107.8 [1]	0.986	>1.0	0.741
	W21	HAZ	0.112	0.095	0.370	0.256	105.5	123.2	107.8 [1]	0.980	>1.0	0.848
	W38	HAZ	0.224	0.102	0.405	0.252	None	146.2	107.8 [1]	–	>1.0	0.455 [2]

[1] Weld Nugget Yield Strength

[2] Apparent Failure Stress Intensity of 91 Ksi $\sqrt{\text{In}}$

Table V: STATIC FRACTURE TESTS OF INCONEL 718 IN AIR/GN_2 AT -190°F (PART I)

MATERIAL	SPECIMEN NUMBER	FLAW LOCATION	THICKNESS, t (Inch)	INITIAL FLAW DEPTH, a_i (Inch)	INITIAL FLAW LENGTH, $2c_i$ (Inch)	$(a/2c)_i$	GROSS STRESS AT FAILURE, σ_F (Ksi)	YIELD STRENGTH, σ_{ys} (Ksi)	σ_F/σ_{ys}	a_i/t
Forging	B1	–	0.061	0.050	0.203	0.246	169.0	189.2	0.894	0.820
	B2	–	0.062	0.036	0.148	0.244	187.3	189.2	0.989	0.581
Weldment	W1	℄	0.111	0.056	0.245	0.228	152.2	110.3 [1]	>1.0	0.505
	W2	℄	0.112	0.082	0.355	0.231	139.9	110.3 [1]	>1.0	0.732
	W3	HAZ	0.106	0.081	0.350	0.232	133.5	110.3 [1]	>1.0	0.765
	W4	HAZ	0.111	0.092	0.366	0.251	137.7	110.3 [1]	>1.0	0.828
	W39 [2]	HAZ	0.218	0.109	0.413	0.264	151.0	110.3 [1]	>1.0	0.500

[1] Weld Nugget Yield Strength

[2] Tested at -160°F

Table VI: STATIC FRACTURE TESTS OF INCONEL 718 IN LN_2 AT -320°F (Part I)

MATERIAL	SPECIMEN NUMBER	FLAW LOCATION	THICKNESS, t (Inch)	INITIAL FLAW DEPTH, a_i (Inch)	INITIAL FLAW LENGTH, $2c_i$ (Inch)	$(a/2c)_i$	GROSS STRESS AT FAILURE, σ_F (Ksi)	YIELD STRENGTH, σ_{ys} (Ksi)	σ_F/σ_{ys}	a_i/t
Forging	B20	–	0.061	0.047	0.196	0.240	185.8	192.5	0.965	0.771
	B21	–	0.061	0.052	0.208	0.250	179.8	192.5	0.932	0.853
Weldment	W20	℄	0.112	0.091	0.363	0.251	135.8	150.8 [1]	0.900	0.812
	W36	HAZ	0.112	0.088	0.365	0.241	150.0	150.8 [1]	0.996	0.785
	W37	HAZ	0.102	0.089	0.390	0.228	138.5	150.8 [1]	0.919	0.873

[1] Weld Nugget Yield Strength

Table VII: STATIC FRACTURE TESTS OF INCONEL 718 IN AIR AT 70°F (PART II)

MATERIAL	SPECIMEN NUMBER	FLAW LOCATION	THICKNESS, t (Inch)	INITIAL FLAW DEPTH, a_i (Inch)	INITIAL FLAW LENGTH, $2c_i$ (Inch)	$(a/2c)_i$	GROSS STRESS AT FLAW BREAK THROUGH, σ_T (Ksi)	GROSS STRESS AT FAILURE, σ_F (Ksi)	YIELD STRENGTH, σ_{ys} (Ksi)	σ_T/σ_{ys}	σ_F/σ_{ys}	a_i/t
Forging	LB-4	–	0.030	0.020	0.134	0.149	162.7	178.2	179.6	0.905	0.993	0.667
	LB-7	–	0.030	0.024	0.170	0.141	161.0	165.0	179.6	0.896	0.918	0.800
Weldment	LW-4	℄	0.062	0.047	0.280	0.168	130.0	142.5	175.6 [1]	0.740	0.811	0.758
	LW-21	℄	0.062	0.055	0.382	0.144	103.2	120.8	175.6 [1]	0.588	0.688	0.887
	LW-3	HAZ	0.060	0.041	0.272	0.151	144.3	164.0	175.6 [1]	0.823	0.934	0.683
	LW-22	HAZ	0.060	0.055	0.380	0.145	67.8	133.8	175.6 [1]	0.386	0.762	0.918

[1] Weld Nugget Yield Strength

Table VIII: SUSTAINED TESTS OF INCONEL 718 FORGING IN LOX AT -190°F AND 1000 PSI (PART I)

SPECIMEN NUMBER	THICKNESS, t (Inch)	INITIAL FLAW DEPTH, a_i (Inch)	INITIAL FLAW LENGTH, $2c_i$ (Inch)	$(a/2c)_i$	APPLIED GROSS STRESS, σ_A (Ksi)	YIELD STRENGTH, σ_{ys} (Ksi)	σ_A/σ_{ys}	a_i/t	SUSTAINED TIME (Hrs)	OBSERVATIONS
B6	0.062	0.051	0.203	0.251	140.0	189.2	0.740	0.823	20.0	Growth (Δa = 0.001")
B8	0.058	0.048	0.203	0.237	120.0	189.2	0.634	0.826	20.0	No Growth [1]
B9	0.059	0.048	0.199	0.241	91.0	189.2	0.481	0.814	20.0	No Growth [1]
B10	0.059	0.038	0.152	0.250	91.0	189.2	0.481	0.644	20.0	No Growth
B13	0.058	0.035	0.136	0.258	140.0	189.2	0.740	0.603	20.0	Growth (Δa = 0.005")
B17	0.060	0.047	0.200	0.235	130.0	189.2	0.687	0.784	20.0	Growth (Δa = 0.002")
B18	0.061	0.037	0.138	0.268	125.0	189.2	0.661	0.606	34.0	No Growth

[1] Specimen Unloaded Due to Pressure Leak and Then Re-Loaded

Table IX: SUSTAINED TESTS OF INCONEL 718 WELDMENT IN LOX AT -190°F AND 1000 PSI – FLAWS IN ℄ (PART I)

SPECIMEN NUMBER	THICKNESS, t (Inch)	INITIAL FLAW DEPTH, a_i (Inch)	INITIAL FLAW LENGTH, $2c_i$ (Inch)	$(a/2c)_i$	APPLIED GROSS STRESS, σ_A (Ksi)	YIELD STRENGTH [1], σ_{ys} (Ksi)	σ_A/σ_{ys}	a_i/t	SUSTAINED TIME (Hrs)	OBSERVATIONS
W5	0.113	0.057	0.217	0.263	50.0	110.3	0.453	0.505	20.0	No Growth
W6	0.112	0.074	0.303	0.244	50.0	110.3	0.453	0.660	20.0	No Growth
W7	0.110	0.088	0.370	0.238	50.0	110.3	0.453	0.800	20.0	No Growth
W8	0.112	0.089	0.368	0.242	85.0	110.3	0.770	0.794	20.0	No Growth
W11	0.113	0.093	0.368	0.253	120.0	110.3	>1.0	0.823	0.62	Grew Through-The-Thickness In 37 Min. (Δa = 0.020")
W15	0.112	0.101	0.365	0.277	102.0	110.3	0.925	0.902	–	Grew Through-The-Thickness On Loading (Δa = 0.011")
W26	0.112	0.076	0.297	0.256	95.0	110.3	0.861	0.678	20.0	No Growth
W29	0.109	0.100	0.395	0.253	80.0	110.3	0.725	0.918	–	Grew Through-The-Thickness On Loading (Δa = 0.009")

[1] Weld Nugget Yield Strength

Table X: SUSTAINED TESTS OF INCONEL 718 WELDMENT IN LOX AT -190°F AND 1000 PSI – FLAWS IN HAZ (PART I)

SPECIMEN NUMBER	THICKNESS, t (Inch)	INITIAL FLAW DEPTH, a_i (Inch)	INITIAL FLAW LENGTH, $2c_i$ (Inch)	$(a/2c)_i$	APPLIED GROSS STRESS, σ_A (Ksi)	YIELD STRENGTH, σ_{ys} (Ksi) [1]	σ_A/σ_{ys}	a_i/t	SUSTAINED TIME (Hrs)	OBSERVATIONS
W9	0.108	0.054	0.222	0.243	50.0	110.3	0.453	0.500	20.5	No Growth
W10	0.110	0.089	0.363	0.245	50.0	110.3	0.453	0.810	20.5	No Growth
W12	0.114	0.094	0.363	0.259	85.0	110.3	0.770	0.825	20.5	No Growth
W14	0.112	0.095	0.372	0.255	100.0	110.3	0.907	0.848	20.3	Growth (Δa = .004")
W17	0.112	0.093	0.368	0.253	94.0	110.3	0.852	0.851	20.0	No Growth
W25	0.112	0.066	0.278	0.238	100.0	110.3	0.907	0.590	20.0	No Growth

[1] Weld Nugget Yield Strength

Table XI: LOAD/UNLOAD TESTS OF INCONEL 718 IN AIR/GN_2 AT $-190^{o}F$ (PART I)

MATERIAL	SPECIMEN NUMBER	FLAW LOCATION	THICKNESS, t (Inch)	INITIAL FLAW DEPTH, a_i (Inch)	INITIAL FLAW LENGTH, $2c_i$ (Inch)	$(a/2c)_i$	APPLIED GROSS STRESS, σ_A (Ksi)	YIELD STRENGTH, σ_{ys} (Ksi)	σ_A / σ_{ys}	a_i/t	OBSERVATIONS
Forging	B14	–	0.061	0.049	0.200	0.245	140.0	189.2	0.740	0.803	Growth (Δa = 0.003")
Weldment	W16	℄	0.112	0.102	0.372	0.274	102.0	110.3 ▷1	0.925	0.911	Grew Through-The-Thickness (Δa = 0.010")
	W23	HAZ	0.113	0.089	0.370	0.241	102.0	110.3 ▷1	0.925	0.788	Growth (Δa = 0.002")

▷1 Weld Nugget Yield Strength

Table XII: SUSTAINED TESTS OF INCONEL 718 FORGING IN GOX AT 70°F AND 1000 PSI (PART II)

SPECIMEN NUMBER	THICKNESS, t (Inch)	INITIAL FLAW DEPTH, a_i (Inch)	INITIAL FLAW LENGTH, $2c_i$ (Inch)	$(a/2c)_i$	APPLIED GROSS STRESS, σ_A (Ksi)	YIELD STRENGTH, σ_{ys} (Ksi)	σ_A/σ_{ys}	a_i/t	SUSTAINED TIME (Hrs)	OBSERVATIONS
LB-1	0.032	0.018	0.140	0.129	140.0	179.6	0.780	0.563	20.0	Growth (Δa = 0.002")
LB-2	0.032	0.019	0.141	0.135	120.0	179.6	0.668	0.594	20.0	No Growth
LB-3	0.032	0.017	0.130	0.131	96.0	179.6	0.535	0.532	20.0	No Growth
LB-6	0.029	0.023	0.174	0.132	130.0	179.6	0.724	0.794	20.0	Growth (Δa = 0.001")
LB-8	0.030	0.027	0.172	0.157	96.0	179.6	0.535	0.900	20.0	Growth (Δa = 0.001")
LB-9	0.032	0.023	0.185	0.124	110.0	179.6	0.613	0.719	20.0	No Growth
LB-10	0.032	0.027	0.182	0.148	80.0	179.6	0.446	0.844	20.0	No Growth

Table XIII: SUSTAINED TESTS OF INCONEL 718 WELDMENT IN GOX AT 70°F AND 1000 PSI – FLAWS IN ℄ (PART II)

SPECIMEN NUMBER	THICKNESS, t (Inch)	INITIAL FLAW DEPTH, a_i (Inch)	INITIAL FLAW LENGTH, $2c_i$ (Inch)	$(a/2c)_i$	APPLIED GROSS STRESS, σ_A (Ksi)	YIELD STRENGTH, σ_{ys} (Ksi) [1]	σ_A/σ_{ys}	a_i/t	SUSTAINED TIME (Hrs)	OBSERVATIONS
LW-1	0.061	0.051	0.364	0.140	100.0	175.6	0.570	0.836	20.0	Growth (Δa = 0.001")
LW-6	0.060	0.049	0.362	0.135	65.0	175.6	0.370	0.816	20.0	No Growth
LW-11	0.060	0.042	0.273	0.154	65.0	175.6	0.370	0.700	20.0	No Growth
LW-13	0.061	0.041	0.273	0.150	120.0	175.6	0.684	0.672	20.0	Growth (Δa = 0.002")
LW-15	0.060	0.038	0.283	0.134	90.0	175.6	0.513	0.634	20.0	No Growth
LW-16	0.056	0.051	0.363	0.140	80.0	175.6	0.456	0.911	7.1	No Flaw Growth Indicated on Fracture Face But Slight Pressure Rise on Back of Specimen [2]
LW-19	0.060	0.054	0.385	0.140	65.0	175.6	0.370	0.900	20.0	No Growth

[1] Weld Nugget Yield Strength

[2] Pressure Indicated on Back Side of Specimen, Initiating After 1 Hour at Load and Increasing to 50 PSI After 7.1 Hours

Table XIV: SUSTAINED TESTS OF INCONEL 718 WELDMENT IN GOX AT 70°F AND 1000 PSI - FLAWS IN HAZ (PART II)

SPECIMEN NUMBER	THICKNESS, t (Inch)	INITIAL FLAW DEPTH, a_i (Inch)	INITIAL FLAW LENGTH, $2c_i$ (Inch)	$(a/2c)_i$	APPLIED GROSS STRESS, σ_A (Ksi)	YIELD STRENGTH, σ_{ys} (Ksi) [1]	σ_A/σ_{ys}	a_i/t	SUSTAINED TIME (Hrs)	OBSERVATIONS
LW-2	0.066	0.041	0.275	0.149	120.0	175.6	0.684	0.621	20.0	Growth (Δa = 0.002")
LW-7	0.059	0.049	0.362	0.135	65.0	175.6	0.370	0.831	20.0	No Growth
LW-10	0.057	0.040	0.278	0.144	90.0	175.6	0.513	0.702	20.0	No Growth
LW-12	0.063	0.040	0.276	0.145	65.0	175.6	0.370	0.635	20.0	No Growth
LW-14	0.060	0.050	0.358	0.140	100.0	175.6	0.570	0.833	20.0	Growth (Δa = 0.001")
LW-17	0.061	0.050	0.364	0.137	80.0	175.6	0.456	0.820	20.0	No Growth
LW-20	0.063	0.053	0.386	0.137	65.0	175.6	0.370	0.842	20.0	No Growth

[1] Weld Nugget Yield Strength

Table XV: LOAD/UNLOAD TESTS OF INCONEL 718 IN AIR AT 70°F (PART II)

MATERIAL	SPECIMEN NUMBER	FLAW LOCATION	THICKNESS, t (Inch)	INITIAL FLAW DEPTH, a_i (Inch)	INITIAL FLAW LENGTH, $2c_i$ (Inch)	$(a/2c)_i$	APPLIED GROSS STRESS, σ_A (Ksi)	YIELD STRENGTH, σ_{ys} (Ksi)	σ_A/σ_{ys}	a_i/t	OBSERVATIONS
Forging	LB-5	–	0.030	0.017	0.140	0.122	140.0	179.6	0.780	0.567	Growth (Δa = 0.003")
Weldment	LW-8	℄	0.062	0.052	0.362	0.144	100.0	[1] 175.6	0.570	0.838	Growth (Δa = 0.001")
	LW-9	HAZ	0.062	0.042	0.276	0.152	120.0	[1] 175.6	0.684	0.678	Growth (Δa = 0.003")

[1] Weld Nugget Yield Strength

Table XVI: SUSTAINED/CYCLIC (SUSLIC) TESTS OF INCONEL 718 FORGING IN LOX AT -190°F AND 1000 PSI (PART I)

SPECIMEN NUMBER	THICKNESS, t (Inch)	INITIAL FLAW DEPTH, a_i (Inch)	INITIAL FLAW LENGTH, $2c_i$ (Inch)	$(a/2c)_i$	MAX APPLIED GROSS STRESS $(\sigma_A)_{Max}$ (Ksi)	$R = \frac{(\sigma_A)_{Min}}{(\sigma_A)_{Max}}$	YIELD STRENGTH, σ_{ys} (Ksi)	$\frac{(\sigma_A)_{Max}}{\sigma_{ys}}$	a_i/t	NUMBER OF CYCLES [1]	OBSERVATIONS
B4	0.062	0.035	0.150	0.233	96.2	0.895	189.2	0.509	0.565	20	No Growth
B5	0.062	0.049	0.203	0.241	96.2	0.895	189.2	0.509	0.791	20	No Growth
B11	0.058	0.051	0.203	0.251	126.8	0.895	189.2	0.670	0.879	20	Growth (Δa = 0.002")
B14	0.061	0.048	0.202	0.238	123.1	0.950	189.2	0.651	0.786	72	Growth (Δa = 0.002")
B19	0.061	0.030	0.112	0.268	123.1	0.950	189.2	0.651	0.492	20	No Growth

[1] See Figure 18 For Load Profile

Table XVII: SUSTAINED/CYCLIC (SUSLIC) TESTS OF INCONEL 718 WELDMENT IN LOX AT -190°F AND 1000 PSI – FLAWS IN HAZ (PART I)

SPECIMEN NUMBER	THICKNESS, t (Inch)	INITIAL FLAW DEPTH, a_i (Inch)	INITIAL FLAW LENGTH, $2c_i$ (Inch)	$(a/2c)_i$	MAX. APPLIED GROSS STRESS, $(\sigma_A)_{Max}$ (Ksi)	$R = \frac{(\sigma_A)_{Min}}{(\sigma_A)_{Max}}$	YIELD STRENGTH, σ_{ys} (Ksi) [2]	$\frac{(\sigma_A)_{Max}}{\sigma_{ys}}$	a_i/t	NUMBER OF CYCLES [1]	OBSERVATIONS
W18	0.112	0.091	0.369	0.247	52.1	0.895	110.3	0.472	0.813	20	No Growth
W22	0.112	0.091	0.361	0.252	87.2	0.950	110.3	0.790	0.813	20	Growth ($\Delta a < 0.001''$)
W28	0.112	0.070	0.298	0.235	87.2	0.950	110.3	0.790	0.625	20	No Growth
W30	0.112	0.091	0.370	0.246	87.2	0.950	110.3	0.790	0.813	55.5	Growth ($\Delta a < 0.001''$)

[1] See Figure 18 For Load Profile

[2] Weld Nugget Yield Strength

Table XVIIIa: CYCLIC TEST OF INCONEL 718 FORGING IN AIR/GN_2 AT -190°F (PART I)

SPECIMEN NUMBER	TEST CONDITION	THICKNESS, t (Inch)	INITIAL FLAW DEPTH, a_i (Inch)	INITIAL FLAW LENGTH, $2c_i$ (Inch)	$(a/2c)_i$	MAX. APPLIED GROSS STRESS $(\sigma_A)_{Max}$ (Ksi)	YIELD STRENGTH, σ_{ys} (Ksi)	$\frac{(\sigma_A)_{Max}}{\sigma_{ys}}$	a_i/t	OBSERVATIONS
B16	15,000 Cycles at R = 0.95, 90 cpm	0.060	0.049	0.197	0.249	102.6	189.2	0.542	0.817	Growth ($\Delta a < 0.001''$)

Table XVIIIb: CYCLIC TEST OF INCONEL 718 WELDMENT IN AIR/GN_2 AT -190°F – FLAW IN HAZ (PART I)

W24	15,000 Cycles at R = 0.95, 90 cpm	0.112	0.102	0.365	0.280	87.2	110.3	0.790	0.911	Growth ($\Delta a < 0.001''$)

Table XVIIIc: CYCLIC/LOAD TO LEAKAGE TEST OF INCONEL 718 WELDMENT IN AIR/GN_2 AT -190°F – FLAW IN HAZ (PART I)

W32	15,000 Cycles at R = 0.95, 90 cpm; Loaded at 1000 lb/min Until Leakage	0.112	0.097	0.372	0.261	52.1	110.3	0.472	0.865	Growth ($\Delta a = 0.001''$)

Table XVIIId: PROOF/CYCLIC/LOAD TEST OF INCONEL 718 WELDMENT IN AIR – FLAW IN HAZ (PART I)

W31	12 Cycles to 75 Ksi at R = 0 and 70°F	0.112	0.096	0.363	0.265	75.0	107.8	0.696	0.857	No Growth
	15,000 Cycles at R = 0.95 and -190°F, 90 cpm					52.1	110.3	0.472		
	Loaded at 1000 lb/min to 67.7 Ksi at -190°F					67.7	110.3	0.614		

Table XIXa: COMPARISON OF FLAW EXTENTION METHODS AND SPECIMEN WIDTH ON 3 HOUR SUSTAINED LOAD TESTS IN AIR/GN_2 AT -190°F – FLAWS IN ℄ (PART I)

METHOD OF FLAW EXTENSION	SPECIMEN NUMBER	THICKNESS, t (Inch)	WIDTH, w (Inch)	INITIAL FLAW DEPTH, a_i (Inch)	INITIAL FLAW LENGTH, $2c_i$ (Inch)	$(a/2c)_i$	APPLIED GROSS STRESS, σ_A (Ksi)	YIELD STRENGTH, σ_{ys} (Ksi)	σ_A/σ_{ys}	a_i/t	OBSERVATIONS
Tension σ =45 Ksi	W33	0.112	1.50	0.066	0.352	0.188	80.0	110.3	0.725	0.590	No Growth
Tension σ =45 Ksi	W34	0.111	1.00	0.065	0.353	0.184	80.0	110.3	0.725	0.586	No Growth
Bending σ_{Max}=45 Ksi	W35	0.111	1.00	0.064	0.337	0.190	80.0	110.3	0.725	0.577	Growth (Δa = 0.001") ($\Delta 2C$ = 0.008")

Table XIXb: BATTELLE INCONEL 718 WELDMENT (T.I.G.) SUSTAIN LOADED FOR 3 HOURS IN LOX AT -297°F (PART I)

Bending σ_{Max}= 45 Ksi	72W	0.100	1.00	0.065	0.348	0.186	80.0	–	–	0.630	Growth (Δa = 0.011")

Table XXa: CYCLIC TESTS TO LEAKAGE AT R = 0 OF INCONEL 718 FORGING IN AIR AT 70°F (PART I)

SPECIMEN NUMBER	THICKNESS, t (Inch)	FLAW DEPTH, a (Inch)	FLAW LENGTH, 2c (Inch)	a/2c	MAX. APPLIED GROSS STRESS, $(\sigma_A)_{Max}$ (Ksi)	YIELD STRENGTH, σ_{ys} (Ksi)	$\frac{(\sigma_A)_{Max}}{\sigma_{ys}}$	a_i/t	$\Delta a/Q/\Delta N$ (Micro-Inch/Cycle)	$(K_I)_{Avg}$ (Ksi $\sqrt{In}$)	OBSERVATIONS
B3	0.061	Initial 0.030 Final 0.061	Initial 0.112 Final 0.190	Initial 0.268 Final 0.321	105.0	169.8	0.619	0.492	1.25	48.7	Flaw Grew Through-The-Thickness in 13,450 Cycles—Cyclic Rate of 40 cpm
B22	0.061	Initial 0.039 Final 0.061	Initial 0.195 Final 0.195	Initial 0.241 Final 0.313	105.0	169.8	0.619	0.639	1.25	54.2	Flaw Grew Through-The-Thickness in 7,640 Cycles – Cyclic Rate of 40 cpm
B23	0.061	Initial 0.046 Final 0.061	Initial 0.206 Final 0.222	Initial 0.223 Final 0.275	105.0	169.8	0.619	0.755	2.10	60.4	Flaw Grew Through-The-Thickness in 3,136 Cycles—Cyclic Rate of 40 Cpm

Table XXb: CYCLIC TEST TO LEAKAGE AT R = 0.095 OF INCONEL 718 WELDMENT IN AIR/GN_2 AT -190°F – FLAW IN HAZ (PART I)

W27	0.111	Initial 0.090 Final 0.111	Initial 0.368 Final 0.390	Initial 0.245 Final 0.284	87.2	1 110.3	0.790	0.811	16.9	70.5	Flaw Grew Through-The-Thickness in 491 Cycles – Cyclic Rate of 10 Cpm

Table XXc: CYCLIC TEST TO LEAKAGE AT R = 0 OF INCONEL 718 WELDMENT IN AIR AT 70°F – FLAW IN HAZ (PART II)

LW-18	0.054	Initial 0.030 Final 0.054	Initial 0.200 Final 0.208	Initial 0.150 Final 0.260	50.0	1 175.6	0.285	0.556	0.30	24.2	Flaw Grew Through-The-Thickness in 37,000 Cycles—Cyclic Rate of 40 Cpm

1 Weld Nugget Yield Strength

DISTRIBUTION LIST FOR FINAL REPORT NASA CR-108485

CONTRACT NAS 9-10913

"INVESTIGATION OF CRACK GROWTH THRESHOLD OF INCONEL 718 EXPOSED TO HIGH PRESSURE OXYGEN"

The Boeing Company
Seattle, Washington

		Copies
National Aeronautics and Space Administration Manned Spacecraft Center Houston, Texas 77058		
Attention:	Procurement Officer J. W. Wilson Mail Code JC 721 (23)	1
	Library R. Shirkey Mail Code BM 6	4
	Management Service Division J. T. Wheeler Mail Code BM 7	1
	Structures and Mechanics Division R. G. Forman Mail Code ES 8	59